Closing the Wound: an Eye-Opening Mechanism

Development of a Bi-planar Incision Mechanism Used in Vitrectomy

by Jesse Schuurman

TU Delft

Closing the Wound: an Eye-Opening Mechanism

Development of a Bi-planar Incision Mechanism Used in Vitrectomy

DELFT UNIVERSITY OF TECHNOLOGY

MASTER OF SCIENCE

MECHANICAL ENGINEERING - BIOMECHANICAL DESIGN

Author:
J. Schuurman

Thesis committee:
Prof. Dr. ir. P. Breedveld
Prof. dr. J.J. van den Dobbelsteen
Ir. Jette Bloemberg
Ir. Esther de Kater

May 3, 2023

ABSTRACT

Background: Treatment of eye conditions, such as retinal detachment, macular pucker or macular holes, ask for an intervention named "vitrectomy". In a vitrectomy, multiple surgical instruments are brought into the eye, to facilitate removal of the vitreous humor. The instruments enter the eye through trocar ports that are placed in the sclera. Post operation, this passageway is removed, leaving an incision wound in the sclera. These wounds that remain after removal may cause complications such as hypotony and endophthalmitis. Current studies suggest that the frequency of these complications decreases when the incision architecture (i.e., the number of incision planes that are used to construct the wound) , made during insertion of the trocar port, has better self sealing properties. The objective for this study is to *develop and verify a surgical instrument that can consistently create the most effective self-sealing scleral incisions.*

Method: An analysis is performed that investigates the relation between the incision architectures and the corresponding self-sealing characteristics. This analysis is done through information found in literature and an experiment. In this experiment, incisions with a variety of incision architectures are made in a setup that imitates the characteristics of the human eye. Based on the analysis, incisions with a bi-planar architecture hold the greatest potential for consistent self-sealing incisions. A set of requirements are formulated that are used to generate a functional prototype that is capable of creating bi-planar incision. This concept consist of a high precision pin and slot mechanism linked to an actuation handle. Verification of the established requirements and evaluation of the prototype performance are achieved by incisions in silicone slabs (i.e., eye phantoms).

Results: The defined Bi-planar architecture is set to have an oblique plane of $0.500\ mm$, a vertical plane of $0.250\ mm$ and the angle between the two planes of $60.0°$. The Bi-Planar Incision Mechanism showed to have an mean oblique plane of $0.530\ mm$ ($SD = 0.043$), a mean vertical plane of $0.248\ mm$ ($SD = 0.0286$) and a mean angle of $60.08°$ ($SD = 2.40$). The incision were performed with an average time to completion of 5.0 seconds ($SD = 1.5$).

Conclusion Using the Bi-Planar Incision Mechanism showed to be a successful method to make the desired bi-planar incisions. The result showed precise, accurate and fast incisions. The next step is to validate the self-sealing statistics in conditions that resemble those found in the operation room.

TABLE OF CONTENTS

1 Introduction

1.1 Vitrectomy

The human eyes are one of the most intricate organs in the human body that play a crucial role in our daily lives. Any surgical intervention in this area requires the utmost precision and care. Due to advanced surgical techniques, the highest levels of minimal invasive surgery are found in ophthalmology. One type of such ophthalmic surgery is a "pars plana vitrectomy", a procedure that helps to regain vision or prevent further damage. In this procedure, a clear gel called the vitreous humor, as seen in Fig. 1, that fills the posterior segment of the eye, is removed. Eye conditions which require such intervention are retinal detachment, macular pucker or macular holes [1]. The primary functions of the vitreous humor include transmitting light, supporting the posterior surface of the lens, holding the neural layer of the retina firmly against the pigmented layer, and contributing to intraocular pressure [2]. The vitreous humor consist out of a fibrillar network filled with 98% water and 2% collagen and hyaluronan [1]. During pars plana vitrectomy, a hollow needle enters the eye, cuts the vitreous humor into small fragments, and sucks the gel-like structure out of the eye. Besides this needle, a light source and a transfer-tube are brought into the eye, as seen in Fig. 2. The light source illuminates the intraocular workspace helping the surgeon to see the structures inside the eye more clearly. The transfer-tube replaces the vitreous humor with a saline solution in order to maintain the shape of the eye. In order for these instruments to enter the eye, a passageway through the sclera (i.e., the white wall of the eye) must be constructed. This passageway is created by placing a trocar port (i.e., a tunnel with an inner diameter of $0.4\ mm$ and the outer diameter of $0.5\ mm$ for 27 gauge vitrectomy [3]) in the scleral wall. Unfortunately, complications may arise from the wound that remains after the trocar port has been removed, as is discussed in the following section,.

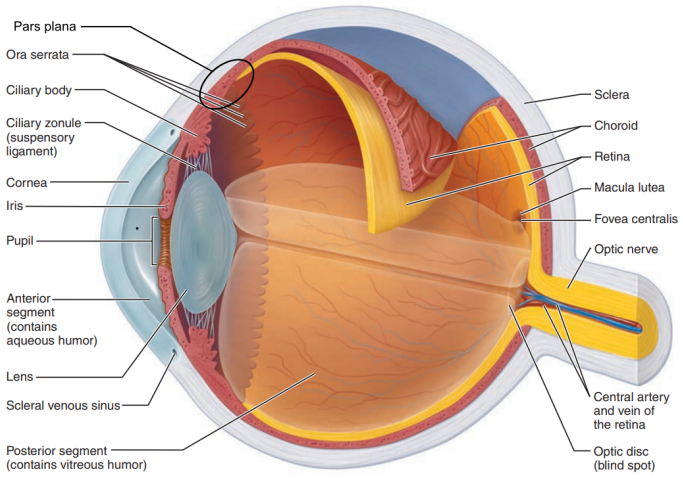

Figure 1: *Anatomy of the human eye [2].*

1.2 Problem Definition

Throughout the years, pars plana vitrectomies improved a lot, increasing gauge sizes (i.e., smaller needle diameter) and going from perpendicular to oblique incisions. These enhancements result in an improved seal of the incision wound that remains after the surgery. Although progress has been made, complications following a vitrectomy caused by insufficient self-sealing of the wound still occurs. Hypotony, defined as an intraocular pressure (IOP) of $5\ mmHg$ or less, can be developed after a vitrectomy. Bamonte *et al.* [5] conducted a study on 122 25-gauge vitrectomies where the incisions are created in an oblique fashion. They found 13.1% cases of hypotony one day after the operation. Not only is it important to prevent fluid from escaping the eye, bacteria entering the eye must be prevented as well. Endophthalmitis, an infection of the eye, is found at 0.11% of 25-gauge vitrectomies [6]. While this number seems small, prevention is of great concern since it can lead to loss of vision or even loss of the eye [7]. Both hypotony and endophthalmitis can be reduced through improved wound sealing. One method to improve the sealing is by improving the incision architecture (i.e., the number of incision planes that are used to construct the wound) through the sclera. Instead of penetrating the sclera in a straight line (uni-planar), one can choose to make a bi- or tri-planar incision. These different types of incisions can be seen in Fig. 3. It can be argued that such incision architectures provide better sealing [8], [9]. Mahajan *et al.* [8] conducted a study in which they performed 23-gauge tri-planar sclerotomies on fresh human donor eyes. They found a low incidence of postoperative day 1 hypotony, only being 1.7% instead of the previously mentioned 13.1%. Mahajan *et al.* [8] do state that better sealing does not necessary mean better wound closure. Next to this, due to their experimental method (that includes resection of the overlying conjunctiva and Tenon capsule), they were able to perform a tri-planar incision with great precision. Unfortunately, such precision is not achievable in other conditions. This is shown in the study of Singh *et al.* [10], they let surgeons perform 25-gauge oblique incisions. While surgeon performed the cuts with the same insertion technique, great inconsistencies were

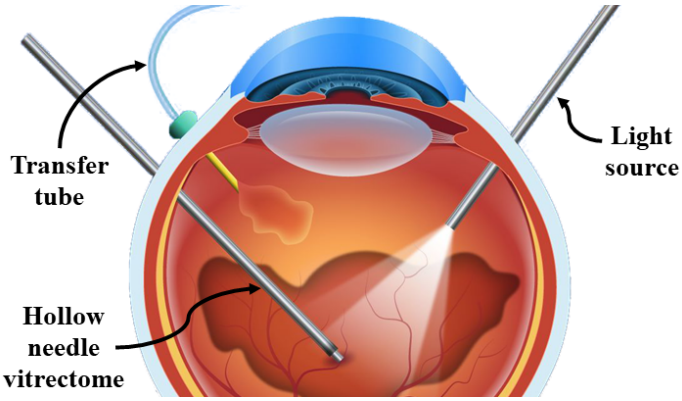

Figure 2: *Cross section of the human eye during a vitrectomy. Showing the needle of the vitrectome, the light source and the transfer-tube containing the substitute of the vitreous humor (i.e., saline solution) [4].*

found. After examination of the cuts, between 45% and 67% of those "oblique" were actually accidental bi-planar cuts. It shows that more plains create better sealing, however, the execution of the incisions remain a challenge.

1.3 Goal of the research

The goal of this study is to: **develop and verify a surgical instrument that can consistently create the most effective self-sealing scleral incisions**. As mentioned before, the incision architecture affects the self sealing properties. In order to develop a tool that has the best sealing properties, one must gain more insight into the different incision architectures. Since there is little research done that directly compares the self sealing performance of different types of scleral incisions, an experiment is designed that fills this knowledge gap. Once determined what type of architecture is most effective, an instrument is designed that must perform this specific type of incisions consistently.

1.4 Layout of the report

In this report, a step-by-step process that begins with problem definition and ends with the verification of a final design is presented. First, as seen previously, Section 1 presented an introduction to eye surgeries and the complication found in vitrectomies. Section 2 brings a more in depth understanding of the state-of-the-art in vitrectomies, introduces methods to improve self sealing incisions and different possible incision architectures are shown. Section 3 shows an experiment that investigates the self sealing properties of the different types of incision architectures. In Section 4, the analysis is translated in a set of requirements for the development of an instrument capable of creating the most effective self sealing scleral incisions. Section 5 describes the verification process of the new design to validate whether the requirements are met and to measure its performance. In Section 6 and Section 7 a discussion and a conclusion of this report is found.

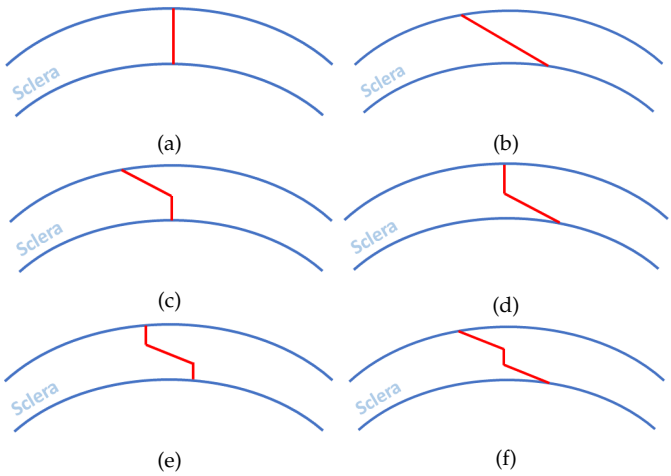

Figure 3: *Marked in red, the incision architectures penetrating the sclera. (a) Perpendicular uni-planar incision architecture. (b) Oblique uni-planar incision architecture. (c) Bi-planar incision architecture 1. (d) Bi-planar incision architecture 2. (e) Tri-planar incision architecture 1. (f) Tri-planar incision architecture 2.*

2 Analysis of Sclerotomy

2.1 Anatomy of the eye

The eyeball consist of three layers: the fibrous, vascular and inner layer. The eye is filled with a clear gel called the vitreous humor. The lens, responsible for focusing the light, divides the eye into two segments, the anterior and the posterior segment. The anterior segments contains the aqueous humor and the posterior segment is filled with the vitreous humor. The fluids help to transmit light in the eye and their pressure maintain the shape of the eye. Fig. 1 displays the terms used in this section to describe the anatomy of the eye.

Fibrous layer The outer layer of the eyeball, the fibrous layer, consists out of dense avascular connective tissue. This layer is divided into two parts: the sclera and the cornea. The sclera is found at the posterior side the eye. It makes up the largest part of the fibrous layer which can be identified on the outside as the white of the eye. The tendon like characteristic of the sclera protects and shapes the eyeball. The cornea is situated on the anterior part of the eye. This transparent layer allow light to enter into the eye.

Vascular layer The middle layer of the eyeball is named the vascular layer. This layer has three regions, It starts as the choroid at the posterior side of the eye. It then becomes the ciliary body and finally, most anterior, the iris is found. The choroid is responsible for more than 80% of the vascular layer and is found at the posterior part of the eye [2]. All of the eye's layers are nourished by its blood vessels. Its brown pigment aid in the absorption of light, since it reduces light from reflecting in the eye. The ciliary body consists out of smooth muscles bundles which control the shape of the lens. The iris is the colored part of the eye that lies between the cornea and the lens. The shape of the iris determines the size of the pupil, thereby controlling the amount of light entering the eye.

Inner layer The inner layer of the eye is the retina. The retina consist of two layers: a neural layer and a pigmented layer. The pigmented layer lies against the inside of the choroid. Just like the choroid, it helps to absorb light in the eye by preventing it from scattering. The actual "seeing" is done by the photoreceptors of the neural layer. The neural layer lies on top of the pigmented layer and consist out of rods and cones. The rods are responsible for peripheral and low light vision. Compared to the cones, rods are far more sensitive to light. However, opposite to cones, rods cannot provide sharp or color vision. At the centre of the retina, a highly pigmented section called the macula lutea is found. The macula contains a pit called the fovea centralis. Here you find closely packed cones. The light focusing on this point provide sharp images. The nerves transmitting the information from the photoreceptors to the brain exit through the optic disc. The optic disc is also called the blind spot, since there are no photoreceptors at this location.

Internal chambers and fluids The lens is the barrier between the posterior and anterior fluid chamber of the eye. The posterior fluid chamber is the biggest volume of the eye, taking up around 65% ($4,5\ ml$) of the total volume. It is

filled with a clear gel called the vitreous humor. Its function is to transmit light, to support the posterior surface of the lens, to hold the neural layer of the retina firmly against the pigmented layer and to contribute to the intraocular pressure [2]. The anterior fluid chamber is filled with a clear fluid called the aqueous humor. Contrary to the vitreous humor, the aqueous humor continually renews itself.

Lens The lens is a flexible structure that is responsible for the light to be correctly focused on the retina. The ciliary muscles are able to pull on the lens, changing the lens from a rounded to a more flat shape, hereby changing its point of focus.

2.2 Vitrectomy

Unfortunately, the eye does not always function as desired, resulting in the need for medical care. Treatment of certain eye conditions such as Retinal Detachment, Macular pucker or Macular holes ask for the removal of the vitreous humor [1]. The removal of the vitreous humor is done in a vitrectomy. In this procedure, a hollow needle is inserted through the sclera, ending in the posterior fluid chamber. This needle is able to cut the gel-like structure of the vitreous humor into smaller fragments in order to extract it through the cavity of the needle. Cutting of the vitreous humor is required for the attached vitreous humor to be cut loose from the retina, preventing the vitreous humor to pull on the retina. Additionally, it ensures for a more constant flow of the vitreous humor through the needle. At the end of the procedure, the removed vitreous humor is replaced with a saline solution to maintain the desired intraocular pressure. During a vitrectomy, three instruments are inserted through the sclera into the eye: the vitrectome, responsible for the suction and cutting of the vitreous humor, a light source and a transfer tube that fills the eye with the saline solution. The instrument setup found in vitrectomy are shown Fig. 2.

2.3 Current cannula placement method

All of the instruments enter the eye through a cannula that is placed in the wall of the sclera. This passageway can be seen as a tunnel through which the instruments move. A popular way to create this passage is by means of a 'one-step trocar-cannula system'. This approach enables the surgeon to create an incision wound and position the cannula during a single operation. Such trocar cannula systems are developed by D.O.R.C. (Dutch Ophthalmic Research Center). Fig. 4a shows the complete trocar cannula system that contains scleral markers on one side of the pen-shaped device and on the other side a trocar knife over which the cannula is placed. Fig. 4b shows a cannula that is placed in the eye. On one side of the pen shaped device, scleral markers are found, on the other side a trocar knife over which the cannula is placed. The cannulas are inserted at the "pars plana", a specific location of the eye which is encircled in Fig. 1. At this location few vital structures are found, minimizing damage done to the eye during the puncture. The procedure placing the cannula is manually done by the surgeon and goes as follows:

1) The scleral markers at the back of the device are pressed against the sclera at the position of the pars plana, leaving small dents in the surface. These dents provide a reference for the trocar knife to enter.
2) The trocar knife is inserted in an oblique fashion, meaning that the knife enters the sclera with an angle of 60°relative to a perpendicular incision. The eye is stabilized using a forceps on the surface of the eye.
3) The knife is pushed through until the complete knife, together with the shaft of the cannula, has penetrated the sclera. The rim of the cannula act as a natural stop.
4) The trocar knife is extracted while the cannula is held into place by clamping the rim of the cannula with a forceps. This causes the cannula to stay in the wall of the sclera.
5) This process is repeated until the desired amount of cannulas are placed.
6) At the end of the intervention, the cannulas will be removed. Forceps are used to pull on the rim of the trocar, extracting them out of the wall of sclera.

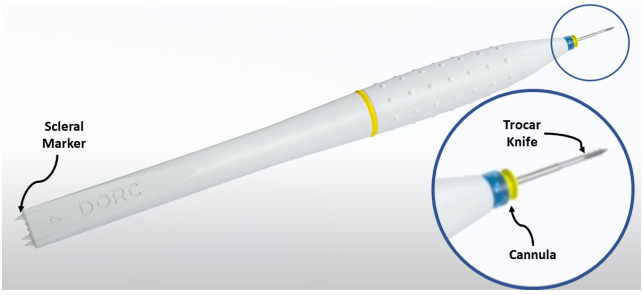

(a)

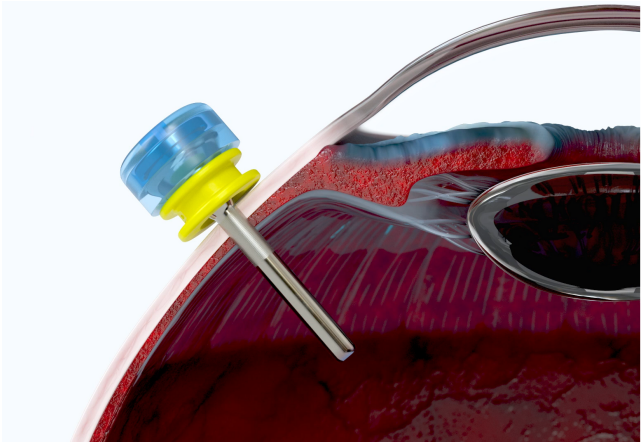

(b)

Figure 4: *(a) Trocar cannula system by D.O.R.C. (Dutch ophthalmic Research Center) [11]. The cannula is placed over the trocar knife. (b) Installed cannula by D.O.R.C. (Dutch ophthalmic Research Center) [11]. The tunnel in grey, the rim in yellow and the valve in blue.*

It is worth noting that using the one-step trocar-cannula system is the most commonly used technique for cannula placement. Other techniques require two steps in order to position the cannula. In the first step an incision is made using a separate stiletto blade. Then, a blunt trocar that guides

the cannula is inserted in the previously made incision [12]. Due to the ease of use of the one-step method, it is the most commonly used technique.

2.4 Improvement to gain better sealing

After the removal of the cannula, it is important to seal the wound that is created by the incision. As mentioned in Section 1, insufficient wound sealing can lead to the development of hypotony and endophthalmitis. Currently, there are certain steps that can be incorporated into the surgical procedure to improve the sealing. The surgeon can choose to suture the wound, or apply a tamponade (i.e., a "plug") into the eye. This tamponade agents can be in the form of a gas or a silicone oil. The tamponade is inserted into the cavity of the eye to provide extra surface tension that helps to seal retinal breaks [13], [14]. Alongside the requirement for additional operations by the surgeon, related complications may arise. The use of sutures may result in complications such as irritations and scleral pigmentary changes, whereas the placement of a tamponade can cause elevated IOP and subretinal migration of the tamponade substance [15] [16] [17]. Therefore, the preference is to make these additional steps redundant due to the benefits of improved scleral incisions. These improvements can be in the form of larger gauge sizes (i.e., smaller knife diameters) or an improved incision architecture. Gauge sizes are constantly increasing, starting from a 17 gauge vitrectomy in 1972 to the present day 27 gauge vitrectomies [18]. Besides decreasing cases of hypotony and endophthalmitis, advantages of small gauge vitrectomy is that you will find less traumatic wound construction and closure and less discomfort by the patient during and after the operation [18]. Inevitably, increasing the needle gauge (i.e., decreasing the needle diameter) brings along challenges. Reducing the needle diameter results in a decrease in shaft stiffness, which in turn can cause control issues due to overflexibility [19]. Additionally, the fluid flow through the needle will experience greater resistance due to the smaller radius of the needle's lumen, and manufacturing of the vitrectome will become more challenging. Another method to change the sealing characteristics is to experiment with the architecture of the incision made by the trocar knife. Multiple surgeons mention the influence and importance of the incision architecture. They state that improvements lead to better sealing and reduce postoperative complications [9]. The advantage of an improved incision architecture is that it enhances the sealing process, regardless of the gauge size. In this paper the focus will be on improving sealing by improving the incision architecture of the trocar knife.

2.5 Incision Architectures

2.5.1 Uni-planar

There are multiple ways to create the passage through the sclera. From perpendicular to oblique incisions and from uni- to tri-planar incisions, each with their own characteristics. A uni-planar incision is defined as a straight incision through the sclera. There are multiple ways the trocar knife can penetrate the sclera in a uni-planar fashion; perpendicular to the sclera or as an oblique incision, as seen in Fig. 3a and Fig. 3b respectively. Over the years surgeons moved from a perpendicular to the currently used oblique incision. Studies show the oblique incision technique to be superior to the perpendicular incisions [20], [21]. There are two reasons why an oblique incision seals better compared to a perpendicular incision. First, the greater length of an oblique incision creates more resistance for the intra ocular fluids to escape, and, due to the greater length there is more potential for the two separated layers to bond. Second, the IOP creates a certain tension in the wall of the eye that opens the hole of a perpendicular incision, while it shuts an oblique incision. Due to the IOP, a tangential stress and a radial stress is found in the wall of the eye. The tangential stress components will widen the perpendicular hole. The radial stresses push the two overlying surfaces together. While oblique incisions have better sealing properties, postoperative complications such as hypotony and endophthalmitis still occur, with rates of 13.2% and 0.11% respectively [5], [6].

2.5.2 Multi-planar

A potential method to create a better sealing incision is by introducing multiple planes in the incision. These multi planar incision can be in the form of a bi- or tri-planar incision. Fig. 3c and Fig. 3d show two forms of bi-planar incisions. Such incisions are created by rotating the tip of the knife when it is halfway through the wall of the sclera. A tri-planar incision is created by rotating the tip of the knife twice inside the sclera, as seen in Fig. 3e and Fig. 3f. The shape of these multi planar incision create extra resistance for the fluids to escape. However, due to the small wall thickness of the sclera (i.e., $0.43 \pm 14\ mm$ on average [22]), such incisions are very hard to create manually with the current trocar systems [23]. The study of Singh *et al*. [10] shows that similar insertion methods lead to very inconsistent incision architectures inside the scleral wall. In their study, surgeons intended to create a 25 gauge oblique incision. The aim was to insert the trocar knife in an oblique fashion through the sclera until the tip had fully penetrated, to then turn the knife perpendicular to the sclera and finish the incision. However, controlling the depth of the trocar knife, therefore controlling the location of the rotation, posed a significant challenge. The optical coherence tomography analysis revealed that only a fraction, ranging from 33% to 55%, of the incisions matched the intended oblique incisions, while the rest were bi-planar incisions. This study shows that it is difficult for the surgeon to control the position of the tip of the knife inside of the sclera. Another factor to consider is the damage done to the sclera due to the movements of the needle. By rotating the tip of the needle inside the sclera tissue, the internal wound enlarges. After the surgery there might be less effective surface that reattaches to each other and seals the wound [24]. Currently, there are no devices used by surgeons that are designed to specifically make a multi-planar incision. This is confirmed by a study conducted by Koot [9] on trocar incision mechanisms and needle steering mechanisms. This study, that included a patent review, found only one steerable needle mechanism. However, this mechanism made use of a flexible needle. Other results solely focused on the linear driving mechanism. After his study, Koot [9] designed and build a steerable trocar incision mechanism, his device will be used as a design starting point in the following Section.

3 Verification of Self Sealing Architectures

3.1 Goal of the experiment

In addition to the results found in the state-of-the-art, a practical analysis is performed to gain more insight into the effects the different incision architecture have on the sealing properties. This experiment will examine the following hypothesis: *"more planes in the incision leads to better sealing"*. A test is performed that would simulate a situation similar to a scleral incision. In this test, three different types of incisions (oblique, bi-planar or tri-planar) are made through a slab of silicone after which the level of leakage for each incision is determined.

3.2 Experimental Setup

The experimental setup consist out of two components; a trocar knife carrying incision device for creating desired incision architectures and a silicone-based human-sclera-mimicking phantom. The experiment is designed so that it allows to test the leakage levels of the different incisions in a systematic fashion. This experiment allows each type of incision to be repeated multiple times, after which the quality of each incision and the degree of sealing can be examined.

This experiment cannot be done on a real human eyes. This means that an alternative, that has similar characteristics as the human eye, needs to be used. The device substituting the human eye is seen in Fig. 5a. For this study, a 0.5 mm thick slab of silicone (www.rubbermagazijn.nl) with a 60 shore A hardness is utilized, which has similar thickness and mechanical properties as the human sclera [9], making it a fitting substitute material. Using M4 bolts, the silicon slab is clamped between a "Holder" and a "Lid", as is shown in Fig: 5b. The surface of the Holder, on which the silicon slab is placed, has a radius similar to those of the human eye (i.e., 12.5 mm). Since the incision architectures are in 2D, a curvature along 1 axis will suffice to take account for the shape of an eye. A fluid chamber is located underneath the silicon slab, as shown in Fig. 5b, which can be pressurized to a desired value. The mechanism used for the insertion of the trocar knife is attached on the Holder which can be seen in Fig. 5c. This mechanism has 2 Degrees Of Freedom (DOF's), a linear stage and one rotational axis. By rotating the "insertion screw" at the top of device the needle lowers. An axle is attached to the the silicone Holder over which the incision device can rotate; the "rotation stage". More information about the design and characteristics of incision device is found in the report of Koot [9]. The insertion mechanism is attached in such a way that the rotational axis lies at the same height as the surface of the silicon slab. A 27 gauge needle (i.e., the substitute to the trocar knife) is attached to the insertion mechanism. The needle used in this setup is manually sharpened by DEMO (Electronic and Mechanical Support Division, Delft). The blades of the trocar knifes, as seen in Fig: 4a, show two clear flat sides, while the versions made by DEMO are not as symmetric and have a more conic tip. Therefore, the variants made by DEMO are labeled as "needles" rather than "knifes". The needle is inserted through a hole and clamped by tightening an M3 bolt. This allows the needle to be detached and replaced if needed. The fluid chamber is filled with water and a pressure of 15 $mmHg$, equal to the pressure in the human eye, is applied. This is done by connecting one side of a tube to the fluid chamber and the other side of the tube to an elevated water reservoir. The water reservoir is elevated to a height of 20 cm equivalent to the desired pressure (i.e., 15 $mmHg$). To assist this experiment a digital microscope

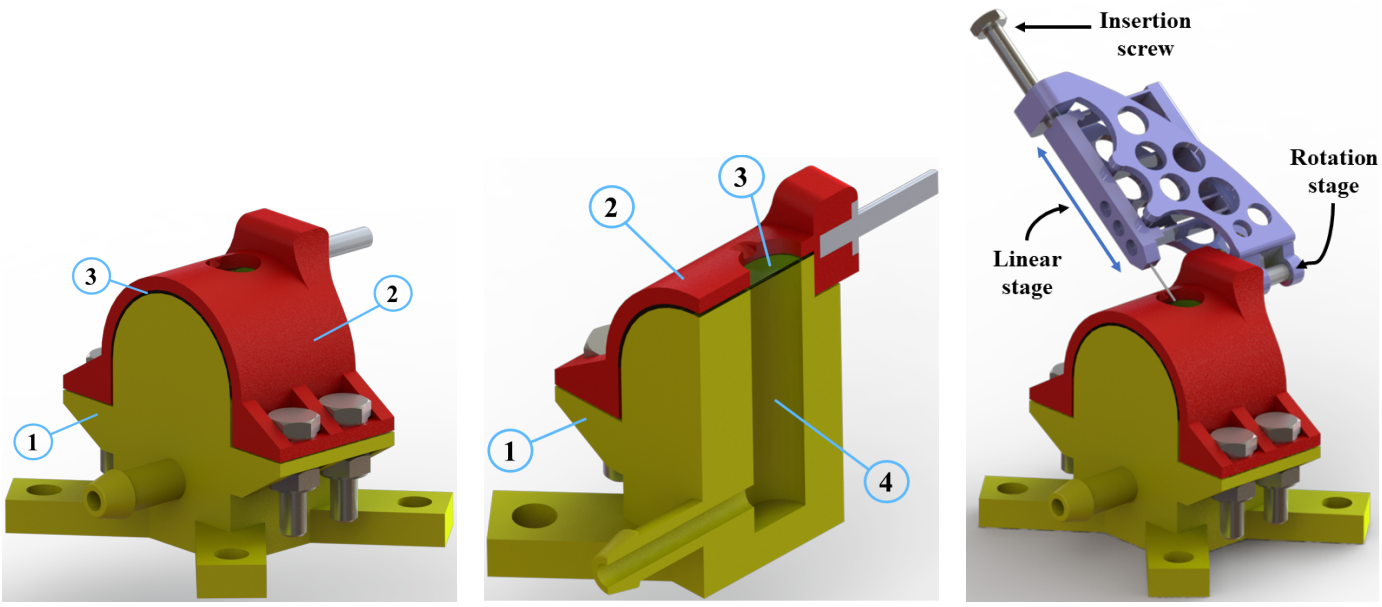

(a) (b) (c)

Figure 5: *Renders of the test components. 1: The base of the Holder, 2: The Lid of the Holder, 3: The silicone slab clamped between the Lid and the Holder, 4: The fluid chamber. (a) Human-sclera-mimicking phantom. (b) Section view of the human-sclera-mimicking phantom. (c) Multi-planar incision device attached to the human-sclera-mimicking phantom.*

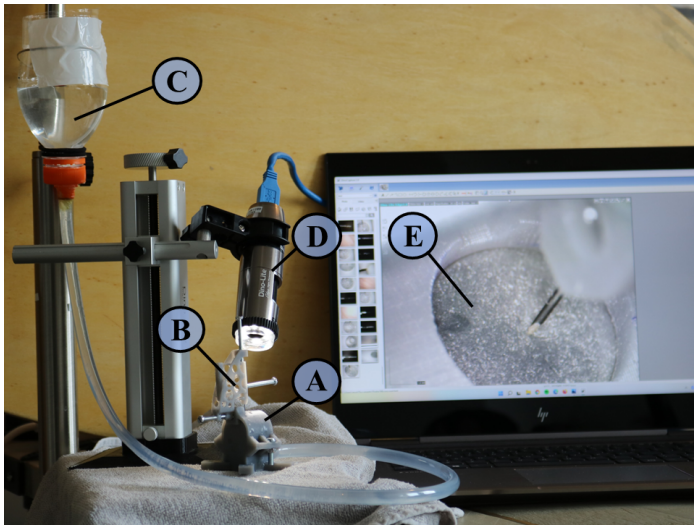

Figure 6: *Complete test setup showing the Holder (A), insertion device (B), water reservoir (C), Dinolite edge digital microscope (D) and a laptop running the DinoCapture software (E).*

(Dinolite edge 3.0) is used to aid during the insertion and used in measuring the amount of leakage. The complete setup can be seen in Fig. 6.

3.3 Procedure

The testing procedure for evaluating the sealing performance of the different incisions is described below:

1) Place a 20 x 20 mm piece of silicon in between Lid and the Holder (do not tighten yet).
2) Fill the water reservoir.
3) Let the water flow all the way through the system, let is pass the silicone slab until all air bubbles disappear.
4) Tighten the Lid of the Holder, making it air tight.
5) Fill the water reservoir to the desired height (i.e., 20 cm).
6) Make the desired incision using the incision device and the digital microscope.
7) Extract the needle.
8) Place the microscope in a vertical line above the sample and measure the diameter of the droplet, using the software corresponding to the microscope (DinoCapture 2.0). Fig. 7 shows an example of a measurement.
9) Remove the slab of silicone and remove the excess silicone on either side of the incision.
10) Determine the quality of the incision by reviewing from the side using the microscope.

For each incision-type, this procedure is repeated until ten incisions are made with a satisfactory architecture (i.e., the number of planes in the incision equal those of the desired architecture). Step 6 requires creating the desired incision, which will be one of four different incision architectures. The different type of incision architectures are shown in Fig. 8 and are made using the following steps:

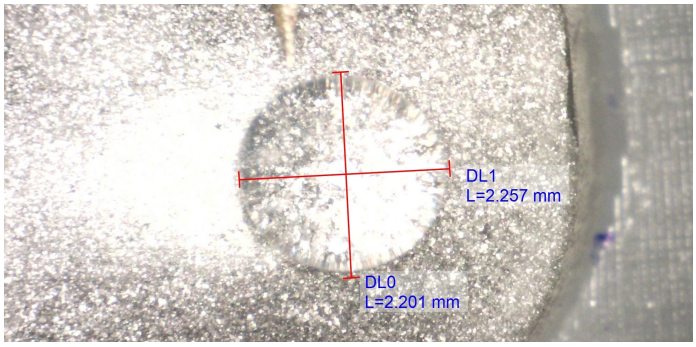

Figure 7: *Example of a droplet measurement.*

Oblique:

1) Place the needle at an angle of $80°$ from vertical.
2) Lower the knife until it touches the silicone surface.
3) Gently rotate the screw so that the needle will penetrate the silicone.
4) Insert the needle up to 7 mm.

Bi-planar:

1) Place the needle at an angle of $80°$ from vertical.
2) Lower the needle until it touches the silicone surface.
3) 1.25 revolutions on the insertion screw (i.e., 0.625 mm), creating an oblique incision in the silicone.
4) Return the device to $0°$.
5) Insert the needle up to 7 mm.

Tri-planar 1:

1) Place the needle at an angle of $0°$ from vertical.
2) Lower the needle until it touches the silicone surface.
3) 0.4 revolutions on the insertion screw (i.e., 0.2 mm).
4) Rotate the insertion mechanism $80°$ from vertical.
5) 1.25 revolutions of the insertion screw (i.e., 0.625 mm).
6) Returning the device to $0°$.
7) Insert the needle up to 7 mm.

Tri-planar 2:

1) Place the needle at an angle of $80°$ from vertical.
2) Lower the needle until it touches the silicone surface.
3) 1.25 revolutions on the insertion screw (i.e., 0.625 mm), creating an oblique incision in the silicone.
4) Returning the device to $0°$.
5) 0.5 revolutions on the insertion screw (i.e., 0.25 mm). Rotate the device back to $80°$.
6) Insert the needle up to 7 mm.

As can be seen in Fig. 8 there are two ways in which the tri-planar incision is performed. Due to the complicated nature of the tri-planar incisions, a test is performed in advance to test the feasibility of both tri-planar incisions. The feasibility experiment follows the same procedure as the evaluation of sealing performance, with the exception that a slab of silicone is supported by a piece of stiff paper rather than relying on the water pressure from bellow. In

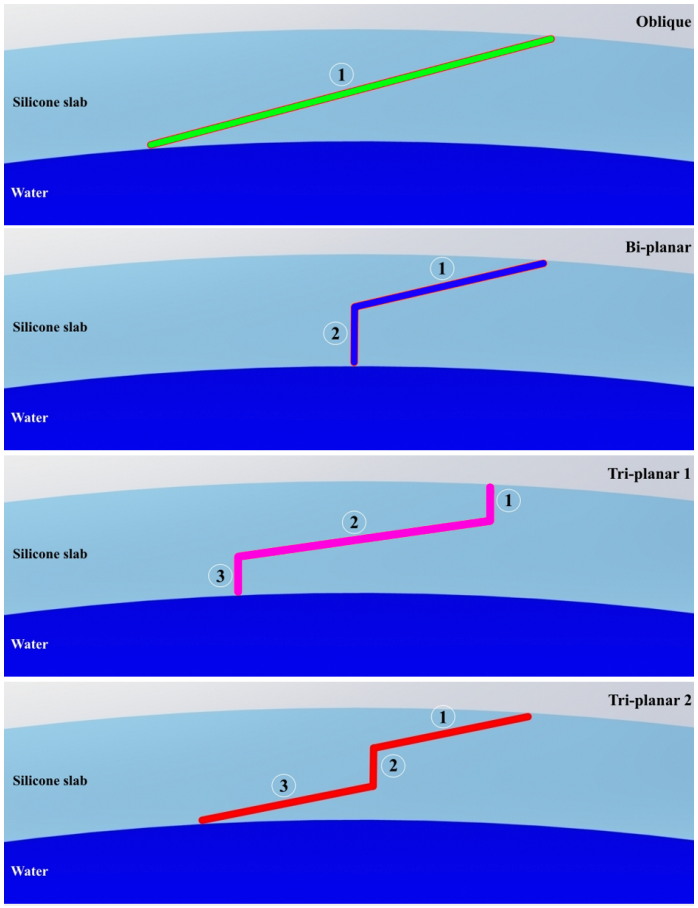

Figure 8: *The colored lines represent the incision architectures. The different types of architectures are: oblique, bi-planar and two tri-planar incisions.*

this setup, underneath the slab of silicone, a second slab of silicone and a similarly shaped piece of stiff paper (i.e., 300 g/m^2) is placed and clamped between the Lid and the Holder. No water is found in the fluid chamber. This setup creates much more stiffness in the radial direction which will "eliminate" one DOF (in the radial direction), making the incision more controlled.

3.4 Experimental Variables

In this experiment, the independent variable is the incision architecture, which is either an oblique incision, a bi-planar incision, or one of two tri-planar incisions. In this thesis, the dependent variables are the amount of leakage, which is determined by measuring the diameter of the droplet present on the silicon surface post-incision and the number of trials to complete ten successful incisions.

3.5 Results

As mentioned before, the experiment is repeated until ten satisfactory incisions were made for each type of incision. The incisions are labeled as failed if the direction and/or the numbers of planes are not equal to those shown in Fig. 8. Appendix A contains all of the images depicting the individual incisions.

3.5.1 *Oblique incision*

The architecture of the first ten incisions were all adequate. Fig. 9a shows an oblique incision. The uncomplicated nature of the oblique incision resulted in a 100% success rate. Examination of the incision architectures under the microscope revealed a distinct similarity in shape. Appendix A displays the resemblance in incision architectures, and Fig. 11 demonstrates the proximity of droplet sizes (in green), affirming this observation. The average droplet size for the oblique incisions were $2.00\ mm$.

3.5.2 *Bi-Planar incision*

The bi-planar incisions were relatively easy to perform, 11 incisions were required to obtain the ten adequate incisions. Fig. 9b shows a bi-planar incision, Fig. 11 shows the droplet sizes (in blue) of the ten incisions. Together they have an average droplet size of $0.727\ mm$. Interesting to note is that four incisions did not produce any droplet on the silicone surface when the needle was extracted.

3.5.3 *Tri-Planar incision*

As previously mentioned, before conducting the evaluation on sealing performance of tri-planar incisions, an experiment is performed that shows the feasibility of a tri-planar incision in the silicone slab. Through the use of a stiff piece of paper, the radial stiffness produced allowed for a more precise and controlled needle penetration into the silicone. Therefore, for both tri-planar incisions, one attempt was required to create the tri-planar incision. Fig.10 shows the two attempts creating both tri-planar incisions. The results demonstrate that, by using this incision device, tri-planar incisions in silicone can be performed. Next, the paper support is removed and exchanged for water pressure, creating a more realistic but flexible setup. The first tri-planar incision starts with a perpendicular incision on the silicon surface. During the process of this radial incision, the silicone will be pushed inwards. The magnitude of flexing of the silicone slab, therefore the incision into the silicon, was inconsistent. This made it very hard to judge the depth of the first plane. Due to the lack of consistency, 23 attempts were necessary to achieve ten tri-planar incisions. Fig. 9c shows a tri-planar incision, Fig. 11 shows the droplet sizes (in purple) of the ten incisions. Together they have an average droplet size of $1.04\ mm$. The second type of tri-planar incision starts with an oblique incision into the silicon. While the incisions of the first plane were consistent, the incision creating the second plane in the radial direction was found to still be inconsistent. This meant that 16 incisions were required to obtain ten tri-planar incisions. Fig. 9d shows a tri-planar incision, Fig. 11 shows the droplet sizes (in red) of the ten incisions. Together they have an average droplet size of $2.02\ mm$. The experiments show that more planes cause for a more challenging incision. Furthermore, this experiment demonstrates that an increase in the number of planes does not necessarily lead to improved sealing, as is summarized in Table 1.

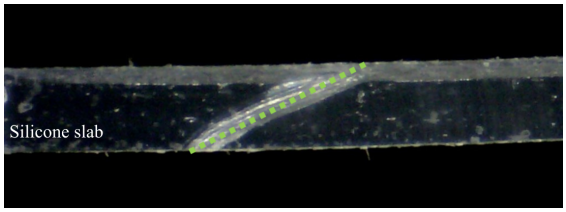

(a)

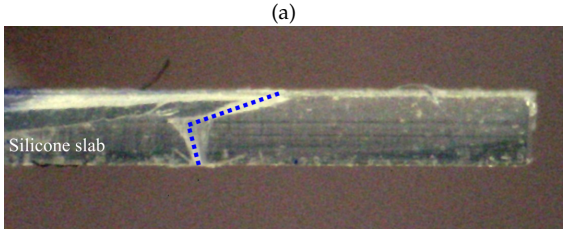

(b)

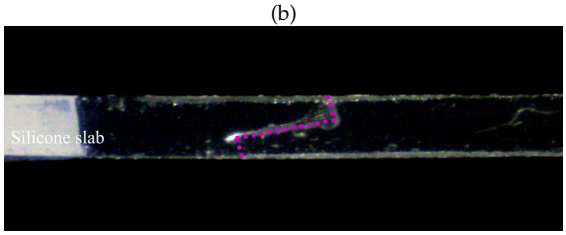

(c)

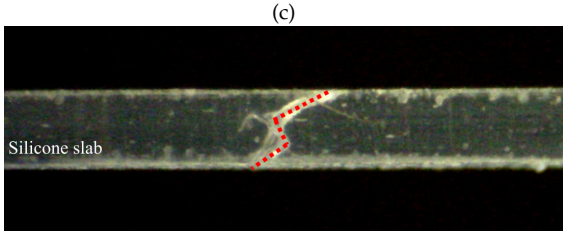

(d)

Figure 9: *Four types of incision architectures penetrating the* 0.5 *mm thick silicone slabs. (a) Side view of an oblique incision. (b) Side view of a bi-planar incision. (c) Side view of a tri-planar 1 incision. (d) Side view of a tri-planar 2 incision.*

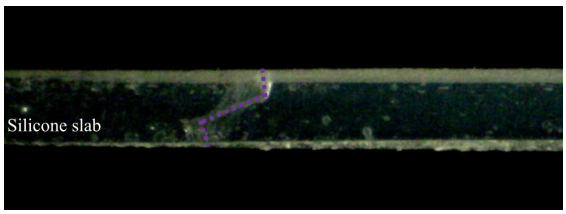

(a)

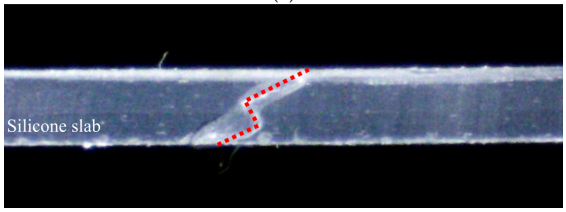

(b)

Figure 10: *Two "feasibility incisions". The two tri-planar incision in this figure were facilitated by using support material to add stiffness in the radial direction, hereby proving the feasibility of the incisions. (a) Side view of an tri-planar 1 incision. (b) Side view of an tri-planar 2 incision.*

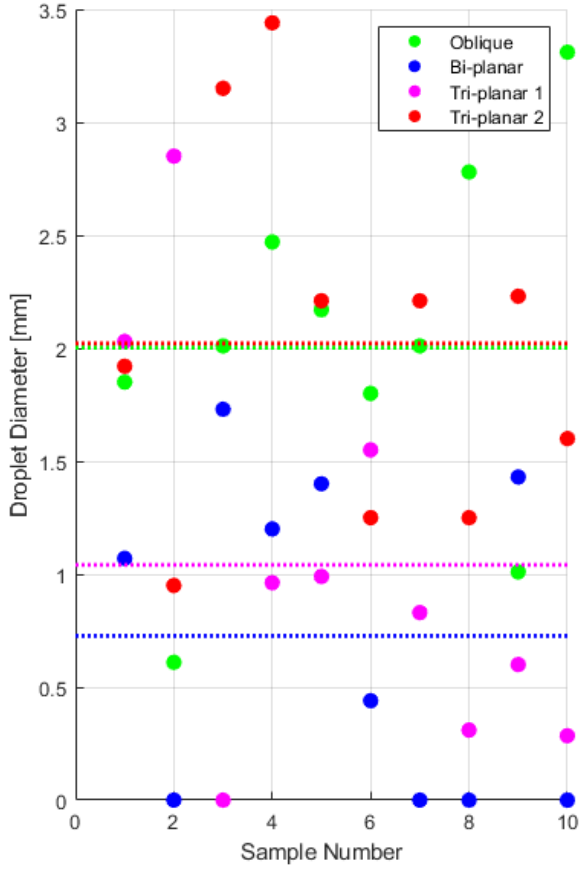

Figure 11: *Measured droplet diameters that correspond with the incisions. The dashed lines represent the average droplet diameter of the ten satisfactory incisions.*

3.6 Interpretation of the Results

3.6.1 Oblique plane vs perpendicular plane

This test showed that the incisions perpendicular to the silicone surface showed more inconsistency compared to the incisions with an oblique plane. This difference became clear comparing the two types of tri-planar incisions. The second type of tri-planar incision starts with an oblique incision into the silicon. This means that, instead of a normal force, the needle predominantly exerts a shear force on the silicone surface. This setup provides more stiffness in the tangential direction than the normal direction. This results in less movement of the silicon during an oblique incision, creating a more predictable and consistent incision. Comparing the tri-planar incision that starts with a perpendicular incision to the one that start with an oblique incision, the former was harder to perform. This is can be seen in the results. In the first tri-planar incision, 23 attempt were required to obtain the ten passable incisions, while for the second tri-planar incision 16 attempts sufficed. Besides the difference in difficulty of the first incision-plane, a learning curve could have affected the difference in the amount of attempts of the two tri-planar incisions. In the experiment all the 23 incisions of the first tri-planar incision were performed consecutively

Incision Architecture	Number of Attempts	Average Droplet Size [mm]
Oblique	10	2.00
Bi-planar	11	0.727
Tri-planar 1	23	1.04
Tri-planar 2	16	2.02

Table 1: *Table showing the various types of incision architectures, their corresponding average droplet size, and the number of attempts required to obtain ten satisfactory incisions.*

to then perform the second type of tri-planar incision. This means that the experience gathered in using the test setup could have results in a better 'hit-rate' during the second tri-planar incision. In future test one should mix the sequence of the different types of incisions. The preferred method for achieving a controlled incision, as demonstrated in this experiment, is to begin with an oblique plane. Therefore, bi-planar incision 2, as shown in Fig. 3 was not considered in the experiment due to its perpendicular entry plane.

3.6.2 Best vs worst sealing incision

Judging the best sealing incision solely on the average droplet size, a bi-planar incision performs best. This means that the hypothesis stated, that more length and planes in the architecture leads to a better sealing, is false. A reason for this is that in the process of creating more planes, more movement by the needle in the silicone is found. This means that there is more damage done to the silicone, creating a wider hole through which the water can escape. The incision device has a fixed rotation axis that lies at the height of the silicone surface. Damage to the silicon may be exacerbated by the use of a fixed rotation axis. To minimize damage in the silicon, the needle should pivot around the tip of the needle during the change of the direction of the plane. Therefore, for a tri-planar incision, the system needs to have points of rotation at two different locations. In this setup, the needle does not pivot around the tip of the needle, but around an axis located at the height of the silicone surface. Creating more planes may cause the silicone to tear, leading to a more damaged silicone, resulting in more leakage. The results show that a bi-planar incision has a better sealing than that of the tri-planar incisions. It is not certain if this is the result of the shape of the architecture or as a result of the quality of the incision. Nevertheless, based on the analysis, incisions with a bi-planar architecture hold the greatest potential for consistent self-sealing incisions. Therefore, as a results of this investigation, a bi-planar incision device has been designed.

3.6.3 Test-setup vs reality

While this setup finds many similarities with an intervention on a human eye, the differences need to be recognized. For example, the needle used in this setup is manually sharpened by DEMO in Delft. The needles will not be as sharp as the single use trocar knifes used in the operation room. Reviewing the needles used in this test, they showed some asymmetry at the sharp end. Next to this, the elastic characteristics of an human eye is different than the silicone substitute. While the silicone used matches the modulus of the sclera tissue as close as possible, it does deviate from the less homogeneous nonlinear scleral tissue, which contains elastic fibers [25], [26]. This all means that the interaction between the needle and the silicone might be different compared to the interaction of a real trocar knife into the sclera tissue. The fluid used in this setup varies from the more viscous vitreous humor found in a human eye. The vitreous humour consist out of a fibrillar network filled with 98% water and 2% collagen and hyaluronan [1]. Compared to vitreous humor, the use of water in the test setup increases the likelihood of leakage. When judging the performance of the different incisions made in this test, these differences need to be considered.

4 Design

4.1 Introduction

The experiment done in Section 3 gave insights into three main challenges that are present when creating bi-planar incisions. First, creation of an architecture that precisely follows the prescribed bi-planar path. Second, controlled depth penetration in soft tissue. The knife will only advance through the tissue when the force applied by the surgeon exceeds those of the resistance of the tissue exerted on the knife. This resistance will vary during the course of the incision due to dynamic and static resistance characteristics. In practise, when the knife enters the tissue, it first dents in the surface of the tissue before penetration. Upon breaking the surface by the tip of the knife, the knife experiences a decrease in resistance, enabling it to move through the tissue with less resistance. This causes the tissue to bounce back from its indented position over the blade of the knife. This event leads to uncontrolled depth penetration in the soft tissue. Third, positioning the incision device relative to the eye presents a challenge. During the incision, the eye ball is not fully constraint and able to make small movements when forces are applied. However, maintaining a constant relative position between the incision location and the trocar knife is crucial during the incision process. While these three factors are all critical, this article is mainly focused on the creating of the best self-sealing architecture (i.e., the first challenge); the bi-planar incision. The objective is to develop a functional prototype which complies with the formulated requirements. This concept must repeatedly perform bi-planar incisions at scale. Verification is necessary to assess the conceptual design's working principles and manufacturing method for its ability to execute bi-planar incisions at scale within the set tolerances.

4.2 Design requirements

The design requirements for the Bi-Planar Incision Mechanism are formulated, using a technique as taught by Bob van Vliet (TU Delft), in the following 4 categories; functional requirements, specifications, constraints and performance

criteria. The generated concepts need to meet all the requirements found in the first three categories (functional requirements, specifications and constraints). In the last category (performance criteria) concepts can differentiate from and compete with each other. Table 3 shows an overview of all the design requirements.

4.2.1 Functional requirements

This section presents the functional requirements of the concepts, which define what the design must be able to do.

- **Incision Architecture**:
  In order to define the incision architecture, the thickness of the sclera, into which the architecture is made, needs to be set. Vurgese *et al.* [22] investigated the thickness of multiple regions of the sclera. They found that the thickness around the ora serrata region is $0.43 \pm 0.14\ mm$. This region is most interesting since its closest to the pars plana. However, at this stage it is more valuable to design for a thickness that benefits the testing phase. As previously done, the first tests will be done on a slab of silicone. Since previous tests made use of a $0.50\ mm$ thick silicone, the concepts will be designed for a sclera with a thickness of $0.50\ mm$. Fig. 12 shows in red the bi-planar architecture that must be made by the trocar knife. The values of the parameters of this bi-planar architecture are found in Table 2. Currently, a manual incision is done with the trocar knife at angle that is around $60°$ from the vertical axis. Therefore, the trocar knife of the new device must enters the sclera with an angle of $60°$ from the vertical axis, to then penetrate the sclera for $0.48\ mm$, at this point the tip of the knife reached the middle of the sclera. Then, it turns back to 0 degrees from vertical and continues the penetration with a translation of at least $4\ mm$ to achieve complete placement of the cannula in the sclera, and up to $8\ mm$ to prevent the trocar knife from damaging tissue in the eye. The depth of the first plane is set to the middle of the sclera. This is done to maximize the probability of a bi-planar incision, accounting for the trocar knife to over- or undershoots during the creating of the first plane. It is not realistic for the bi-planar incision to follow the exact path as shown in Fig. 12. Bi-planar incisions that stay within the following range as seen in Variables 1, are considered as successful bi-planar incisions:

Parameter	Value
Bi-planar angle, $\boldsymbol{\alpha}$	$60°$
Height of the rotation point, $\boldsymbol{h}$	$0.25\ mm$
Oblique incision length, $\boldsymbol{o}$	$0.48\ mm$
Vertical incision length, $\boldsymbol{v}$	$0.25\ mm$

Table 2: *Bi-planar architecture parameters.*

$$\begin{aligned} 0.125mm \leq h \leq 0.375mm \\ 50° \leq \alpha \leq 70° \end{aligned} \tag{1}$$

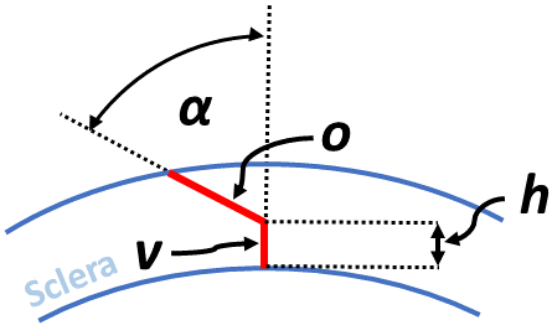

Figure 12: *Bi-planar architecture in red. Bi-planar angle,* $\boldsymbol{\alpha}$*. Height of the rotation point,* $\boldsymbol{h}$*. Oblique incision length,* $\boldsymbol{o}$*. Vertical incision length* $\boldsymbol{v}$*.*

- **Fixed Motion Path**:
  In order to simplify the usability of the device it should only be able to operate in one way. Using the device of Koot [9], an infinite number of architectures can be made. Contrary, this design should only be able to make one pre-defined bi-planar incision.
- **Maximum Incision Time**:
  Currently, the placement of the cannulas is a quick and straight forward procedure which takes around 5 seconds. Using this device, a time limit of 20 seconds to place the cannula is set. This is done to increase the probability of the device being adopted by the surgeons.
- **Manually Operated Handheld Device**:
  The current incision system is relatively simple and inexpensive due to its minimal number of parts and the materials used. Should the new design consist out of many expensive complicated parts, like in a tele surgical system, chances of adaptation is low. Therefore, in this research, only handheld manually operated systems will be investigated.
- **Single Handed Operation**:
  The system should be actuated using one hand. This means the surgeon is able to simultaneously use their other hand for other manipulations, such as stabilizing the eye (as is currently done).
- **Visual Feedback**:
  Since the incision is done manually, the surgeon needs to rely on visual feedback. The surgeon must be able to position the device at the right location. The view of surgeon must not be obstructed by any components that could affect the precision of the incision.
- **Radial Insertion Direction**:
  The incision orientation of the trocar knife relative to the fibers of the tissue should influence the self sealing properties once the trocar knife is removed. One can imagine that if the fibers are separated by the trocar knife instead of being cut, better self sealing properties are found. Unfortunately, contrary to the fibers in the cornea, the collagen fibers in the sclera have an irregular and intermingling pattern [27]. Madanagopalan *et al.* [24] conducted a study to find the best incision orientation in the sclera's

tissue.There are multiple ways to initially position the trocar knife relative to the eye. Fig. 13 shows 4 distinctive orientations the blade is able to enter the eye. Madanagopalan *et al*. [24] studied the self sealing properties of 25 gauge oblique incision in these 4 orientations. Madanagopalan *et al*. [24] makes a distinction between radial and circumferential entry wounds. The incision created using method 1 and 2 in Fig. 13 leave an external circumferential entry wound. Incision 3 and 4 create a radial external linear entry wound. The second way they distinguish the orientation of the incision is by the direction of the intrascleral path, which can be parallel or perpendicular to the limbus (i.e., parallel or perpendicular to the border between the cornea and the sclera). Incision 1 and 4 have an internal incision path that is perpendicular to the limbus, incision 2 and 3 have have an intrascleral path that is parallel to the limbus. Madanagopalan *et al*. found that radial incisions provided best sealing properties due to better mechanical closure of the scleral wound [24]. Parallel incision are preferred over perpendicular incisions, since the direction of perpendicular incisions may cause retinal damage. In the new design an incision will be created that leaves a radial entry wound with an intrascleral path that is parallel to the limbus (number 3 in Fig. 13).

- **Device Support on Eye Surface**:
  As stated previously, this research will not focus on stabilizing the eye with respect to the incision device. This research is focused on systems that support itself onto the surface of the eye. As a result it minimizes the size of the device, increasing its maneuvrability. Appendix B shows a tree with alternatives on how devices can be positioned relative to the eye.
- **Minimum Insertion Force**:
  The system must be able to insert the needle with a minimum force of 0.7 Newton. This is force is required to puncture the sclera using a 27 gauge needle [28].

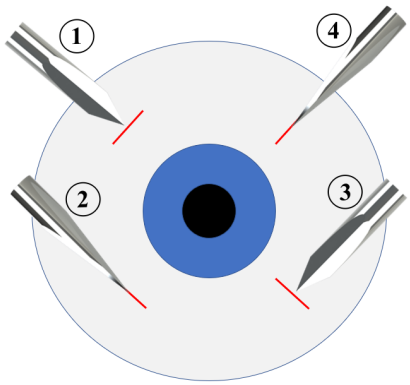

Figure 13: *Four blade penetration orientations. circumferential entry wound (1 & 2). Radial external linear entry wound (3 & 4). Internal incision path perpendicular to the limbus (1 & 4). Internal incision path parallel to the limbus (2 & 3).*

4.2.2 Specifications

This section contains pre-defined specifications that were determined before the design process.

- **Type of Trocar**:
  The smallest trocar knife available needs to be used to minimize the damage done. Currently, the state of the art is a trocar knife that is 27 gauge. This size will be used in the new designs.

4.2.3 Constraints

In this section constraints, limitations are found that are imposed by external factors.

- **Geometric Constraints**:
  The geometric constraints set in this sections are particularly relevant to the final design. The geometric constraint are divided in two categories. Limitations originating from the patient or limitations originating from the surgeon. Geometric limitation caused by surgical instruments found in the operation room (e.g, microscope situated above the patient's head) are not taken into account. Their positions should adjust to the geometry of the incision mechanism.
  - ***Geometric constraint patients:***
    These geometric constraints are set by the physical constraints of the human head. There are two main obstacles around the eye that limit the design freedom, as illustrated in Fig. 14. First, medial to the eye the nose is situated, which is a potential obstacle to the incision mechanism. Besides the nose, the orbit of the eye (i.e., the eye socket) limits the workspace. Fig. 14a shows the position of the eyeball relative to the orbit. Fig. 14c shows the three locations at which the cannulas are places. The location with the most critical geometric constraints is incision location one. The geometric constraint will be sett with respect to this location. The trocar is inserted $1.5\ mm$ nasal from the limbus (i.e., the border between the cornea and the sclera) [29]. The limbus average width is $11.8\ mm$ [30]. Worst case, the trocar is inserted $7.4\ mm$ nasal form the centre of the eye. The width from the centre of the eye towards the nose is lager than $20.0\ mm$ for 95%. [31]. Meaning that, seen from the centre of the cut, the width of the device should stay below $12.6\ mm$. The vertical distance from the center of the eye to the inferior orbital rim is $18.7\ mm$ (95% CI) [31], As is illustrated in Fig.14b. Therefore, the device cannot exceed this distance in this direction during the incision.
  - ***Geometric constraint surgeon:***
    This constraint concerns the maximal size of the handle of the incision mechanism. The maximal grip diameter for 95% of the adults is $43\ mm$. The handle cannot exceed this diameter [32]. The width of a human hand is smaller than $97\ mm$ (without the thumb) for

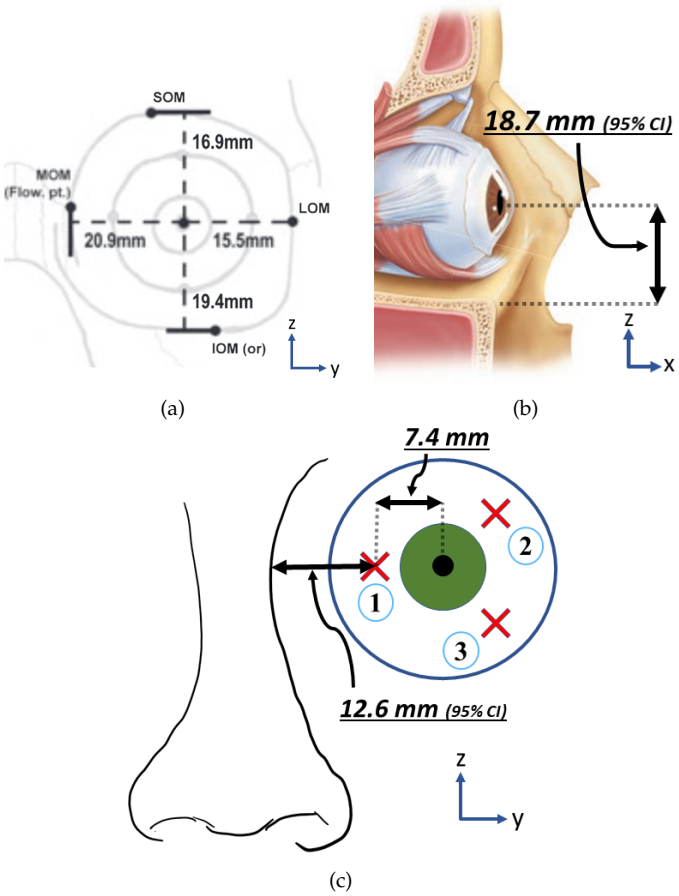

Figure 14: *Most critical geometrical constraints of the patient. (a) Relative position of the eyeball in the orbit. [31]. (b) Vertical distance between incision point 1 and the orbital rim. (c) The three incision locations. Distance from incision location 1 to the nose.*

95% percent of the population between 20-60 years old [33]. The height of the handle cannot exceed this length.

4.2.4 Performance criteria

In this section points are found that judge the performance of each design. These points can be positioned on a scale. As light/stiff/fast as possible are typical performance criteria.

- **Number of Contact Point as Few as Possible:** It is desired to leave as little damage to the eyeball after surgery. Contact points on the surface of the eye may lead to more damaged to the tissue.
- **Cost as Low as Possible:** In order to increase adaptation of the device cost must be as low as possible.
- **Ease of Use:** Since ease of use is a vague criteria that is hard to quantify, it will be divided into separate points.

  - *As few operations/manipulations (with hands) as possible:* The surgeon preferably completes the incision in as few operations as possible. An operation is defined as any change in the directions of motion by the hand. Suppose the surgeon requires to first translate his hand, then a rotation to finish the incision, two operations are made.
  - *Time to complete incision as low as possible:* The time to complete the action is an indicator on the effort it takes to carry out a task.
  - *Time to train the surgeon as short as possible:* One quantity that assesses the ease of use, is to measure the time the surgeon needs to train to perform as desired. This means a level of performance needs to be defined (a certain operation in a certain time within certain margins). These test needs to be done in real life by multiple surgeons.
  - *Task effectiveness as high as possible:* A higher effectiveness suggest an easy to use system. A system with high success rate (i.e., the amount of attempts to perform an adequate incision) should be preferred.

The last three point can only be measured with physical models, not in the concept generation phase. Unfortunately, in this study, only one working physical model will be produced. Therefore, the concepts will not be evaluated on these points.

Functional Requirements	
Incision Architecture	- Oblique cut at 60°, with length of $0.48\ mm$. - Rotation around the tip of the the knife to $0.°$ - Vertical incision with length between $4\ mm$ up to $8\ mm$.
Fixed Motion Path	Device should only be able to make the defined architecture.
Maximum Incision Time	Maximum incision time of 20 second.
Manually Operated Handheld Device	Only handheld manually operated systems are investigated.
Single Handed Operation	System must be operated with one hand.
Visual Feedback	Components must allow sufficient visual feedback, so that the location and quality of the incision meet the necessary standards.
Radial Insertion Direction	Trocar knife will enter the sclera with a radial entry wound and an intrascleral path that is parallel to the limbus.
Device Support on Eye Surface	To aid maneuverability and simplicity, the system will be supported on the sclera.
Minimum Insertion Force	Minimum trocar knife insertion force = $0.7\ N$.
Specifications	
Type of Trocar	27 Gauge trocar knife
Constraints	
Geometric Constraints	- Geometric constraint patient: Device cannot make contact with patient's head (i.e., the nose and the orbit of the eye) - Geometric constraint surgeon: Device must be operable by 95% of all surgeons.
Performance Criteria	
Number of Contact Point as Few as Possible	To minimize damaged surface area on the sclera, contact point should be as low as possible.
Cost as Low as Possible	To increase adaptation of the device, cost should be as low as possible.
Ease of Use	- As few manipulations as possible - Time to complete incision as low as possible - Time to train the surgeon as short as possible - Task effectiveness as high as possible.

Table 3: *Design Requirements.*

4.3 Final Design

4.3.1 Functional overview

First the complete final design and its working principle is shown. Afterwards, more detailed information is given on the design process of each subsystem. The final design is shown in Fig. 16, this device can be divided into two halves, at the lower end a high precision path generator, at the upper end an actuation handle. The precision-end consist out of metal plates with slots. Three metal pins are guided through these slots. A small housing, named the "Needle Carrier" holds these pins into relative position and connects the needle with the pins. Hereby, the Needle Carrier is constraint to only move through the slots following one predetermined path. On top of the plates a handle is placed, the surgeon holds the handle using a power grip with its thumb at the top of the handle. The components in the handle are used to actuate the movement of the Needle Carrier through the slots. The movements through the slots can be divided into three stages. Fig. 15a show the the four positions of the Needle Carrier. First an oblique downward linear movement from position P1 to P2. Second, an upward movement along an arc from position P2 to P3. Third, a second downward linear movements from P3 to P4. The surgeon will push the button (in green) on top of the handle to move to Needle Carrier from P1 to P2. The pressure applied to the button is then released by the surgeon. An internal extension spring pulls the Needle Carrier upwards to position P3, consequently moving the Push Button upwards. Finally, to complete the movement, the surgeon will again push downwards on the button to move the Needle Carrier to P4. Placing this device on the sclera, the needle at the bottom of the device will penetrate the surface and create an incision that has a bi-planar architecture.

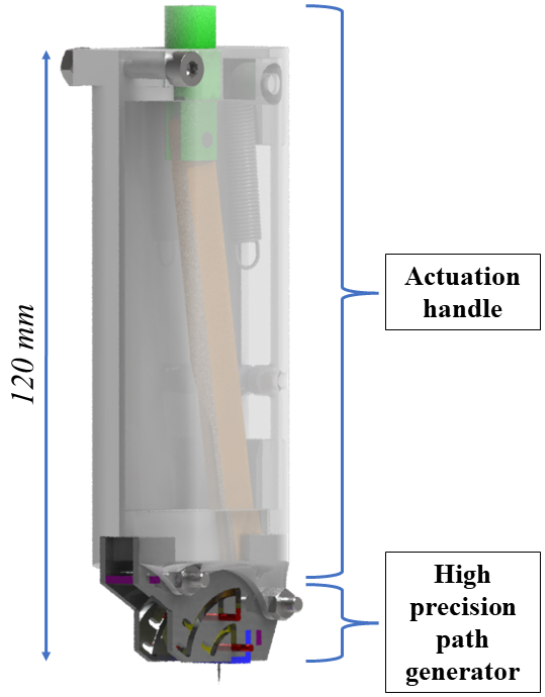

Figure 16: *Final Design. Showing the "Push Button" in green, the "Handle" in white, the "Slots" in grey, the "Contact Surface" in blue and the "Pins" in red.*

4.3.2 High precision path generator

The new mechanism must follow a certain path in order for the tip of the knife to follow a bi-planar architecture. The required movements by the mechanism can be divided into two types of operations; a translation or a rotation. In order for the knife to make a bi-planar incision, the end-effector of the mechanism should follow the orange line that is illustrated in Fig. 15b. This path consist out of a curved

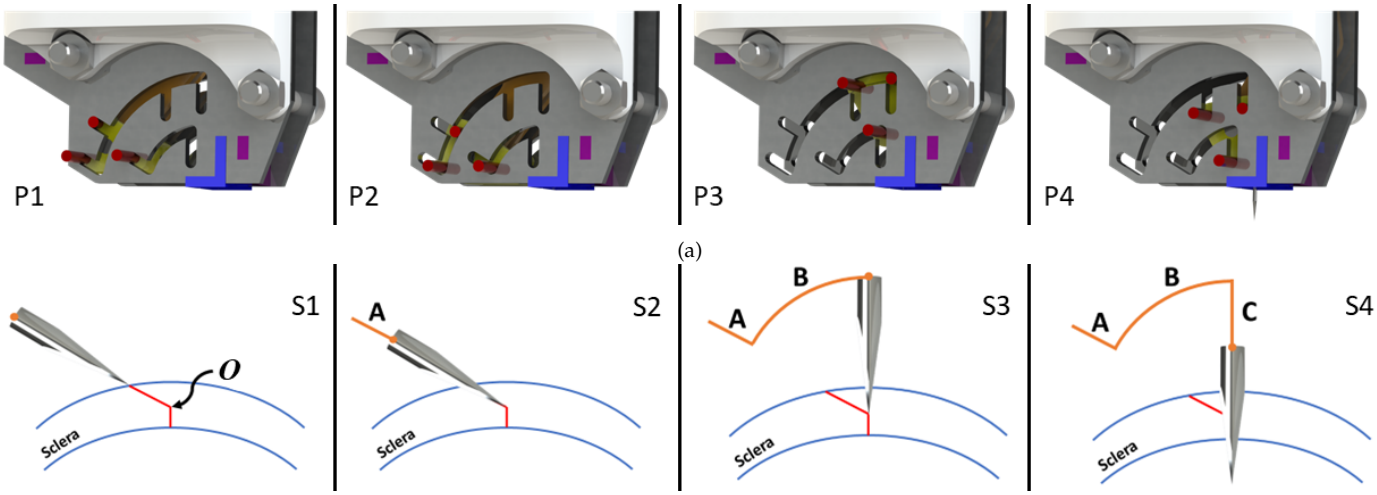

Figure 15: *Four steps corresponding to the four positions in the Bi-planar incision device. (a) The four positions, P1 to P4, of the Needle Carrier. The pins are represented in red. (b) Four steps, S1 to S4, to create a bi-planar incision. Path (orange line) of the knife realizing a bi-planar cut (red line). 1) Trocar knife approaches the the surface of the sclera with a 60° angle. 2) A linear translation creating the first half of the incision. 3) Rotation with tip of the trocar knife around point O. 4) Second translation at 0 degree, inserting the trocar knife into the eye.*

path ″B″ with its centre at rotation point ″*O*″ and two linear translations ″A″ and ″C″. Such a path can be created by adding a translation stage to a rotation stage.

Rotation stage

The center of the rotation is located at the midpoint of the height of the sclera. The tip of the trocar knife must rotate in this point. The rotation mechanism cannot be placed at this exact location in the tissue of the sclera. This means a ″Remote Center of Motion (RCM)″ mechanism must be used. Fig. 17 shows three types of ″ 1-DOF RCM mechanisms″ as described by Zong *et al*. [34]. These RCM mechanisms are found in three directions relative to the bi incision. Out of plane in front of the incision architecture (Figure 17A), in plane sideways of the incision architecture (Figure 17B) and in plane above the incision architecture (Figure 17C). Fig. 17A shows a single revolute joint at the same height sideways of the rotation point. Fig. 17B shows a RCM mechanism based on a parallelogram. Similar to the single-revolute-joint mechanisms, the joints that connect the mechanism to the world, are placed in line with the point of rotation. Fig. 17C shows an instantaneous RCM, a four bar linkage above the point of rotation. Rotation systems such as A and B, must place their rotation joints at the same height as the rotation point in the sclera. This means that bodies will be found on a plane that is tangential to surface of the eye. Such construction will most likely ask for support structures on this plane, leading to multiple contact point on the surface of the sclera [9]. Next to this, the available workspace on the tangential plane is more limited compared to workspace found above the surface of the eye. Systems placed above the eye have more available workspace, allowing for more design freedom. In addition, it is expected that systems above the eye do not need as much widespread support structures around the eye. For this reason the new design will focus on a system with its rotation bodies found above the eye (i.e., Fig 17C). Fig. 18 shows multiple methods to generate a rotation point in the middle of the sclera, while the bodies lie above the sclera surface. First, a slider with rollers on a rails is seen. The slider moves along a beam with a curvature that has its centre at the rotation point in the sclera. Here the moving slider encloses the curved structure. In the second mechanism, the moving slider is enclosed by the stationary curved structure. The knife is attached to a slider that moves through the curved slot (that has a curvature with its centre at the rotation point). Such concept can be considered as slot-pin mechanism. Third, a four bar mechanism is seen with an instantaneous RCM. Assuming that the angular rotation is small, the motion of the trocar knife can be seen as a rotation around the rotation point O. By replacing the joints with compliant substitutes, this mechanism can be converted to a compliant mechanism. A compliant mechanism is also shown in the fourth concept. The fourth system is a compliant 2-link RCM mechanism as is described by [35]. The advantage of compliant mechanisms is their kinematic predictability, minimal number of parts and 3D-printability. However, compliant mechanisms are in general limited to small movements. Large movements bring along parasitic motions (an event that is undesired at the tip of the trocar knife) or are limited to the elastic limit of the compliant elements. If one stacks multiple layers of the the compliant mechanism on top of each other, larger angles can be created. However, multiple layers create a mechanism with a larger thickness.

Mechanisms 3 and 4 will not be investigated further to be used as the rotation stage, since they are not suited to create large angles (i.e., angles of 60°, required for the bi-planar incision) without converting them into complex compliant systems (which does not fit the scope of this research). Mechanism 2 is preferred over mechanism 1 to be investigated further. The eventual required small system scale is expected to be attainable through the simplicity of this concept's individual parts. In addition, a pin and slot mechanism can be integrated with a linear stage, as is shown later in this section. The slot-slider mechanism concept has multiple variants on its own, as shown in Fig. 19. The shape of the slider, the number of the sliders and the number

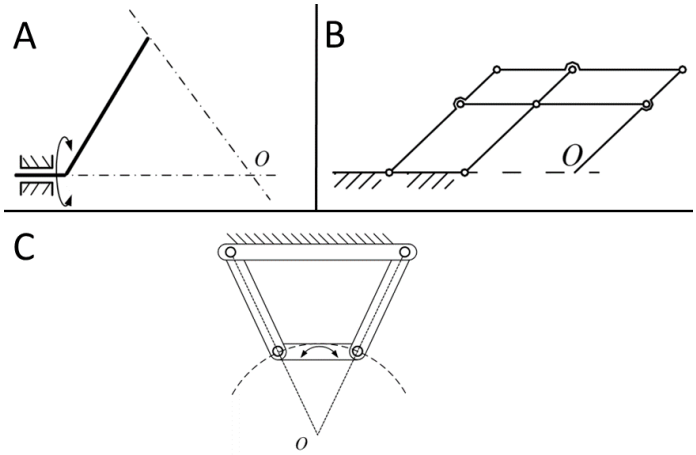

Figure 17: *1-DOF remote centre of motion (RCM) mechanisms as described in Zong et al. [34]. A) Single-revolute-joint RCM mechanisms. B) Parallelogram-based RCM mechanisms. C) Instantaneous RCM mechanisms.*

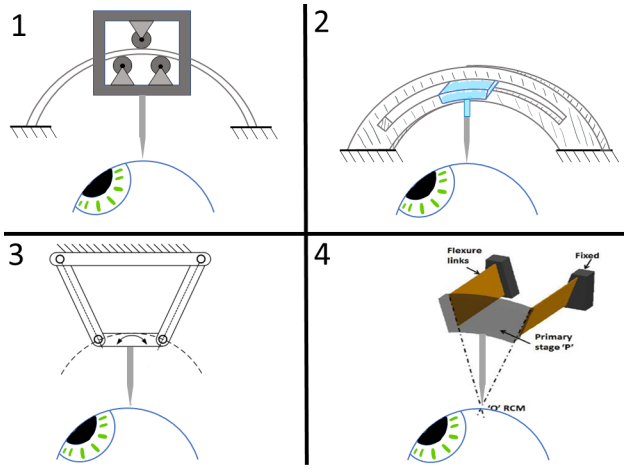

Figure 18: *Three above the eye RCM mechanisms. 1) Trocar knife attached to rollers travailing over a rails. 2) Trocar knife attached to a pin that is guided through a slot. 3) Trocar knife attached to the coupler link of an instantaneous RCM mechanism. 4) A 2-link compliant RCM mechanism [35].*

of slots, can be altered. In order for the slider to move through the slots, a small gap must be found between the two bodies. However, this gap leads to play in the system which affects the precision in the system. By changing the shape or the number of sliders, constraints are added to the system. These additional constraints will decrease this play in the system. Before deciding what slot sliding mechanism is used let us first look at the linear stage.

Linear stage

It is possible to ”paste” any linear stage on top of the slider found in the rotation stage. Such linear stages can be in the form of rails, sliding surfaces, rollers, compliant linear motion mechanisms. Appendix C shows a classification of these 2D linear stage mechanisms. It is however desirable to make the system as compact and simple as possible. For that reason the slots are also used to facilitate the linear movements. In order to integrate the linear slot with the rotational stage, a slider-slot mechanism with circular pins is used, as seen in the concepts of B and C of Fig. 19. The three pin mechanism is chosen due to its superior precision characteristics compared to the two pin mechanism. Appendix C shows the difference in precision between the two and shows the maximum tolerances between the pin and the slots to guaranty a successful bi-planar architecture, as was set in the requirements.

Geometry of the slots

The geometry of the slots are a result of compromises made between factors that are beneficial for precision and those that ensure the mechanism to stay within geometric constraints. For example, one of the factors that improves precision is by placing the pins as far apart as possible. However, this distance is limited due to the geometry constraints. One solution that provides precision while making the mechanism more compact is by allowing two of the three pins partially share one slot. All the parameters that are forming the slots are found in Table 4 and Fig. 20. The remaining recces seen on the plate of Fig. 20 are there for assembly and alignment purposes. In this mechanism, two parallel plates with the slots are found. It is critical for the two plates to be correctly aligned and kept at the right distance form each other. This is done by the two ”Spacer Plates” as seen in Fig. 21, they guaranty alignment and keeps the plates at the right distance.

Needle Carrier

The pins and needle are fixed to the ”Needle Carrier”, as can be seen in Fig. 22a. the Needle Carrier moves between the two walls in which the slots are found. The two longer pins go all the way through the carrier and are used to ”reload” the system (i.e., move the Needle Carrier to it initial position). The needle is inserted through the designated hole at the right depth by using a 3D printed alignment tool. This tool can only push the needle so far inwards that it protrudes $8.65\ mm$ from the Needle Carrier. Using the digital microscope (Dino-Lite edge 3.0), the insertion depth is measured to confirm a successful placement and is then glued into place. At the upper and lower edge a protruding surface is found to aid the guidance of the carrier along the walls of the plates. Fig. 22c and 22a show how the Needle Carrier connects to the rest of the system. An axle located at the center of the Needle Carrier connects the carrier to the ”Push Rod”. A ”Tension Cord” found around the axle is connected to the extension spring on the opposite end. The Push Rod is connected to the ”Push Button”.

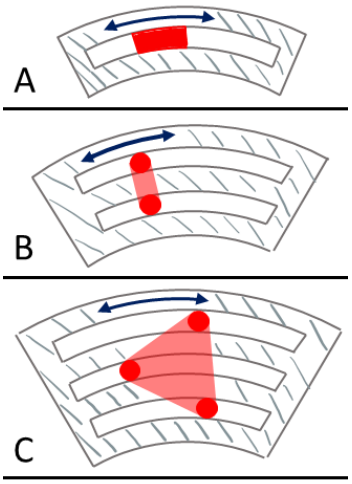

Figure 19: *Types of slider/pin-slot mechanisms. A) Single slot with curved slider. B) Two slots with two circular sliders. C) Three slots with three circular sliders.*

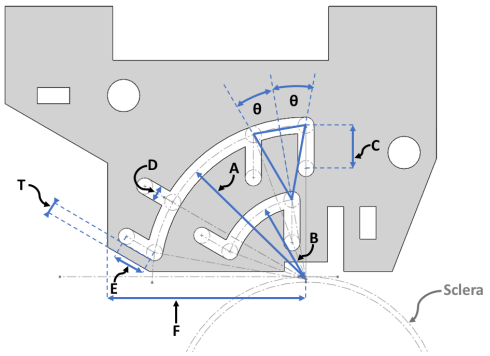

Figure 20: *The parameters which define the geometry of the slots.*

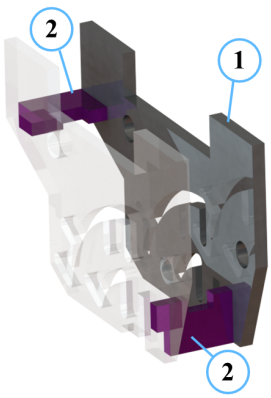

Figure 21: *Two parallel plates (one is made transparent) aligned using two ”Spacer Plates”. 1: Plates with slots. 2: ”Spacer Plates”.*

Parameters	Value	Argument
Length Between Rotation Centre and Large Arc, $\boldsymbol{A}$	14.25 mm	To increase precision, length "A" should be as large as possible but not exceed "F".
Length Between Rotation Centre and Small Arc, $\boldsymbol{B}$	7.5 mm	To increase precision, length "B" should be as small as possible, while the minimum thickness "T" is respected.
Length Second Linear Stage (Vertical), $\boldsymbol{C}$	4 mm	Currently, the length of the cannula is around 4 mm. The minimum length of the vertical stage should be 4 mm for the cannula to be placed in the sclera.
Pin Diameter, $\boldsymbol{D}$	1.5 mm	Smaller pins take up less space, however, when to small bending of the pins may occur. After consultation with DEMO, pins with a diameter of 1.5 mm were sett as they were the right combination of strength size and availability.
Length First Linear Stage (Oblique), $\boldsymbol{E}$	3 mm	The minimal length of the oblique stage must be larger than 0.50 mm to create the oblique incision plane. However, such a slot length may cause accidental triggering. A length of 3 mm is chosen to reduce this probability and gives the operator more feedback that the incision has been initiated.
Length Between Incision Centre and Inferior Orbital Rim, $\boldsymbol{F}$	18.7 mm	To facilitate for 95 % , Distance "F" cannot be lager than 18.7 mm, as illustrated in Fig 14b.
Wall Thickness, $\boldsymbol{T}$	1 mm	The minimum wall thickness is set to 1 mm to provide enough strength during use and fabrication.
Angle Between Lower- and Upper Pins, $\boldsymbol{\theta}$	20.74 degree	The larger θ, the higher the precision. To large and the arc will go past the tangent plane of the eyeball.

Table 4: *Parameters of the Pin and Slots.*

Contact Surface

Fig. 22b shows the part of the concept that is in contact with the underlying surface into which the incision is made. This part is interchangeable for use on a flat surface, for use on a cylindrical surface (as seen in Section 3) or on a spherical surface (eyeball). Into this Contact Surface, a small slot and hole are cut for the needle to pass through. A small cut out benefits controlled penetration into soft tissue. By making this cut out small, the Contact Surface lies closely to location of penetration. This creates a more stable area of penetration. The relative height difference of the tissue found at the edge of the cut out and the tissue that is situated at the penetration location, is smaller when it has close proximity than when these locations are further apart.

4.3.3 Actuation handle

Actuation

The pin and slot mechanism force the Needle Carrier to move along a fixed path, resulting in a motion that is able to create a bi-planar incision. The next step is to determine the manner of actuation of this movement. Since one of the requirements is to use the device single handed, only this hand can be used to activate the motion of the Needle Carrier. The type of grip determines the placement of the fingers, which may influence the location and method of actuation. The new design will use a method of gripping that has proven itself in surgery. The two most well known gripping types are the pinch grip and the power grip [36]. The pinch grip allows for for great precision, this grip is preferred when the outcome of the surgical intervention relies on the dexterity of the surgeon. The pinch grip does ask for more tension in the hand muscles compared to the power grip. The power grip may be preferred to improve comfort or strength during manipulations. Another way the pinch- and power grip differentiate from each other is by the size of shaft. The pinch grip asks for a narrow shaft that allows the thumb, index- and middle finger to be at close proximity. Contrarily, the power grip permits to have a wider shaft/handle. In this new design, the responsibility generating the precision lies with the kinematics of the mechanism, not the dexterity of the surgeon. This means the precision advantage of the pinch grip is less interesting.

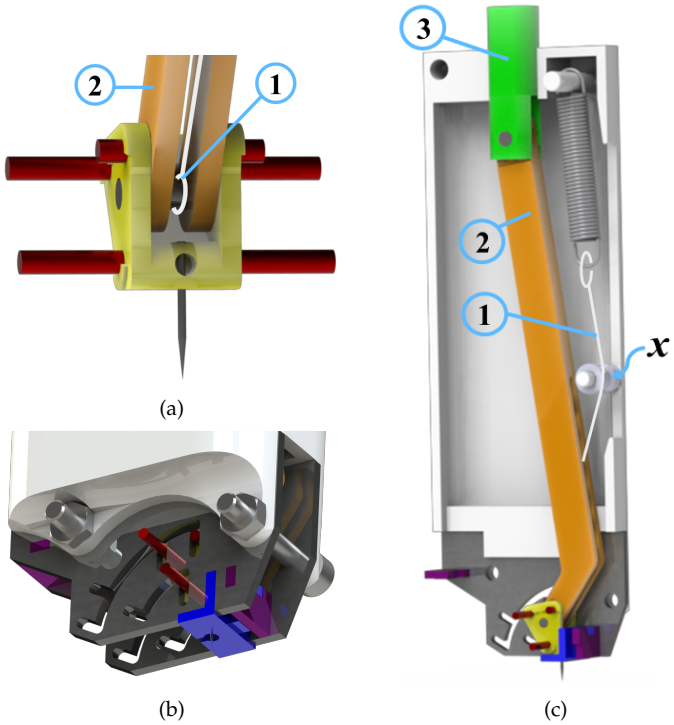

Figure 22: *The Needle Carrier connecting pins and needle to the actuation system. 1: Tension cord that connects the axle at the Needle Carrier to the extension spring. 2: Push Rod. 3: Push Button. x = tension force origin (i.e., the location from which the tension force must be applied on the Needle Carrier). (a) In yellow, the Needle Carrier, connected to the needle, the pin (red) and the Push Rod (orange). (b) In blue, the interchangeable part that makes contact with the to be penetrated surface. (c) Section view of the system.*

While the short intervention duration and low intensity do not require a power grip, the handle size gives more design freedom, making this the preferred grip. Now that there is a broad idea on the position of the fingers, an actuation system can be designed. One criteria states to favor a system with minimal manipulations. This means the ultimate design will make a bi-planar incision after only one manipulation (i.e., one push of a button or even actuating a bi-planar incision by letting the device touche the surface of the sclera). However, such systems may require complex and sensitive mechanisms. While such mechanism do have an advantage in ease of use, designing a less complex and reliable mechanism is favorable in this study. Before showing the internal components that actuate the system, lets first start to analyse the change in direction and forces that need to be applied on the Needle Carrier to force movement along the slots. There are four distinct force direction, as is shown in Fig 23. $F1$ and $F4$ responsible for the translations. A force that starts in the direction of $F2$ and end at in the direction of $F3$ to move the carrier along the arc, this force will be called F_{arc}. Since the pins are guided through slots, it is not essential to apply a force in the exact same direction as $F1$, F_{arc} and $F4$ to move the carrier through the slot. When a force is applied to the carrier and a component of this force vector lies in the same direction as the aforementioned forces, the Needle Carrier will advance through the slots. This means that if a force in the negative y-direction is applied in position P1, the Needle Carrier moves to position P2. Such principle is found in the final design, where a downward force vector is applied that starts at the top of the handle. The power grip allows the surgeon to place its thumb on top of the handle in order to push a button (like clicking on a pen). In this way the force is directly applied to the Needle Carrier without any extra kinematic mechanisms, see Fig 22c. What remains is to force the Needle Carrier to move along the arc. To force this movement, an extension spring is used, as is illustrated in Fig 24.

Spring

There are multiple factors to consider when incorporating an extension spring. First, the strength of the spring. The minimal spring force must be large enough so that it is able to lift the weight of the moving components and overcome the friction forces in the sliding surfaces. However, it is undesired to use an unnecessary stiff spring. Since this spring force has an upward component, it works opposite to the push-direction of the surgeon's thumb. An increased spring strength requires a corresponding increase in force exerted by the surgeon on the system. Higher operation forces through the system increase the risk of forces "spilling over" towards the sclera of the patient's eye. Additionally, an unnecessary stiff spring exerts large forces on the internal components, requiring an increase in their size. The second factor concerns the direction in which the spring pulls on the Needle Carrier. When the Needle Carrier approaches position P3, the length, therefore the strength of the spring, is at its lowest point. It is essential for the Needle Carrier to move from any stationary position along the arc towards position P3. Since the spring tension decreases along its path, it is beneficial for the spring force direction to resemble that of $F3$. However, if there is a constant pull on the Needle Carrier in the same direction as $F3$, it will pull the Needle Carrier away from position P1 and trigger the system automatically. For this to be avoided, F_{spring}, cannot have a projection on $F1$. Therefore, contrary to its current shown position, the origin of the spring force must lie in the green region as is shown in Fig 24. The system is designed such that the origin of the spring force lies in the green region as far to the right as possible while respecting the geometric constraints of the handle. The final factor is the location of the spring inside the system. Fig 22c shows the location of the spring inside of the handle. Instead of connecting one end of the spring to point "x" and the other end directly to the Needle Carrier, the spring is places higher up in the handle. A tension cord (fishing

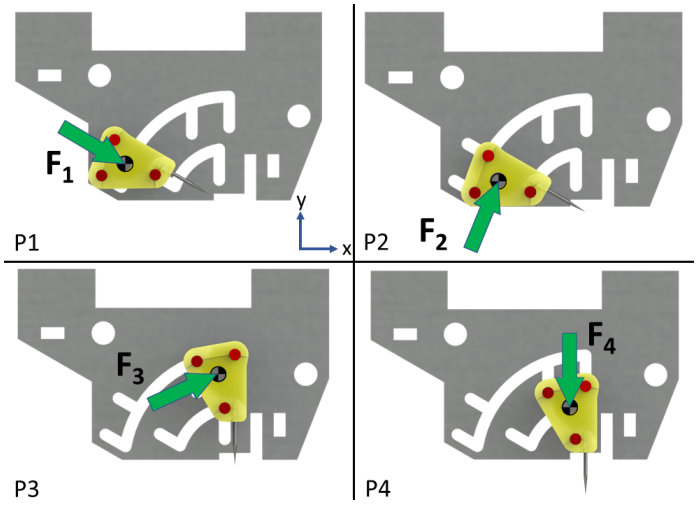

Figure 23: *Required force directions to move the Needle Carrier along the slots.*

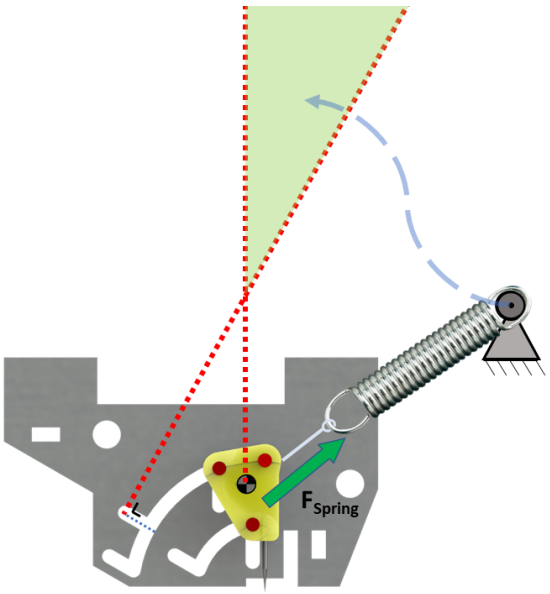

Figure 24: *Spring forcing the carrier through the arc motion. The origin of the tension force must move lie in the green region.*

line) is used to connect the Needle Carrier to the spring. At point "x" a pulley is situated that guides this cord.The spring has more room due to the current placement, thus allowing for more versatility in choosing the ideal spring. Before the selection of a spring, the spring force needs to be determined. However, this minimal required spring force, is closely related to the friction in the system. The existence of multiple sliding surfaces makes it challenging to accurately determine the necessary spring force. The required spring force ranges from a system with minimal friction, where the spring is only necessary to lift the moving components, to a poorly manufactured and assembled system with significant amounts of friction. Due to this reason, a tension spring is chosen as the driving force. Since such springs are easily interchangeable, a spring with minimal stiffness that still is able to move the Needle Carrier, can be placed inside the system. During the assembly three spring were tested with the following stiffnesses: Spring 1 = 0.12 N/mm, Spring 2 = 0.16 N/mm, Spring 3 = 0.42 N/mm . Eventually Spring 2 has been placed inside the mechanism. The springs are bought at www.industriele-veren.nl respectively having the following item numbers: 41030, 31150 and E02400291500S.

Handle
The height of the handle is 100 mm, a width of 40 mm and a depth of 25 mm. The handle is designed so that the hands of 95 % of adults fit, as was described in the requirements. The handle acts as a housing and connects all the subsystems using M3 and M4 bolts nuts and bolts.

4.4 Prototype manufacturing

All, except the spring, the tension cord and bolts and nuts, are specifically designed and manufactured for this concept. The needle, the pins, the plates with the slots and the Spacer Plates are made out of stainless steel and manufactured by DEMO. As previously stated and shown in Appendix D, small tolerances (maximum tolerance of 25 μm) are essential to successfully perform a bi-planar incision. Therefore, the plates are manufactured by means of Electrical Wire Discharge Cutting (EDWC). Using this method of manufacturing, tolerances up to 5 μm can be achieved [37]. The remaining parts are made using a Formlabs 3 SLA 3D printer. The "clear" resin is used, this resin combines the benefits of minimal layer thicknesses and the transparency allows to observe the internal kinematics. The technical drawings of the individual parts are found in Appendix I. The final assembly's off-the-shelf parts and their corresponding supplier and item numbers are shown in Table 5. The final assembled Bi-Planar Incision Mechanism is shown in Fig. 25. The design evolution of this prototype can be observed in Appendix E.

Off-the-shelf parts	Supplier	Item number
Extension spring	www.industriele-veren.nl	31150
Tension cord	Hema	81040087
M4x30	Karwei	450602
M3x20	Karwei	450612

Table 5: *Of-the-shelf parts and their corresponding supplier and item numbers that are used in final assembly.*

Figure 25: *Assembled Bi-Planar Incision Mechanism.*

5 Evaluation

5.1 Goal of the experiment

The purpose of this experiment is to determine the capability of the Bi-Planar Incision Mechanism to meet the predetermined requirements. Next to this, the performance of the device is reviewed. This is done by measuring the time it takes to complete the incision and by analyzing the precision and consistency of the bi-planar architecture. In order to bring these results into context, they will be compared to bi-planar incisions made using a reference device (i.e., the incision mechanism of Koot [9]).

5.2 Experimental Setup

The experimental setup consist out of a flat slab of silicon (i.e, eye phantom) into which the incisions are made. Five participants conduct the experiments to enable a broader range of operator dexterity to be included. The Five participants, comprising two females and three males between the ages of 21 and 29, with healthy eyes and dexterity,

will each perform a total of ten bi-planar incisions. Five incisions using the new Bi-Planar Incision Mechanism and five with the previously build design by Koot [9]. During these procedures the time to completion is recorded and the the quality of the architecture is reviewed afterwards in a similar fashion as was done in the previous experiment, as seen in Section 3. The used test setup is in many ways similar to the one seen in Section 3. There are however two modifications made. First, the curved surface of the silicone is replaces by a flat surface. To test the quality of the bi-planar incision geometry using a silicone slab, a flat surface is sufficient and simplifies the test setup as compared to using a curved surface. Second, the pressure chamber is replaced by a support layer. As previously stated and shown in Section 3, one of the challenges making a multi planar incision is caused by the radial flexibility of the sclera/silicone. In order to minimize this flexibility, hereby focusing on the performance of the architecture, the silicone slab will be supported from below. Fig. 26 and Fig. 27 show the two devices as they will be used in the experiment. They are adjusted to be used on a flat surface. Hence, the Bi-Planar Incision Mechanism has a flat contact patch, and the multi-planar incision device of Koot [9] is attached to a flat feet that rest on the silicone. The incision surface consist out of one $\pm$ 20 x 30 mm layer of 0.5 mm thick shore 60 silicone (www.rubbermagazijn.nl) slab which itself is supported by a block of (Styro) foam. The foam elevates and supports the slab of silicone in order to give the setup stiffness and allows the needle to travel 4 mm vertically through the silicone with minimal friction. The incision location is indicated by a circle of around 3.5 mm diameter that is drawn on the silicone slab. This size is similar to the width of the average pars plana [38]. In the experiment that includes reference multi-planar incision device, a small sheet of brown paper is placed between the foam and the silicon slab increasing contrast to improve the depth perception of the needle in the silicon. In addition, for this setup, a digital microscope (Dino-Lite edge 3.0) is included in the setup to assist with visual feedback during the procedure.

5.3 Instructions to Participants

First, a general explanation is provided towards the participant. This information details the bi-planar incision architecture and explains the general working principle employed by both devices to achieve this type of incision. The

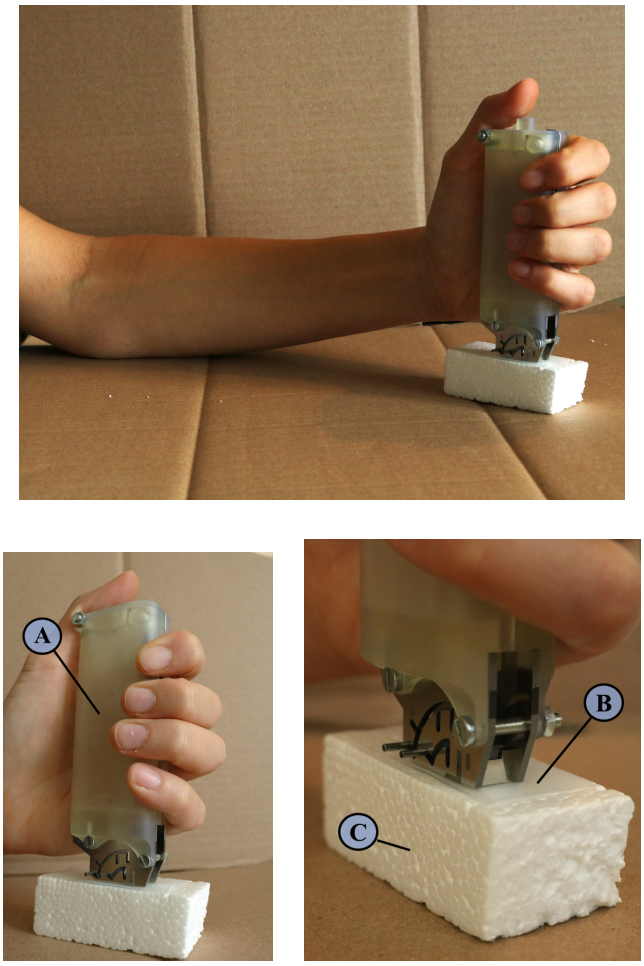

Figure 26: *Complete test setup, showing the Bi-Planar Incision Mechanism (A) and a small silicon (B) slab placed between the foam (C) and the mechanism.*

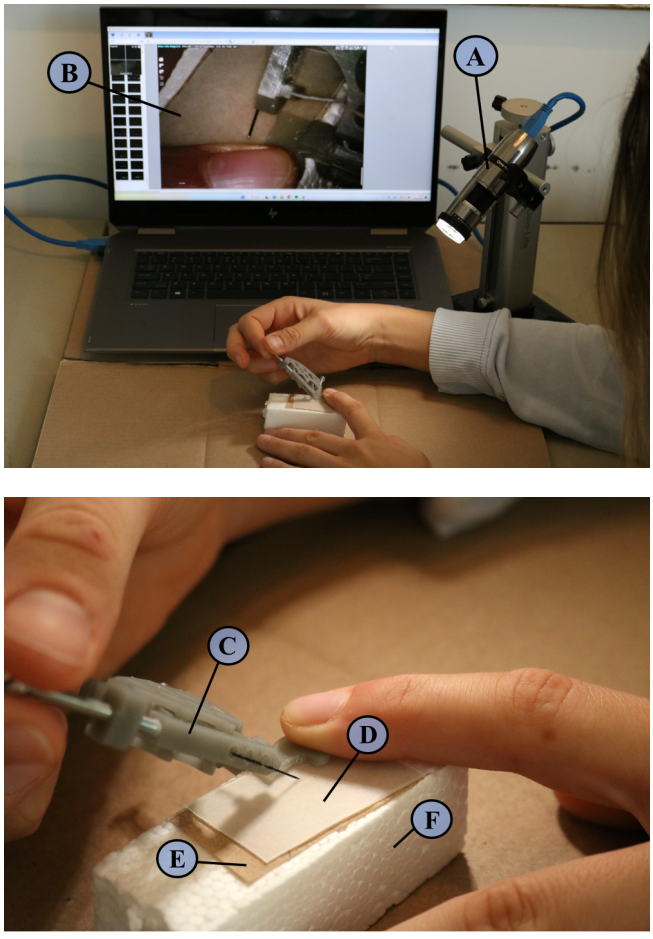

Figure 27: *Complete test setup showing the Dinolite edge digital microscope (A), a laptop running the DinoCapture software (B), the reference multi-planar incision device (C) [9], the silicon slab (D) on top of the contrasting piece of paper (E) and the foam (F).*

participants are instructed to focus on completing all the incisions with as much precision as possible. With the participant now prepared to begin the experiment, the following instructions are provided:

Bi-Planar Incision Mechanism:

1) Pick up the device, hold it with one hand using a power grip.
2) Place it on top of the silicone slab, so that the incision takes place inside of the circle.
3) Place the elbow of the arm performing the incision on the table.
4) Let the weight of the forearm rest on the silicon surface (while holding the Bi-Planar Incision Mechanism).
5) Press the button downward and release afterwards.
6) Repeat the previous action.
7) Remove the device.

Reference multi-planar incision device:

1) Pick up the device, place it on top of the silicone slab so that the incision takes place inside of the circle.
2) Stabilize the base with one hand, perform the incision with the other hand.
3) Place the needle at an angle of 60°from vertical.
4) Lower the needle until it touches the silicone surface.
5) Perform one revolution on the insertion screw (i.e., $0.50\ mm$), creating an oblique cut in the silicone.
6) Return the device to 0°.
7) Insert up to $4\ mm$ (i.e., 8 revolutions).
8) Return the needle to its original position.
9) Remove the device.

First, the participants will performed five test rounds using the multi-planar incision device of Koot [9] to account for the learning curve. The quality of the architecture is reviewed between each round so that the participant is able to adjust and improve their incision technique. For the new Bi-Planar Incision Mechanism only one test round is performed in order to understand the activation of the device. The participants are asked to give comments concerning the incision process, during and after the process.

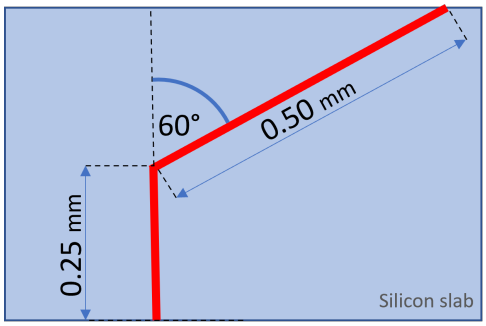

Figure 28: *The red line represents the desired bi-planar architecture in a 0.50 mm thick flat slab of silicone.*

5.4 Experimental Variables

The time to completion is measured during each incision. The time is measured once the system touches the silicone surface, it ends when it leaves this surface. Afterwards, similar to the method found in Section 3, the silicone samples are collected and the incision architectures are analysed through visual inspection using a digital microscope (Dinolite edge 3.0). Fig. 28 shows the "perfect architecture" on a flat silicone slab. The architectures made by the participants are analyzed on three points; the length of both planes and the angle between them. The mean of these values are determined and their corresponding Standard Deviation (STD). Next, the Bi-Planar Incision Mechanism is reviewed to see if it complies with all the requirements set in Section 4.

5.5 Results

The first objective is the verification of the requirements. This experiment validates that the Bi-Planar Incision Mechanism meets all the necessary requirements formulated in Section 4, except for the ability to puncture the sclera. The ability to puncture the sclera could not be measured in this experimental setup. Although the insertion force perceived during the experiment was low, it is expected to increase during real sclerotomies, as discussed in Section 6. The second objective is to determine the performance of the incisions. All incision made using the Bi-Planar Incision Mechanism showed clear Bi-planar characteristics. All Bi-planar incision are labeled as successful considering the criteria in Section 4 and Variables 1. Fig. 29 shows five incision made by participant one using the Bi-planar incision device. The lengths and the angle are measured for each incision using the DinoCapture software, as is shown in Fig. 30. These measurements, as depicted in Fig. 30, are constructed by hand on a visual basis. All 50 individual measurements are shown in Appendix F and Appendix G. The Bi-Planar Incision Mechanism's geometry and incision time measurements are summarized in Table 6, including the mean, standard deviation, and 95% confidence interval. The measurements show a consistent architecture that all closely resembling the intended bi-planar architecture.

As previously stated, to bring the performance of the Bi-Planar Incision Mechanism into perspective, the same experiment is done using multi-planar incision device from Koot [9]. Table 6 shows the mean, standard deviation, and 95% confidence interval for both the geometry and incision time measurements of the reference device. The results show a larger spread in the geometry of the architecture. Considering the criteria in Section 4 and Variables 1, only 7 out of 25 are considered as a successful bi-planar incisions.

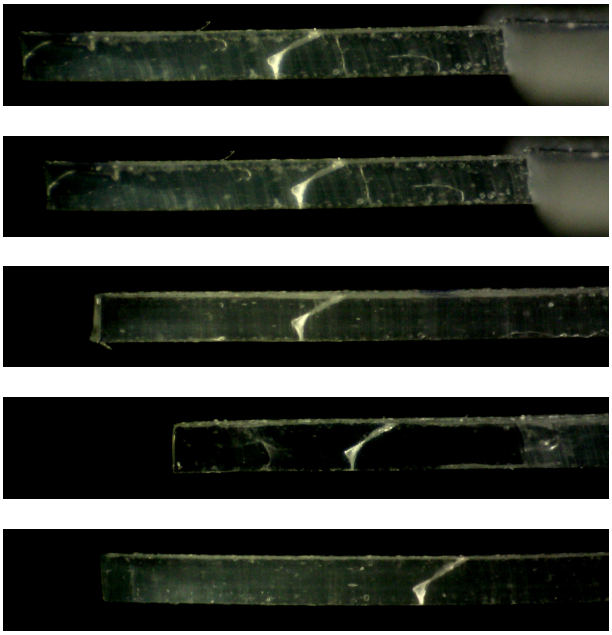

Figure 29: *Five incisions made by participant one, using Bi-Planar Incision Mechanism.*

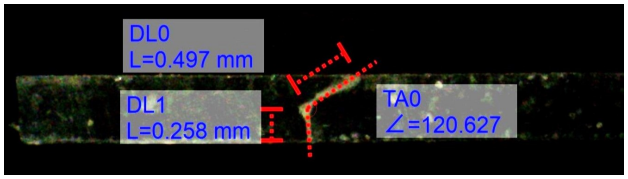

Figure 30: *Measurements of the architecture in silicone slab, created using Bi-Planar Incision Mechanism.*

6 Discussion

6.1 Summary of main findings

6.1.1 Interpretation of the Results

The results demonstrate that the Bi-Planar Incision Mechanism is capable of consistently producing successful bi-planar architectures. The results show that the Bi-planar incision mechanism makes more precise, more accurate and faster bi-planar incisions compared to the reference device of Koot [9]. Judging the position of the needle tip relative to the silicone slab (e.g., judging if the needle tip had entered the silicon) was found to be the most difficult factor using reference multi-planar incision device. This factor has both influence on the time to completion and accuracy of the architecture.

Observing the incisions made using the Bi-Planar Incision Mechanism, the width of the incision is larger at the rotation point compared to the rest of the architecture. There are multiple factors that may contribute to this. First, the length the needle protrudes out of the Needle Carrier does not equal the prescribed distance. If this is true, the needle will not rotate around a stationary point in space; the tip of the needle. Consequently, the tip of the needle will move through the silicon during the rotation, causing more damage to the silicon. Second, participants may apply varying pressure during incision through the mechanism on the silicon surface. The applied pressure could influence the level of indentation of the silicone surface, therefore, changing the depth of the needle in the silicon slab. Third, the play between the pin and slots may cause the Needle Carrier to rotate (as explained in Appendix D) which may lead to the extra damage done to the silicon.

6.1.2 Participant comments

The participants were asked to comment on their experience during and after the incisions. Regarding the Bi-Planar Incision Mechanism, the participant was uncertain whether the mechanism was placed perfectly perpendicular to the silicone surface. However, the device provided the participant with confidence during the incision process, as it performed as intended. On the other hand, the multi-planar incision reference device demanded a high level of visual and physical concentration during the entire incision process. The participant reported that any hand vibration during the incision influenced the movement of the needle relative to the silicone slab, which, in turn, affected the incision. Additionally, the device had play in the system, which affected the participant's confidence in creating a bi-planar incision. It was also challenging for the participant to judge whether the tip of the needle had entered the silicone slab.[1]

6.2 Limitations and recommendations

6.2.1 Measurement errors

The accuracy of the measurements in the DinoCapture software depends on multiple factors. First, the quality of the picture. The picture should be taken normal to the incision plane. Second, the measurements drawn by hand in the software should have the same length and angle as the architecture. Third, it has been assumed that the thickness of all silicone slabs to be constant. However, the length required to penetrate the silicone slab depends on the thickness of the of the slab. Deviations from all these factors lead to deviation from the true value. While precision is sought, the true value cannot be guarantied. Nevertheless, the resolution of the measured values, give a good representation of the quality of the incisions.

1. Note, since the participants are acquaintances of the writer, they might have a positive bias towards the Bi-Planar Incision Mechanism

	Bi-planar incision mechanism		*Reference device [9]*		*Bi-planar incision mechanism*		*Reference device [9]*	
	Mean	**STD**	**Mean**	**STD**	**Min.**	**Max.**	**Min.**	**Max.**
Length Oblique Plane [mm]	0.530	0.043	0.435	0.192	0.508	0.552	0.338	0.532
Length Vertical Plane [mm]	0.248	0.0286	0.304	0.0702	0.233	0.262	0.268	0.340
Angle Between Planes [$Degree$]	60.08	2.40	48.11	8.08	58.87	61.29	44.03	52.21
Time to Completion [$Second$]	5.0	1.5	37.2	5.3	4.2	5.7	34.5	39.8

Table 6: *Mean and STD of the the geometric and time measurements of the Bi-Planar Incision Mechanism.*

6.2.2 Recommendations

Verification recommendations

Incision sample: In this research, the bi-planar incision showed to have the best self-sealing properties in a silicone slab. Next, this research proves that the Bi-Planar Incision Mechanism is able to execute bi-planar incisions with great precision and accuracy, on a slab of silicone. Herewith concluding that the Bi-Planar Incision Mechanism is able to improve the self-sealing properties of scleral incisions. However, all these experiments are performed through silicon samples. Although the silicone used was selected to have material properties as similar as possible to those of the sclera, it has a lower modulus compared to real scleral tissue, which even becomes stiffer with age [25], [26], [39]. Consequently, penetration through the sclera is expected to be more difficult than through the silicone sample, as Koot [9] found in his research. He used the same device to penetrate a silicone slab identical to the one used in this research, as well as a porcine eye. He experienced much more resistance during penetration of the porcine eye, resulting in greater tissue deformation. Although these incisions were performed using the same type of needle made by DEMO, it is expected that more force will be required when using the Bi-planar Incision Mechanism on real eyes, leading to greater tissue deformation prior to penetration, which may impact the incision quality. Additionally, during the experiment, the silicone surface remained stationary in relation to the incision mechanism, whereas in in-vivo sclerotomies, this will not be the case. It is anticipated that eye movement within the eye-socket will occur when force is applied, and slippage between the mechanism and the eye may occur. In future experiments, the mechanisms should be tested in situations that more closely resemble in-vivo sclerotomies. This can be done by making incisions in ex-vivo porcine eyes. The quality of the incision architecture can be reviewed by means of an optical coherence microscopy (OCT). At this stage, the Bi-Planar Incision Mechanism can directly be compared to the currently used trocar knife.

Bi-planar incision type: In the experiment of Section. 3, the second bi-planar incision, as seen in Fig. 3d, was not considered in the experiment. The tri-planar incision revealed superior depth control of the needle with an oblique entry plane compared to a perpendicular plane. Therefore, it was decided to ignore the bi-planar incision with the perpendicular entry wound. However, as the study progressed, the focus was placed on the quality of the architecture, with less importance toward a controlled depth penetration in soft tissue. In the future, a study on the self-sealing properties of bi-planar incision 2, as seen in Fig. 3d, must be investigated.

Design recommendations

Interchangeable Needle: One of the factors influencing the quality of the incisions, is the sharpness of the needle/trocar blade. Originally the Needle Carrier incorporated a feature that allowed the needle to be removed by loosen a small screw. However, the dimensions of the screw thread were to small for the material used (SLA resin). The needle ended up to be glued to the Needle Carrier. This meant one needle performed all incisions, reducing its sharpness after each incision. Next iterations of the mechanism will benefit when the needle is interchangeable. The currently used trocar knife is a single use blade. Their sharpness is superior to the needle that are sharpened by DEMO and used in the concept. This is one of the reasons, these two devices are not compared in the experiments. The second reason is that Singh *et al*. [10] already showed that by using trocar knifes, surgeons are not able to make consistent incision architectures.

Trocar Port: The current trocar knife integrates the trocar port to the trocar knife. A next step to the Bi-Planar Incision Mechanism can be to also integrate the trocar port to the mechanism, hereby the increasing the efficiency of the incision.

Designed for Verification: While designing the Bi-planar mechanism, certain design choices are made that are beneficial during testing. This meant, multi-use, modularity and quick (dis)assembly time was preferred. Future iterations suffice to be single use only. This allows for more integration of the individual parts. In this way, cost and size can be reduced. Alternatively, a combination of single and multi use parts may reduce costs further. The high precision parts can be reused while the parts that come into contact with the patient will be exchanged.

Variable Sclera thickness: The current design assumes the sclera to be $0.50\ mm$ thick. In reality, the sclera thickness varies. Therefore, the height of the rotation point between the two planes should be variable. The current method to adapt for the variable sclera thickness, is to change the thickness of the Contact Surface Part in the mechanism, hereby altering the high of the rotation point. This means, the sclera thickness is must be measured first (e.g., using a B-scan) to then print the Contact Surface Part. An integrated solution, that adjust the height of the mechanism relative to the surface of the sclera, is preferred. However, such procedure (measurement of sclera thickness) might no be realistic. An alternative approach to measuring sclera thickness is to select the location of rotation at a particular height, where the oblique entry plane has a maximum length. This method helps to prevent uni-planar oblique incisions in thin sclerae. The length of the oblique entry plane can be selected such that in 95% of sclera thicknesses a bi-planar incision is created. However, the resulting incision from this method usually consists of a larger perpendicular plane and a smaller oblique plane, which may not be beneficial to the sealing characteristics. The order of the incision planes in bi-planar incision 2, as presented in Fig. 3d, is more suitable for this approach, as the oblique plane will be more dominant.

Over-constrained design: In this design, the Needle Carrier moves between two plates. On both sides, a maximum of three pins make contact with the slots. The symmetry in the setup results in a stable movement of the Needle Carrier when force is exerted to move it. Theoretically, this design also works if the pins only extrude the Needle Carrier on one side. In reality, in this configuration, the unbalanced forces causes the Needle Carrier to tilt between the two plates. This result the Needle Carrier to get stuck. To prevent this unbalanced behaviour, pins must extrude on both sides of the Needle Carrier. The more pins are brought into contact with the slots, the more constraints are added to the system. These constraint restrict the movement of the Needle Carrier, reducing the play found in the system. However, too many constraints may lead to a system that does

not move at all. An over-constrained system fully depends on the alignment of the individual parts. This also hold for the pin and slot mechanism. Insufficient manufacturing in an over constrain situation could lead to failing kinematics. Therefore, in this design, it is possible to reduce or increase the number of pins found on each side of the device, hereby altering the number of constraints. In the final test setup, for the Needle Carrier to move smooth and stable through the plates, five pins were in contact with the slots (two on one side, three on the other side). For future iteration, to be less dependent on the precision of manufacturing, one can investigate solutions that prevent the system to be over-constrained. One possible approach could be a system that uses one plate with slots. However, if this is done on the current design, the Needle Carrier would tilt due to the moment that is created via the Push Rod. A system with one plate must prevent tilting of the Needle Carrier. This can be done by attaching the Push Rod to both sides of the plate, as seen in Fig. 31. Another approach can be in the form of a compliant version of the mechanism.

Alternative Design Directions: In this concept the linear motions are actuated by the surgeon, the rotation is enforced by a spring force. Opposite to this, the rotation is controlled by the surgeon, while the linear motion is activated by a spring force. Such a concept can be seen in Appendix H.

6.3 Future outlook

As mentioned earlier there are three main challenges creating multi-planar incision; consistently creating a prescribed architecture, controlled depth penetration in soft tissue and constraining the relative position between the incision device and the eye. This thesis primarily focused on the first challenge, resulting in a successful development of a Bi-Planar Incision Mechanism. Ultimately, a future design integrates solutions to all these challenges in one device. To achieve this, a combination of the following approaches could be employed: Firstly, the current Bi-planar Incision Mechanism has proven effective in consistently creating bi-planar incisions, thus addressing the first challenge. Secondly, the Contact Surface component helps with controlled depth penetration, but if the needle tip requires greater pressure prior to surface penetration, the tissue surface will deform downwards, necessitating greater pressure from the entire system on the eye, which is undesirable. To address this challenge, fast insertion speeds can be used to take advantage of the tissue's inertia. For example, a fast vibrating needle that moves in the axial direction and overcomes the tissue's inertia could be incorporated. This would result in improved depth penetration in soft tissue. Thirdly, the relative position between the mechanism and the incision location must remain stationary for controlled incisions. However, during insertion, the eye may move in its socket. Ideally, the eye should be anchored in a manner that minimizes damage to the surrounding tissue. This can be achieved by incorporating a suction system into the mechanism. The suction system will ensure a constant relative position between the mechanism and the incision location without causing any harm to the eye. The system of the future will ensure that scleral wounds are self-sealing, leaving no room for complications related to leakage.

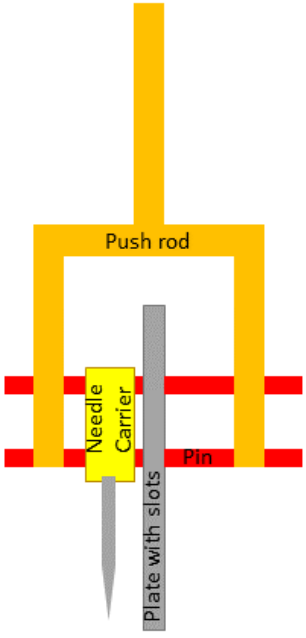

Figure 31: *Design with one plate.*

7 Conclusion

This paper presents the development and verification of an ophthalmic instrument that can consistently create the most effective self-sealing scleral incisions. A study on self-sealing incision architectures was conducted which showed incisions with a bi-planar architecture to hold the greatest potential for consistent self-sealing incisions. A set of requirements was formulated that was used to generate a functional prototype that is capable of creating consistent bi-planar incisions. The study demonstrates a design process that resulted in a Bi-Planar Incision Mechanism, comprising of a high precision pin and slot mechanism that is linked to an actuation handle. Verification of the Bi-Planar Incision Mechanism functional principles and capacity to carry out bi-planar incisions at scale was achieved through experimentation on an eye phantom constructed using a $0.50\ mm$ silicone slab. The experiment revealed that the Bi-Planar Incision Mechanism concept is a fast and reliable system for performing bi-planar incisions on an eye phantom. The next step is to validate the self-sealing incisions of the Bi-Planar Incision Mechanism in conditions that resemble those found in the operation room. The outcomes of this study demonstrate the Bi-Planar Incision Mechanism's great potential to produce precise, accurate, and fast self-sealing incisions.

8 Acknowledgement

First and foremost, I would like to thank Kirsten Lussenburg for always being available to provide me with valuable feedback. Often, her advice was exactly what I needed, which gave me energy after each meeting. I would like to thank Jette Bloemberg, Esther de Kater, and Vera Kortman for their helpful and thorough feedback. Their suggestions helped me refine my work and improve its overall quality.

Furthermore, I would like to thank David from DEMO. Without his precise manufacturing, the mechanism would not have worked so well. I would also like to thank Paul Breedveld for inspiring me to graduate at the BITE department of the TU Delft and for providing valuable feedback. Lastly, I would like to extend my thanks to my friends and family for their support, interest in my thesis, and patience throughout the process.

REFERENCES

[1] H Tan, BAE van der Pol, and Jan Sietse Stilma. *Leerboek oogheelkunde*. Bohn Stafleu van Loghum, 2018.

[2] Elaine Nicpon Marieb and Katja Hoehn. *Human anatomy & physiology*. Pearson education, 2015.

[3] Tatsuya Jujo, Jiro Kogo, Hiroki Sasaki, Reio Sekine, Keiji Sato, Sakura Ebisutani, Yasuhiro Toyoda, Yasushi Kitaoka, and Hitoshi Takagi. 27-gauge trocar-assisted sutureless intraocular lens fixation. *BMC ophthalmology*, 21(1):1–8, 2021.

[4] MD Chris A. Knobbe. Vitrectomy and vitreoretinal eye surgery, Mar 2022.

[5] Giulio Bamonte, Marco Mura, and H Stevie Tan. Hypotony after 25-gauge vitrectomy. *American journal of ophthalmology*, 151(1):156–160, 2011.

[6] Guohai Chen, Radouil Tzekov, Wensheng Li, Fangzheng Jiang, Sihong Mao, and Yuhua Tong. Incidence of endophthalmitis after vitrectomy: a systematic review and meta-analysis. *Retina*, 39(5):844–852, 2019.

[7] Andrzej Grzybowski, Magdalena Turczynowska, and Ferenc Kuhn. The treatment of postoperative endophthalmitis: should we still follow the endophthalmitis vitrectomy study more than two decades after its publication? *Acta Ophthalmologica*, 96(5):e651–e654, 2018.

[8] Vinit B Mahajan, Ryan M Tarantola, Jordan M Graff, H Culver Boldt, Michael D Abramoff, Stephen R Russell, and James C Folk. Sutureless triplanar sclerotomy for 23-gauge vitrectomy. *Archives of Ophthalmology-Chicago*, 129(5):585, 2011.

[9] Berend Koot. *Creation of Tri-Planar Incisions in Vitrectomy, https://repository.tudelft.nl/islandora/object/uuid:07503083-8a2f-416f-a209-42562228fae6?collection=education*. 2021.

[10] Ajay Singh and Jay M Stewart. 25-gauge sutureless vitrectomy: variations in incision architecture. *Retina*, 29(4):451–455, 2009.

[11] D.o.r.c. dutch ophthalmic research center, https://dorcglobal.com/eva-aveta (1-6-2022).

[12] Makoto Inoue, Kei Shinoda, Hajime Shinoda, Ryosuke Kawamura, Kotaro Suzuki, and Susumu Ishida. Two-step oblique incision during 25-gauge vitrectomy reduces incidence of postoperative hypotony. *Clinical & experimental ophthalmology*, 35(8):693–696, 2007.

[13] KAMYAR Vaziri, S Schwartz, C Leffler, and H Flynn. Surgical tamponade in the treatment of retinal detachment. *Retin Physician*, 12:32–7, 2016.

[14] Astha Jain, Thirumalesh MB, and Jivitesh Singh. Tamponading agents in vitreoretinal surgery. In *Cutting-edge Vitreoretinal Surgery*, pages 101–111. Springer, 2021.

[15] Sunil K Warrier, Rajeev Jain, Jagjit Singh Gilhotra, and Henry S Newland. Sutureless vitrectomy. *Indian Journal of Ophthalmology*, 56(6):453, 2008.

[16] Nakhleh E Abu-Yaghi, Yazan A Abu Gharbieh, Ahmad M Al-Amer, Saif Aldeen S AlRyalat, Mohammed B Nawaiseh, Mohammad J Darweesh, Leen R Alkukhun, Alaa M Abed, Omar A Saleh, and Osama H Ababneh. Characteristics, fates and complications of long-term silicone oil tamponade after pars plana vitrectomy. *BMC ophthalmology*, 20:1–7, 2020.

[17] Piotr Kanclerz, Andrzej Grzybowski, et al. Complications associated with the use of expandable gases in vitrectomy. *Journal of ophthalmology*, 2018, 2018.

[18] Sean Yuan, Vishal S Parikh, and Gaurav K Shah. Sutureless small-gauge vitrectomy. In *Cutting-edge Vitreoretinal Surgery*, pages 53–61. Springer, 2021.

[19] Manish Nagpal, Gaurav Paranjpe, Pravin Jain, and Rituraj Videkar. Advances in small-gauge vitrectomy. *Taiwan Journal of Ophthalmology*, 2(1):6–12, 2012.

[20] Lorenzo López-Guajardo, Jesús Pareja-Esteban, and Miguel Angel Teus-Guezala. Oblique sclerotomy technique for prevention of incompetent wound closure in transconjunctival 25-gauge vitrectomy. *American journal of ophthalmology*, 141(6):1154–1156, 2006.

[21] Jason Hsu, Eric Chen, Omesh Gupta, Mitchell S Fineman, Sunir J Garg, and Carl D Regillo. Hypotony after 25-gauge vitrectomy using oblique versus direct cannula insertions in fluid-filled eyes. *Retina*, 28(7):937–940, 2008.

[22] Sujiv Vurgese, Songhomitra Panda-Jonas, and Jost B Jonas. Scleral thickness in human eyes. *PloS one*, 7(1):e29692, 2012.

[23] Steve Charles. Principles and techniques of vitreoretinal surgery. In *Retina*, pages 2147–2162. Elsevier, 2006.

[24] VG Madanagopalan, CK Nagesha, Ashish M Khodifad, and Rajiv Raman. Influence of orientation of the external linear incision created by the 25-gauge trocar and related factors on sclerotomy closure: A clinical and optical coherence tomographic study. *Indian journal of ophthalmology*, 66(12):1809, 2018.

[25] Joseph Park, Andrew Shin, Somaye Jafari, and Joseph L Demer. Material properties and effect of preconditioning of human sclera, optic nerve, and optic nerve sheath. *Biomechanics and Modeling in Mechanobiology*, 20(4):1353–1363, 2021.

[26] Kent Larson. Can you estimate modulus from durometer hardness for silicones. *Dow Corning Corporation*, pages 1–6, 2016.

[27] Bingrui Wang, Yi Hua, Bryn L Brazile, Bin Yang, and Ian A Sigal. Collagen fiber interweaving is central to sclera stiffness. *Acta biomaterialia*, 113:429–437, 2020.

[28] JS Pulido, ME Zobitz, and KN An. Scleral penetration force requirements for commonly used intravitreal needles. *Eye*, 21(9):1210–1211, 2007.

[29] João Pedro Marques, Cátia Azenha, and João Figueira. Microincision vitrectomy trocars–redefining surgical practices through a new range of applications. *Journal-Microincision Vitrectomy Trocars–Redefining Surgical Practices Through a New Range of Applications*, 2015.

[30] Ahmed Abass, Bernardo T Lopes, Ashkan Eliasy, Richard Wu, Steve Jones, John Clamp, Renato Ambrósio Jr, and Ahmed Elsheikh. Three-dimensional non-parametric method for limbus detection. *PLoS One*, 13(11):e0207710, 2018.

[31] Carl N Stephan, Anne JR Huang, and Paavi L Davidson. Further evidence on the anatomical placement of the human eyeball for facial approximation and craniofacial superimposition. *Journal of forensic sciences*, 54(2):267–269, 2009.

[32] Handtools, https://www.ergonomics4schools.com/lzone/tools.htm.

[33] Dined anthropometric, dined.io.tudelft.nl/en/database/tool.

[34] Guanghua Zong, Xu Pei, Jingjun Yu, and Shusheng Bi. Classification and type synthesis of 1-dof remote center of motion mechanisms. *Mechanism and machine theory*, 43(12):1585–1595, 2008.

[35] Prasanna S Gandhi, Rupesh S Bobade, and Chao Chen. On novel compliant mechanisms for remote center motion. *Advances in Mechanical Engineering*, 10(4):1687814018761920, 2018.

[36] Solmon Jeong and Kotaro Tadano. Manipulation of a master manipulator with a combined-grip-handle of pinch and power grips. *The International Journal of Medical Robotics and Computer Assisted Surgery*, 16(2):e2065, 2020.

[37] James G Bralla. *Design for manufacturability handbook*. McGraw-Hill Education, 1999.

[38] HU Moller and Dorte Ancher Larsen. Milestones and normative data. *Taylor and Hoyt's Pediatric Ophthalmology and Strabismus. 5th ed. Edinburgh: Elsevier*, pages 40–9, 2016.

[39] Brendan Geraghty, Stephen W Jones, Paolo Rama, Riaz Akhtar, and Ahmed Elsheikh. Age-related variations in the biomechanical properties of human sclera. *Journal of the mechanical behavior of biomedical materials*, 16:181–191, 2012.

APPENDIX A
INCISIONS AND CORRESPONDING DROPLET SIZE

This section shows four different incision architectures that were analysed in Section 3. Presented within this section are two types of images captured using a digital microscope (DinoLite edge 3.0). One image portrays a side-view of the incision through a silicone slab, while the other depicts the corresponding droplet. Furthermore, alongside the image of the displaying the droplet, the average diameter of that droplet is shown.

Oblique incisions:

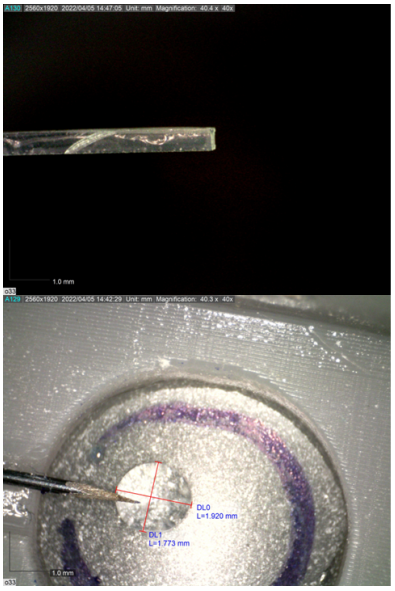

1.85*mm*

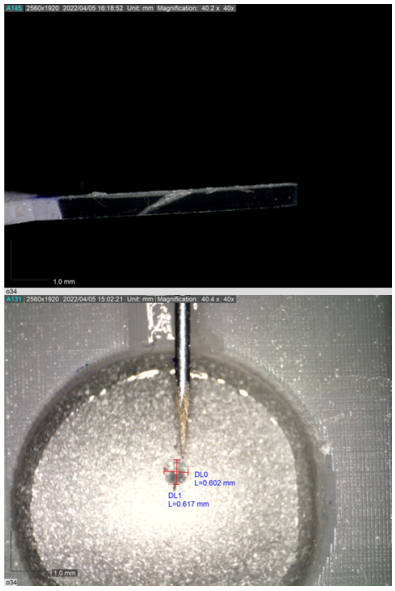

0.61*mm*

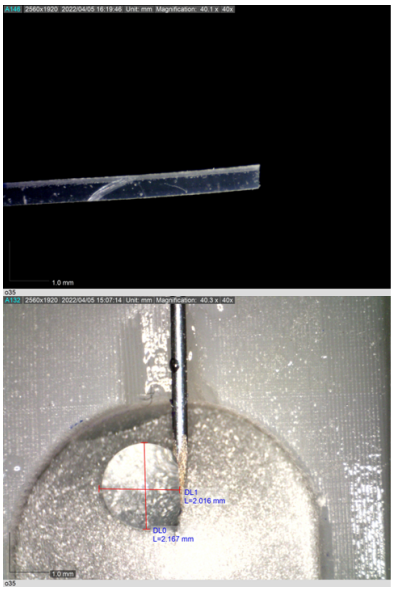

2.01*mm*

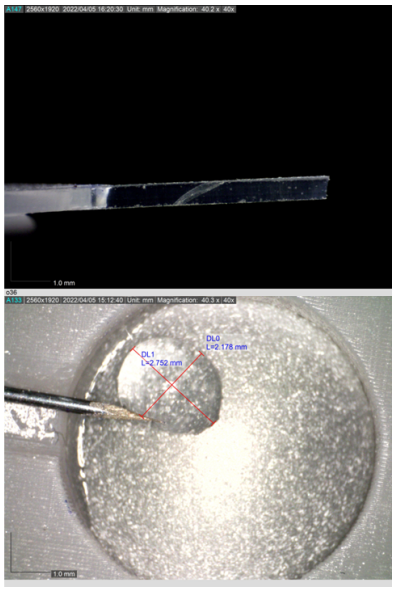

2.47*mm*

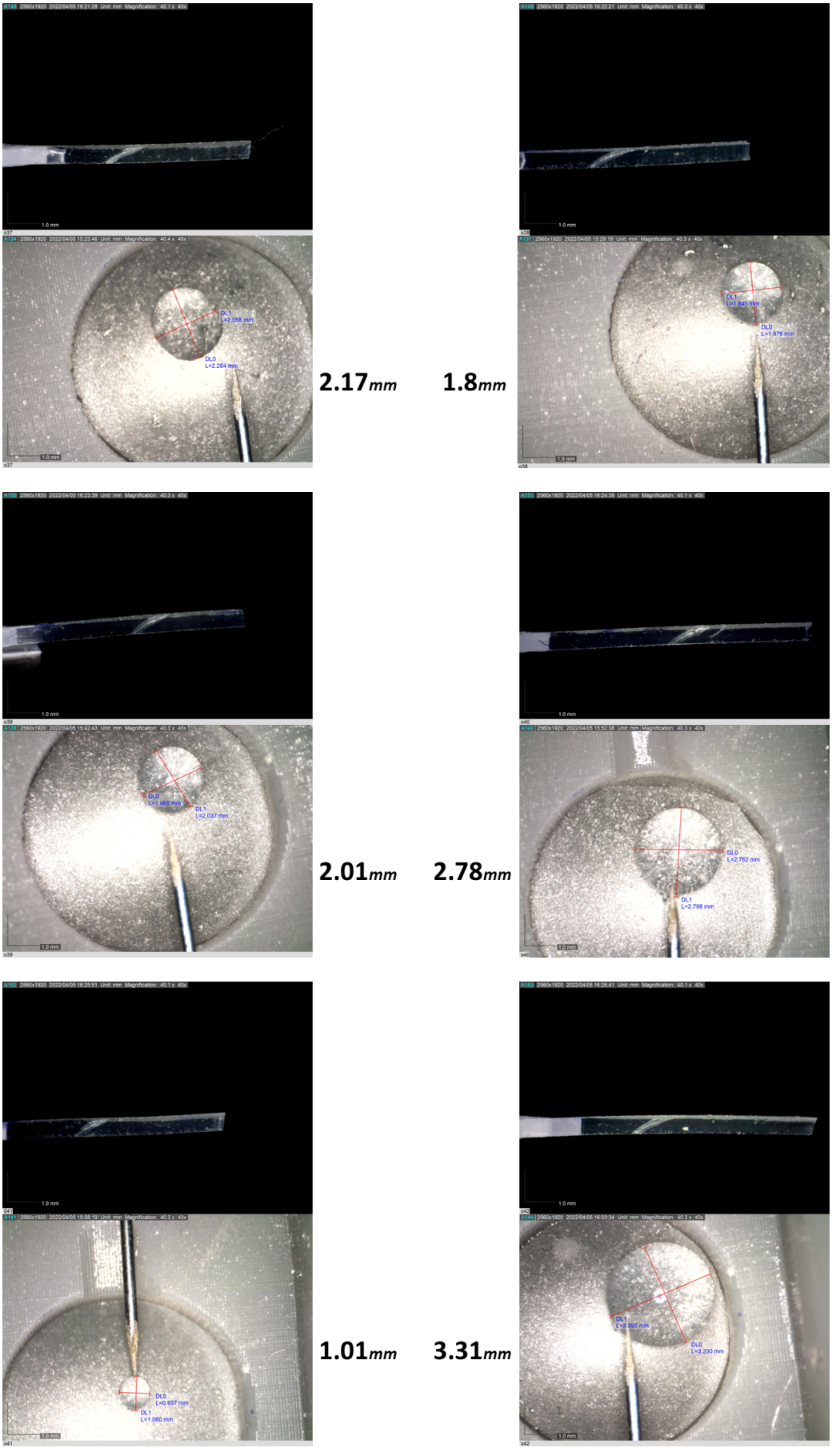

Figure 33: *Oblique incisions and their corresponding droplet size.*

Bi-planar incisions:

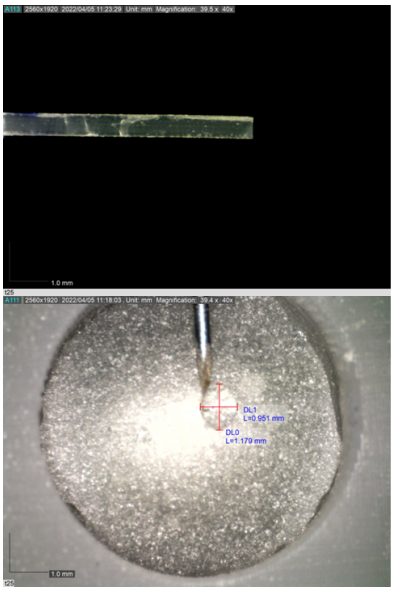

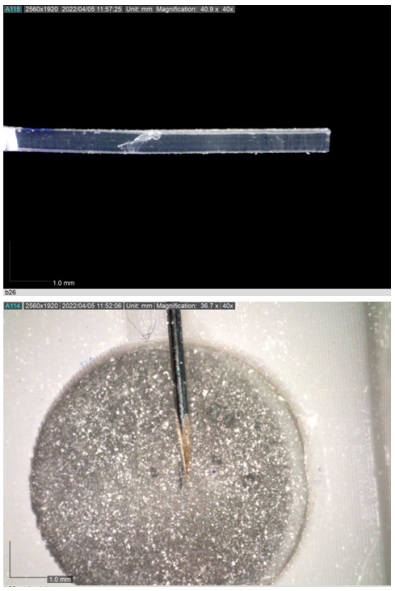

1.07*mm* **0*mm***

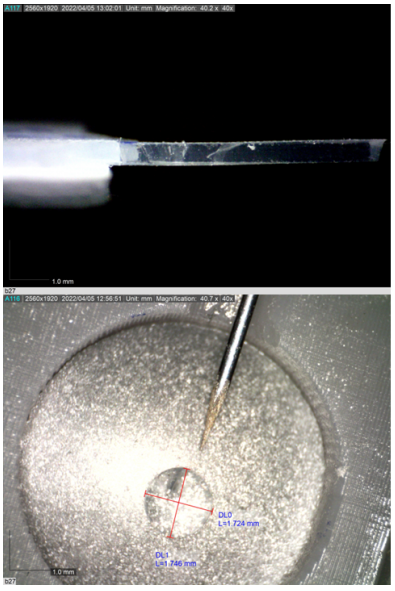

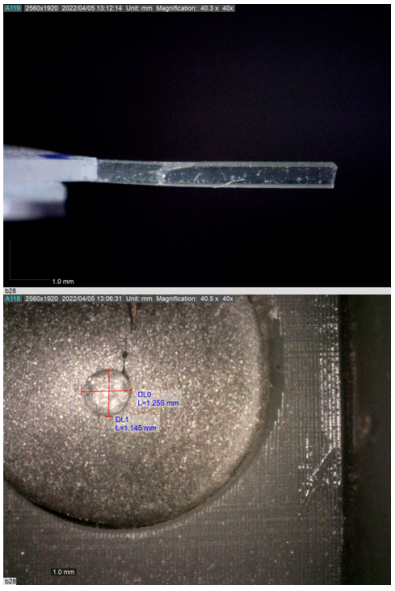

1.73*mm* **1.20*mm***

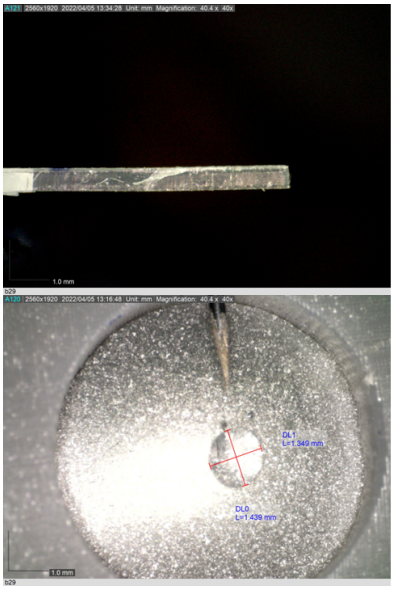

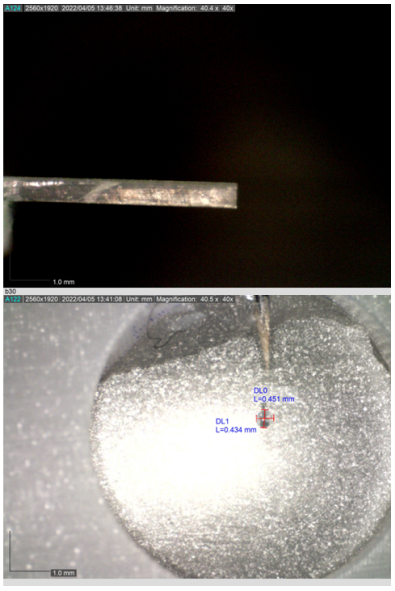

1.4*mm* **0.44*mm***

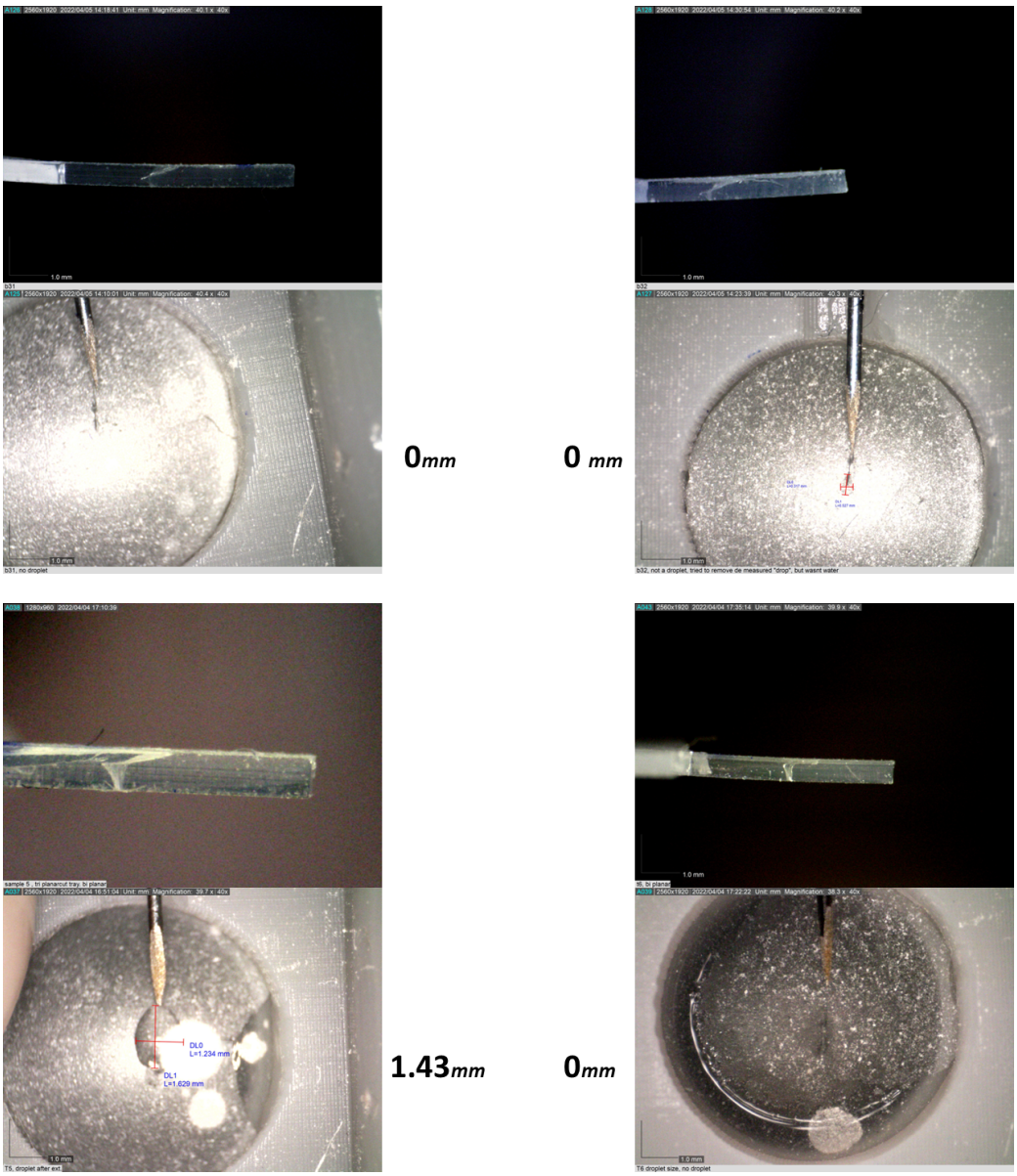

Figure 35: *Bi-planar incisions and their corresponding droplet size.*

Tri-planar 1 incisions:

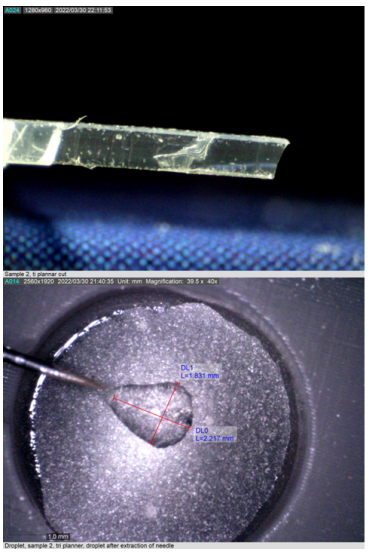

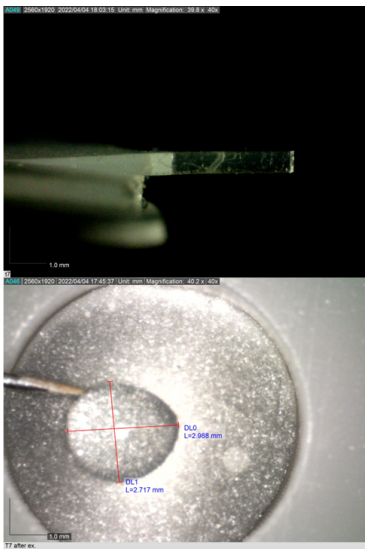

2.03*mm* 2.85*mm*

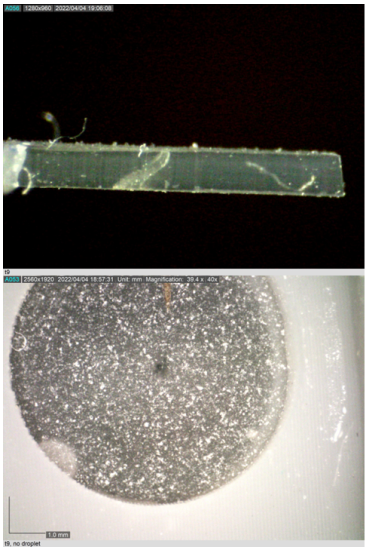

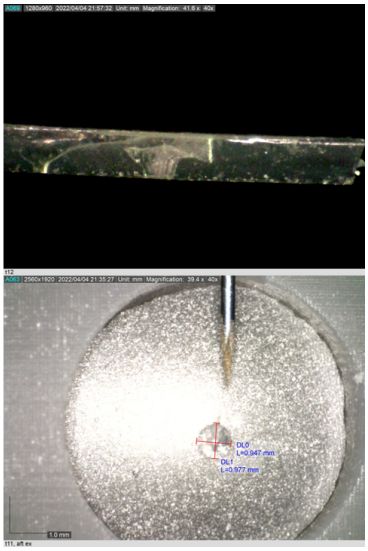

0*mm* 0.962*mm*

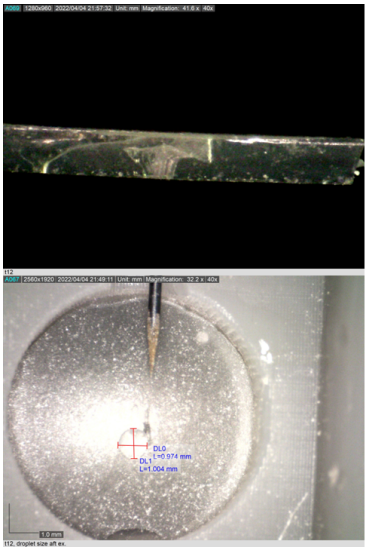

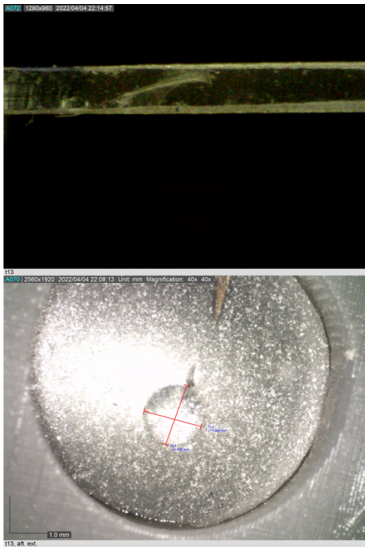

0.99*mm* 1.55*mm*

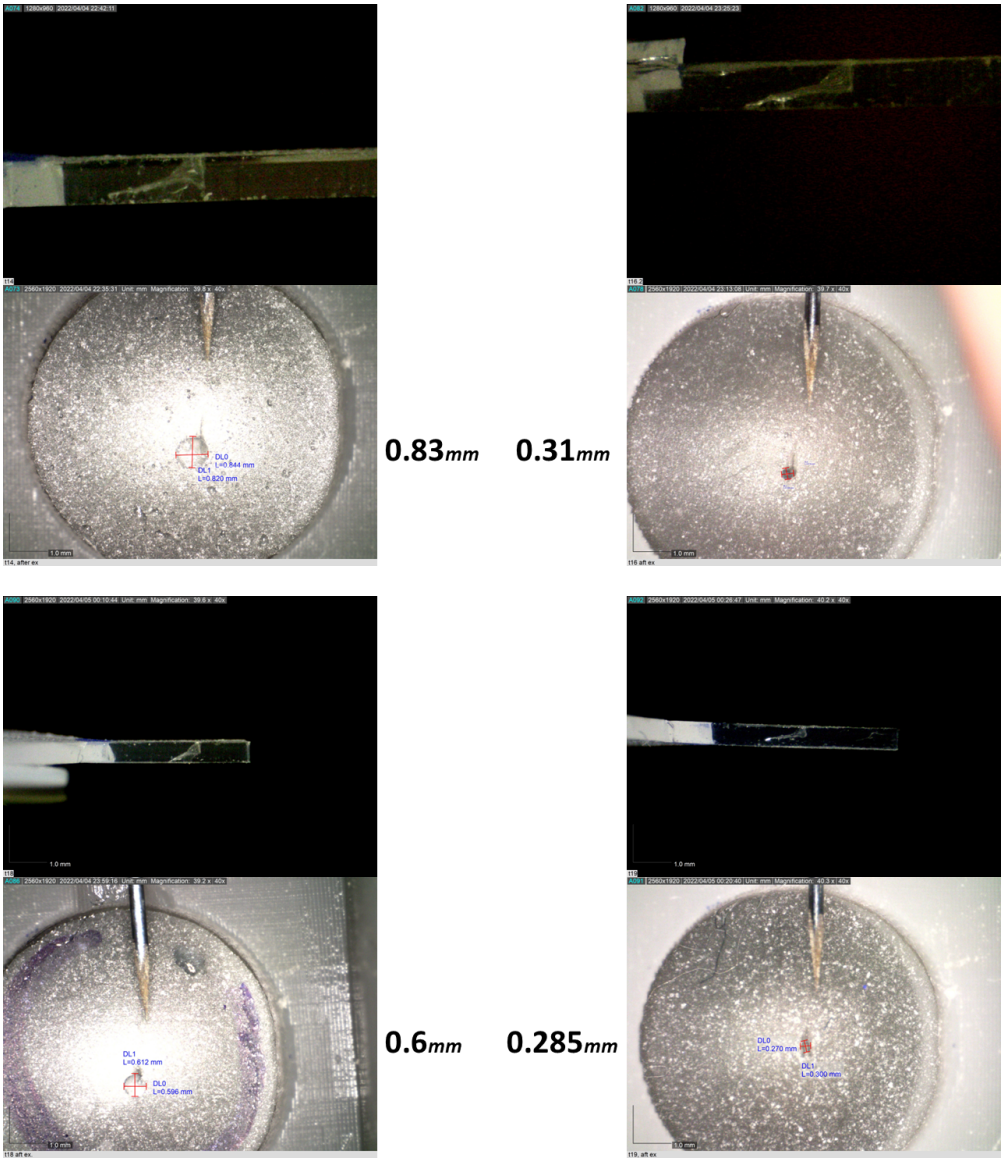

Figure 37: *Tri-planar 1 incisions and their corresponding droplet size.*

Tri-planar 2 incisions:

1.92*mm*

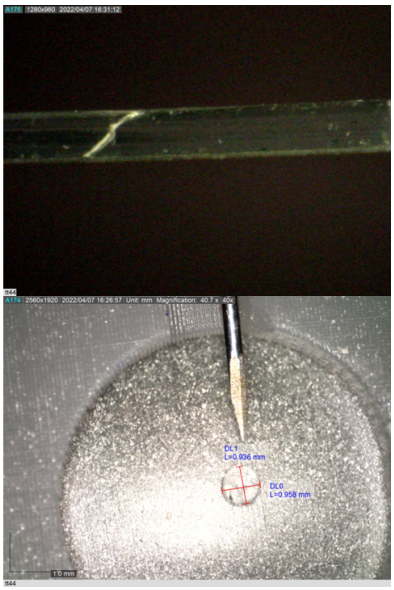

0.95*mm*

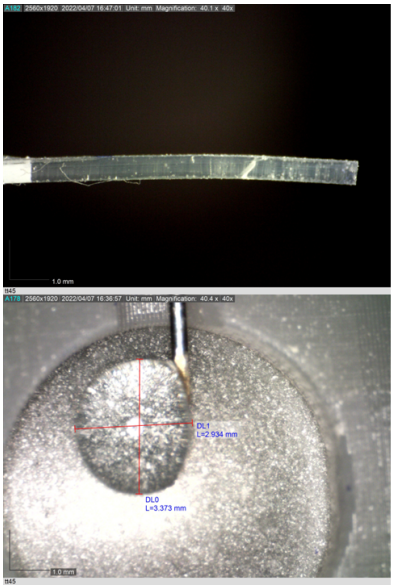

3.15*mm*

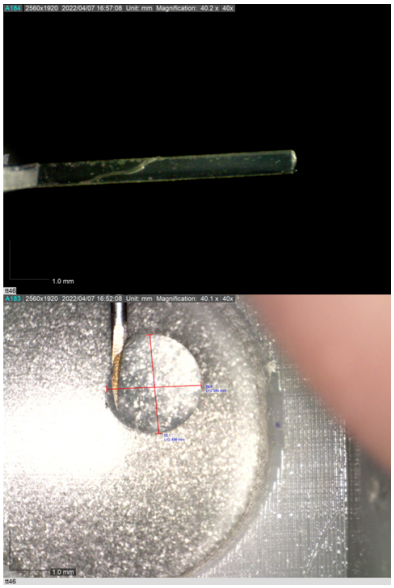

3.44*mm*

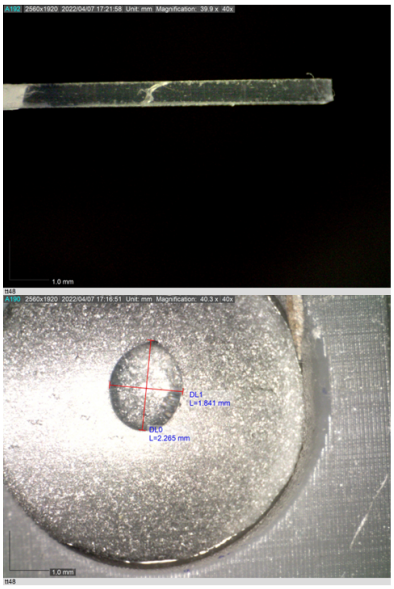

2.21*mm*

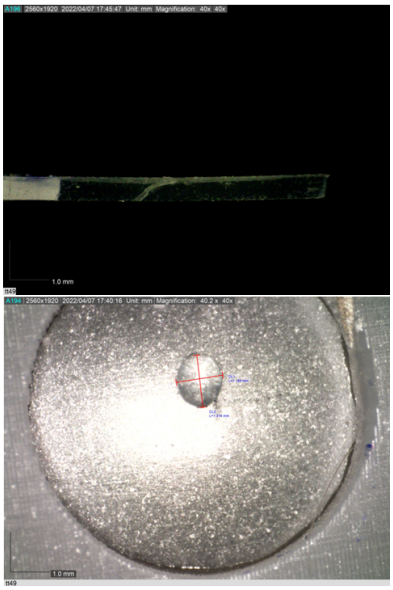

1.25*mm*

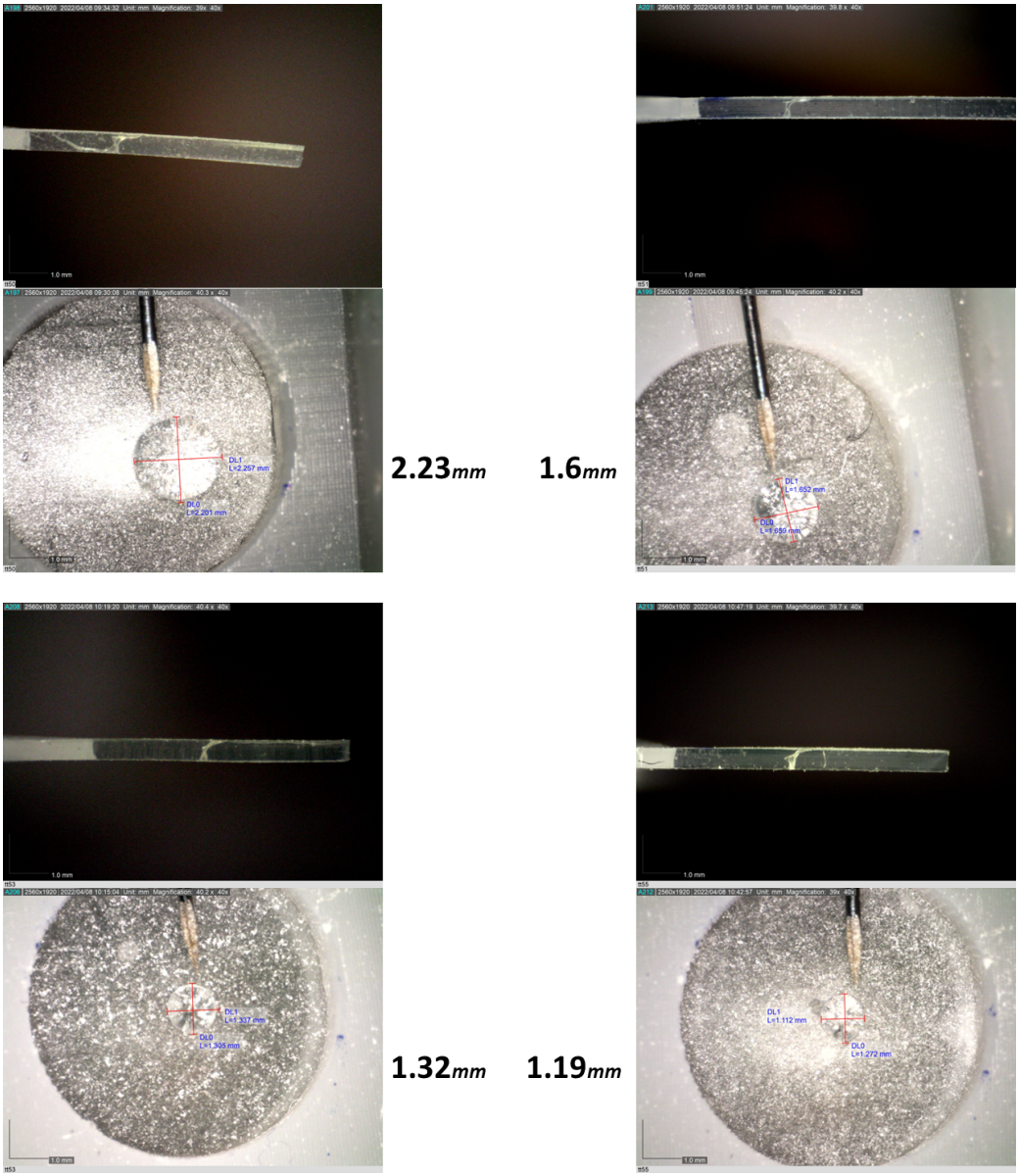

Figure 39: *Tri-planar 2 incisions and their corresponding droplet size.*

APPENDIX B
EYE SUPPORT SOLUTIONS

One of the challenges creating controlled incisions in the eye, is the movement by the eyeball and the movement of the soft tissue of the eye. It is important to have a controlled relative position between the incision location and the incision-knife. This section shows a set of solutions aimed at supporting the ”incision mechanism” relative to the eye.

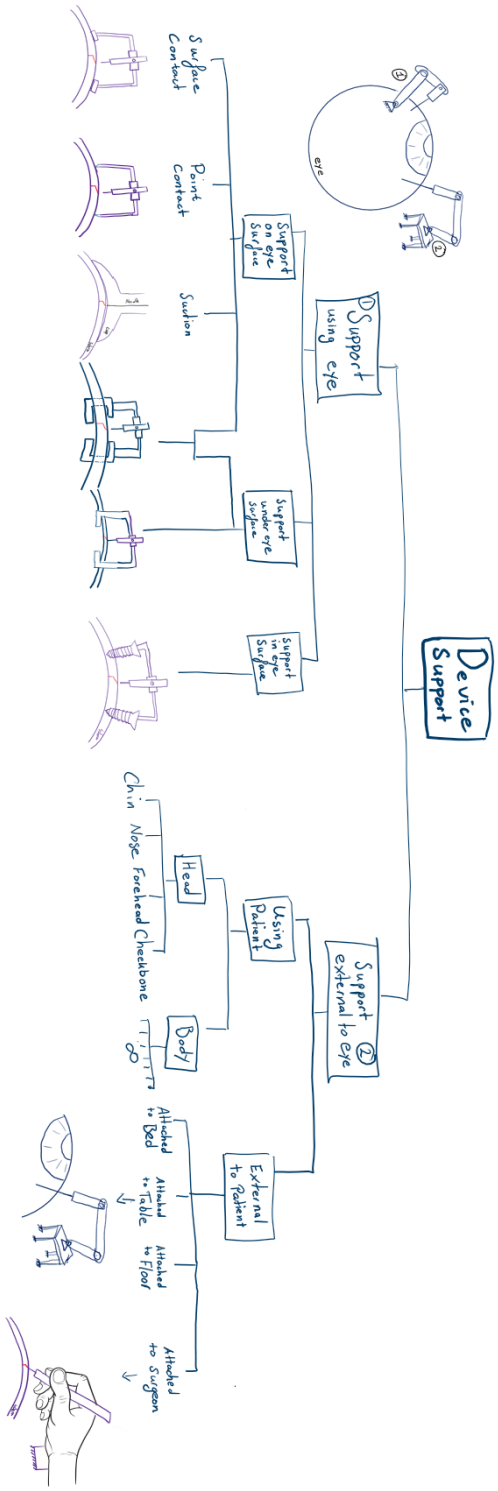

Figure 40: *Tree showing the types of device support.*

APPENDIX C
LINEAR STAGE SOLUTIONS

As discussed in Section 4, linear movement is required to create the desired incision architecture. The tree depicted in this section shows multi solutions to enforce one D.O.F. movement in 2D and can be used during the design process.

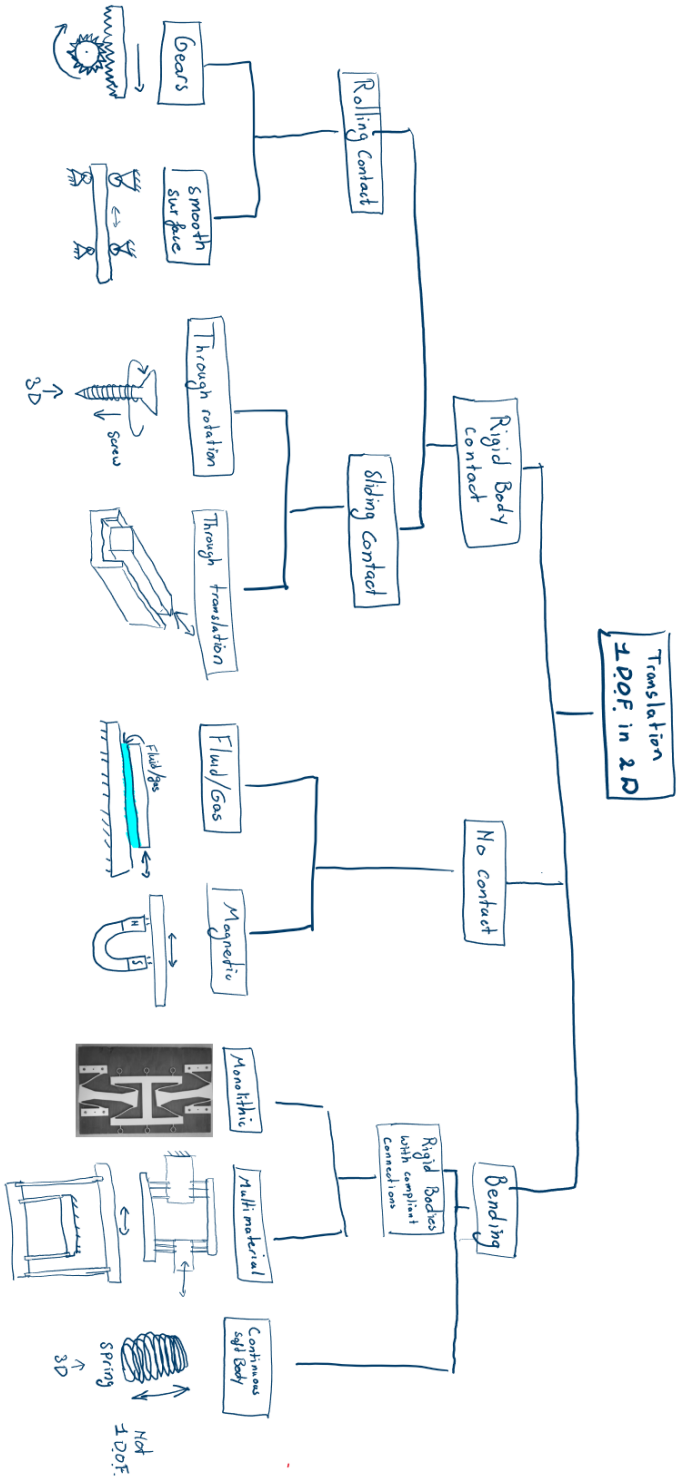

Figure 41: *Tree showing the types of one D.O.F. translation mechanisms.*

APPENDIX D
CALCULATIONS ALLOWABLE PIN-SLOT TOLERANCES

In order for the pin to move through the slots, the width of the slot must be larger than the pin diameter, which creates play in the system. The following section shows what the tolerance of the system must be to guaranty a successful incision. When there is play in the system, the Needle Carrier may deviate from the desired path. This deviation can be in the form of a translation or rotation. While this translation can be neglected, the undesired rotation that occurs must be investigated. This undesired rotation of the Needle Carrier is especially "large" while the carrier moves through the arc. Fig. 42 shows the three types of undesired rotations that are investigated. In upcoming comparisons between three and two pin mechanisms, the rotation as seen in Fig42b is used (this type of rotation causes for the largest deviation at the needle tip).

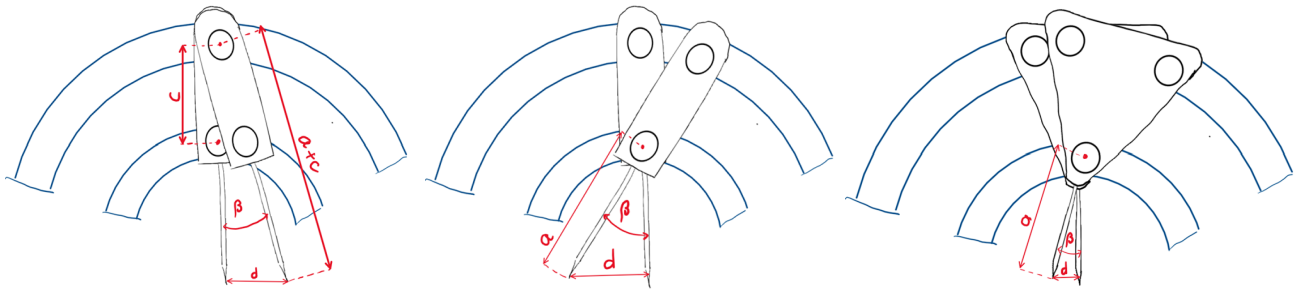

(a) (b) (c)

Figure 42: *Three modes causing play in the systems.*

Due to this play in the system, the location of the needle tip may deviate from the predetermined bi-planar path. This deviation is most critical when the carrier moves from the oblique slot into the arc. If there is to much rotation at this point at the Needle Carrier, the tip of the needle may already penetrate the complete sclera, or leave the sclera surface.

The maximum vertical deviation of the needle tip at this point is $0.125\ mm$. If the tip of the needle exceeds this value, the rotation point of the bi-planar incision, cannot lie within the given boundaries (found in Section 4 and Variables 1) that determine a successful bi-planar incision. Fig.43 shows, with the green dashed lines, the boundaries of the deviation of the needle tip.

The next step is to determine the maximum allowable rotation at the Needle Carrier, in order for the tip of the needle stay within the maximum vertical deviation of $0.125\ mm$. The eventual deviation of the needle tip, depends on the geometry of the Needle Carrier and the tolerance between the pins and the slots. Fig. 44 show the parameters involved in a three pin mechanism and shows the tolerance of the system using parameter: "x". This value represents the space between the pin and the slot.

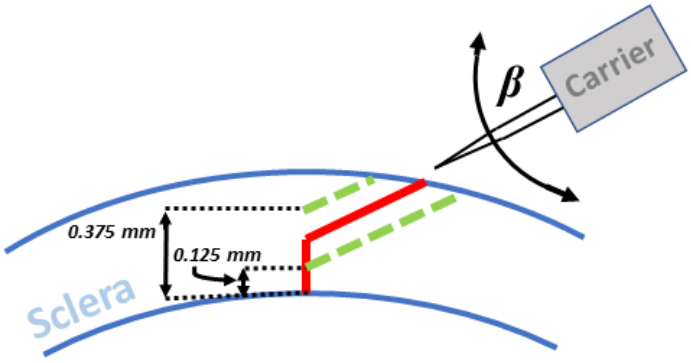

Figure 43: *Allowable height deviation tip of knife for a successful incision.*

The plot seen in Fig. 45 shows on the horizontal axis values for "x", on the vertical axis the corresponding vertical needle tip deviation that. The plot illustrates the superiority of the three pin mechanism over the two pin mechanism, concerning play in the system. The vertical needle tip deviations of two pin mechanism is significantly higher than those of the three pin mechanism, at similar values for "x". The plot shows that one cannot guaranty successful bi-planar incision using a two pin mechanism (with the given geometry). The required value for "x" , thus the required manufacturing technique, is unrealistic.

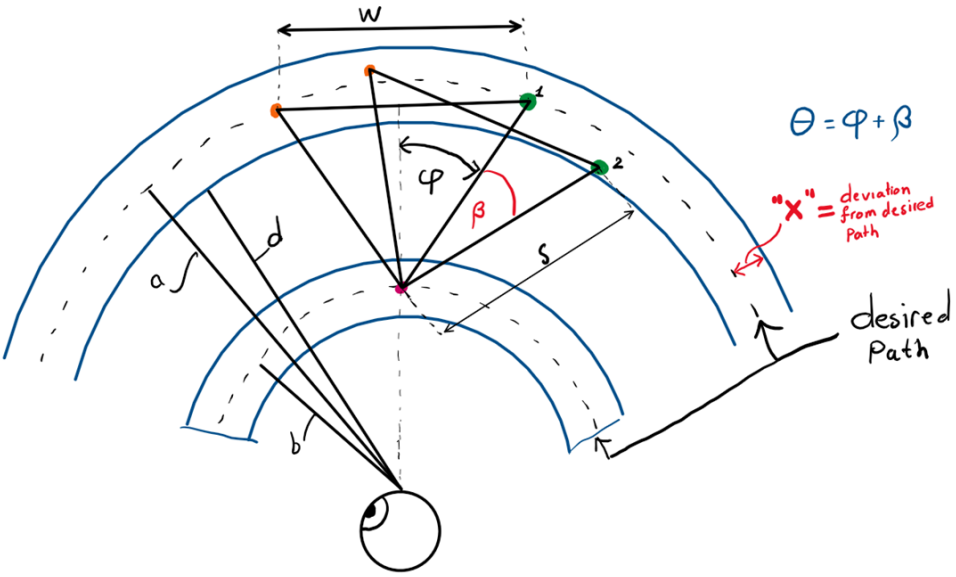

Figure 44: *Parameters required for calculations on a three pin mechanism.*

The plot in Fig. 45 shows that the maximum value for "x" to be $x = 0.0256\ mm$ when using a three pin mechanism. This means, a manufacturing method must be chosen, that guaranties the value of "x" to be larger than $0\ mm$ and smaller than $0.0256\ mm$. For this reason the slots are manufactured by means of electrical discharge wire cutting (EDWC). This method of manufacturing tolerances up to 5 μm can be achieved [37]. The calculation creating the plot of Fig. 45 is found in Fig. 46.

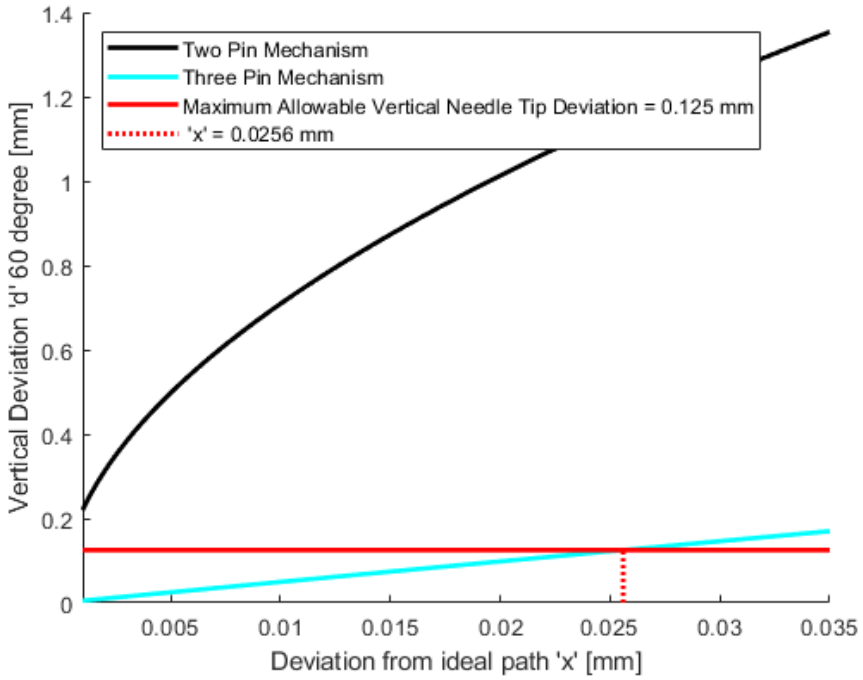

Figure 45: *Plot of the deviation at the needle tip vs deviation from desired path in the slot.*

```
%% Geometry Parameters

x = [0.001:0.0001:0.035];     % "x" = Deviation from desired path

a = 14.25;                    % Disatance from rotation point to large arc
b = 7.5;                      % Disatance from rotation point to small arc
c = a-b;
d = a-x;
e = b+x;
f = b+x;
```

```
%% Three pin parameters
phi = 20.75;
s =(sqrt(2)*sqrt(2.*(a.^2)+(b.^2)*cosd(2.*phi)-(b.^2))-2.*b.*cosd(phi))./(2.*((sind(phi).^2)+(cosd(phi).^2)));
w = 2*s*sind(phi);
```

```
%%
Beta2 = acosd(((-(c.^2)+d.^2-(e.^2)))./(2.*e.*c));  % Rotation of needle carrier, two pin mechanism

Theta = acosd(((d.^2)-(b.^2)-(s.^2))./(2.*b.*s));
Beta3 = Theta-phi;                                  % Rotation of needle carrier, Three pin mechanism


Heightdeviation2 = b.*sind(30)-b.*sind(30-Beta2);   % Hight deviation at tip of knife at an angle of
                                                    % 60 degree two pin mechanism
Heightdeviation3 = b.*sind(30)-b.*sind(30-Beta3);   % Hight deviation at tip of knife at an angle of
                                                    % 60 degree three pin mechanism


 figure
 hold on
plot(x,Heightdeviation2,'k',"LineWidth",2)
plot(x,Heightdeviation3,'c',"LineWidth",2)
plot([0.001 0.035], [0.125 0.125],'r',"LineWidth",2)
plot([0.0256 0.0256], [0 0.125],':r',"LineWidth",2)
xlim([0.001, 0.035])
xlabel("Deviation from ideal path 'x' [mm]")
ylabel("Hight Deviation 'd' 60 degree [mm]")
legend("Two Pin Mechanism", "Three Pin Mechanism", "Maximum Allowable Height Deviation"," 'x' = 0.256 mm")
```

Figure 46: *Matlab script needle tip deviation.*

APPENDIX E
DESIGN EVOLUTION

This section shows the evolution towards the eventual prototype. Firstly, a cardboard version (i.e., A) was created to study the kinematics of the path generator and actuation of the movement. Secondly, a fully 3D-printed PLA version (i.e., B) was made at scale to further examine the working principle of the mechanism and improve understanding of the critical areas. Thirdly, the final prototype (i.e., C) was developed as is described in Section 4.

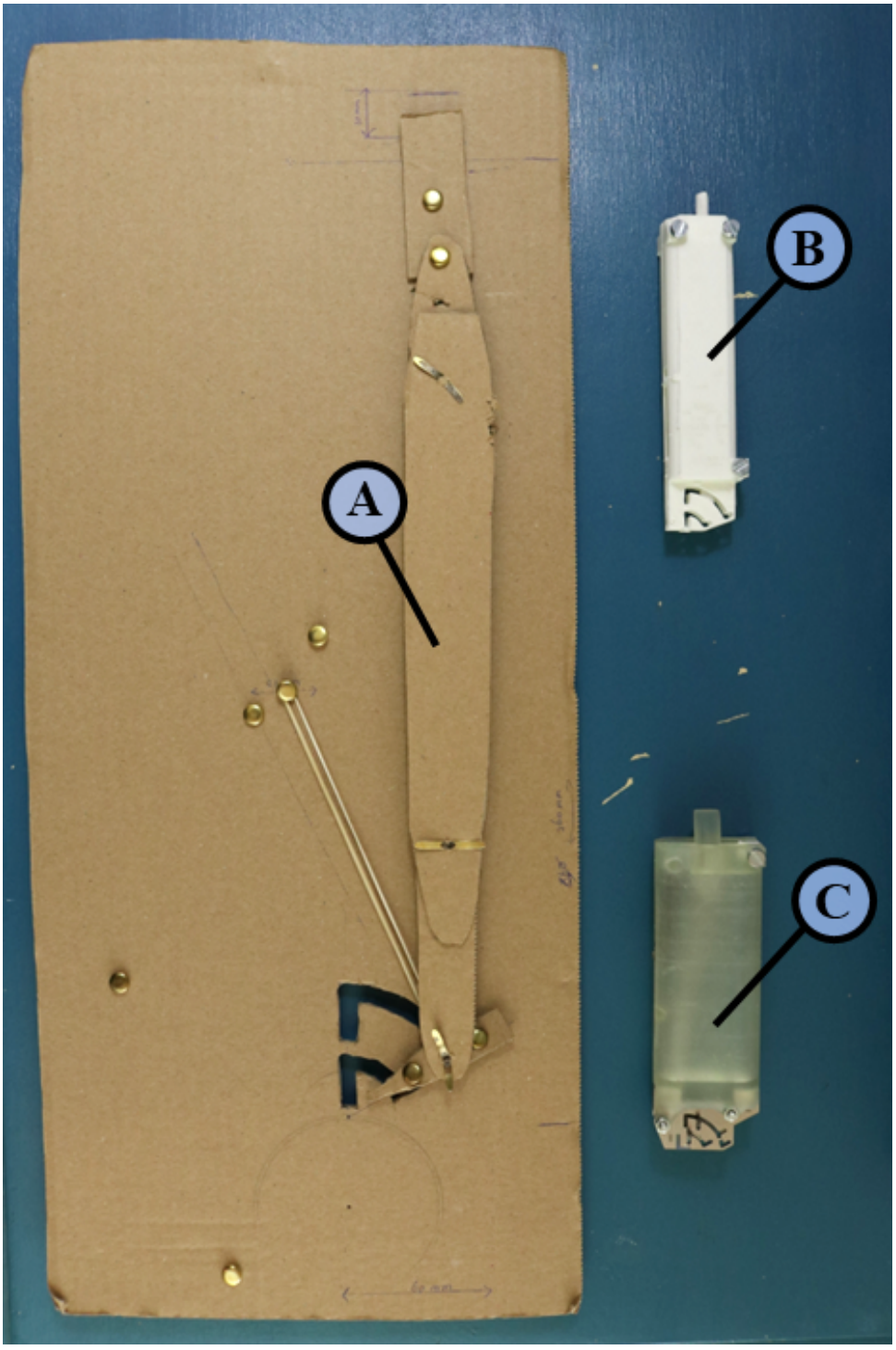

Figure 47: *Design evolution. A) A cardboard kinematic model. B) A fully 3D-printed PLA version. C) The final prototype.*

APPENDIX F
INCISIONS BI-PLANAR INCISION MECHANISM

This section shows 25 bi-planar incisions made by the five participant using the Bi-planar Incision Mechanism, as analyzed in Section 5. Firstly, the side views including the dimensions of the individual incisions are shown. Secondly, the data on the dimensions of the individual incisions are summarized in Table 7.

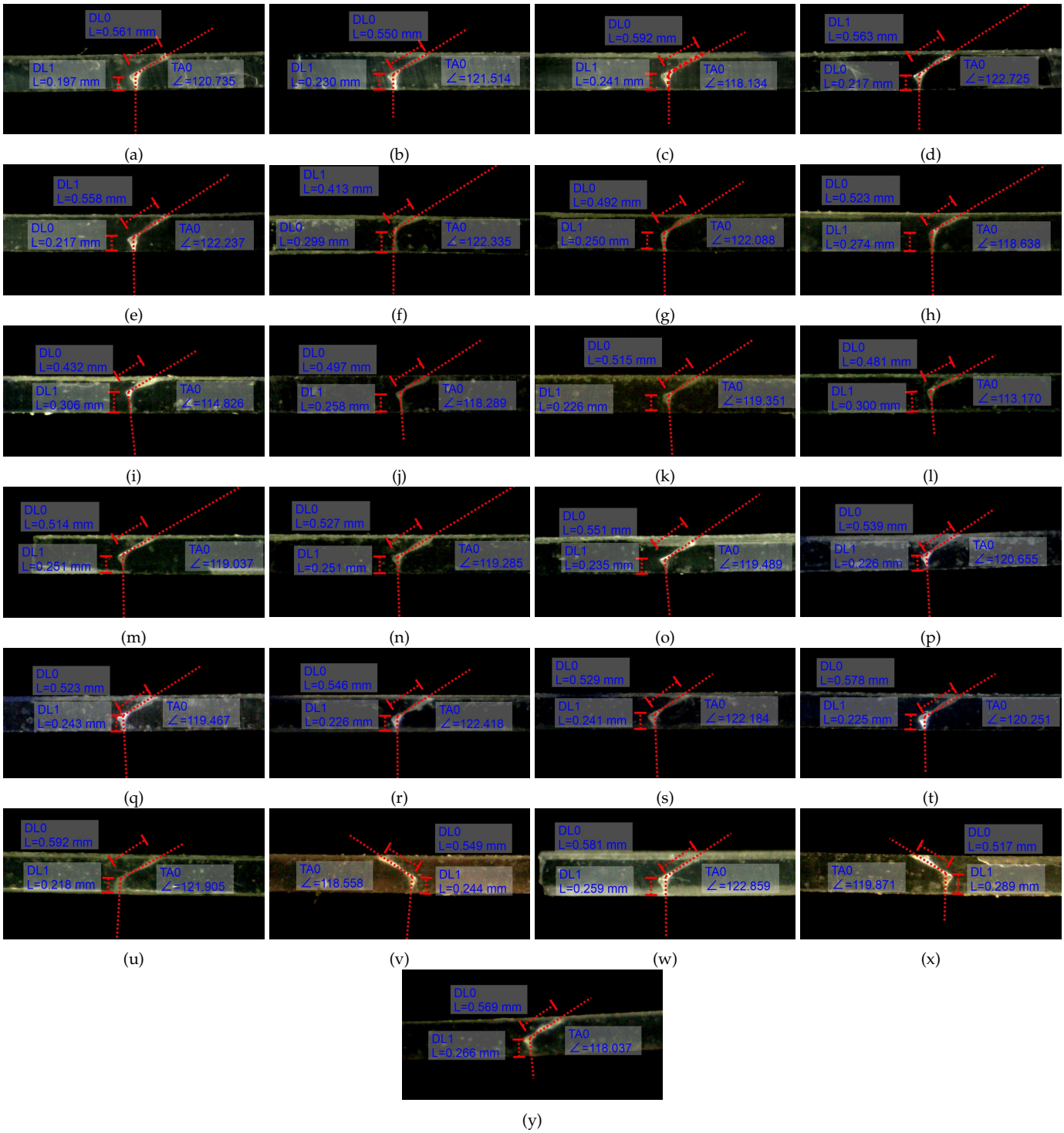

Figure 48: *Bi-planar Mechanism incisions.*

Sample Name	Length Oblique $[mm]$	Length Vertical $[mm]$	Angle $[degree]$	Time $[s]$
L6	0.561	0.197	59.265	7
L7	0.55	0.23	58.486	5
L8	0.553	0.241	61.866	9
L9	0.563	0.217	57.275	8
L10	0.558	0.217	57.77	7
M6	0.413	0.299	57.665	4
M7	0.492	0.25	57.912	3
M8	0.523	0.274	61.362	5
M9	0.432	0.306	65.174	4
M10	0.497	0.258	61.711	4
MY6	0.515	0.226	60.649	5
MY7	0.481	0.300	66.83	4
MY8	0.514	0.251	60.963	5
MY9	0.527	0.251	60.715	3
MY10	0.551	0.235	60.511	3
T6	0.539	0.226	59.345	4
T7	0.523	0.243	60.533	5
T8	0.546	0.226	57.582	6
T9	0.529	0.241	57.816	5
T10	0.578	0.225	59.749	5
J6	0.592	0.218	58.095	6
J7	0.549	0.244	61.442	5
J8	0.581	0.259	57.141	4
J9	0.517	0.289	60.129	4
J10	0.569	0.266	61.963	4

Table 7: *Data individual measurements Bi-Planar Incision Mechanism.*

APPENDIX G
INCISIONS REFERENCE MULTI-PLANAR INCISION DEVICE BY KOOT

This section shows 25 bi-planar incisions made by the five participant using the reference device by Koot [9], as analyzed in Section 5. Firstly, the side views including the dimensions of the individual incisions are shown. Secondly, the data on the dimensions of the individual incisions are summarized in Table 8.

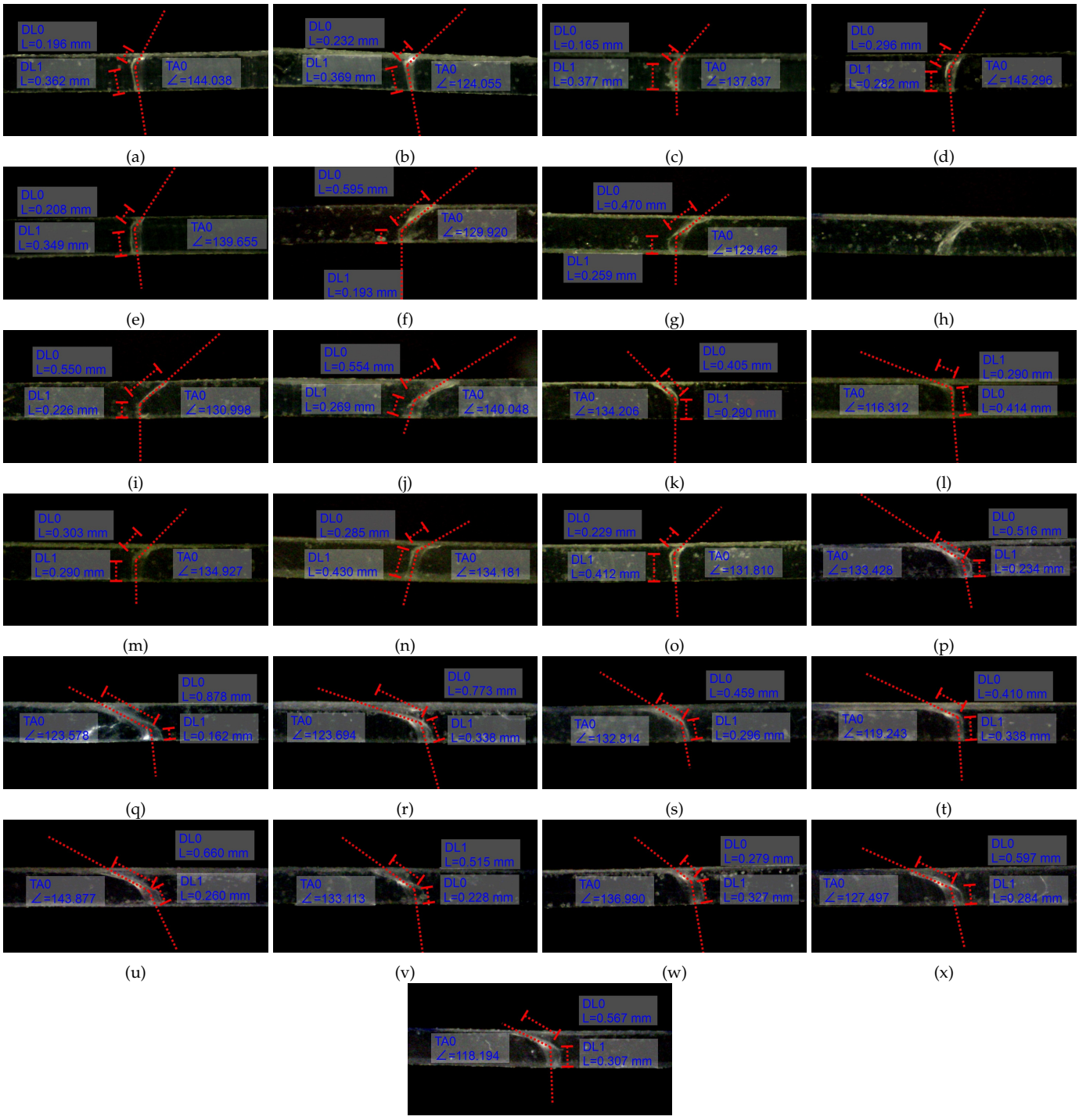

Figure 49: *Incisions reference multi-planar incision device.*

Sample Name	Length Oblique $[mm]$	Length Vertical $[mm]$	Angle $[degree]$	Time $[s]$
L1	0.196	0.362	35.962	32
L2	0.232	0.369	55.945	35
L3	0.165	0.377	42.163	31
L4	0.296	0.282	34.704	43
L5	0.208	0.349	40.345	36
M1	0.595	0.193	50.08	41
M2	0.47	0.259	50.538	32
M3	One Plane			36
M4	0.55	0.226	49.002	38
M5	0.554	0.269	39.952	32
MY1	0.405	0.29	45.794	38
MY2	0.29	0.414	63.688	47
MY3	0.303	0.29	45.073	33
MY4	0.285	0.43	45.819	36
MY5	0.229	0.412	48.19	35
T1	0.516	0.234	46.572	36
T2	0.878	0.162	56.422	33
T3	0.773	0.338	56.306	49
T4	0.459	0.296	47.176	35
T5	0.410	0.338	60.757	41
J1	0.660	0.260	36.123	43
J2	0.515	0.228	46.887	46
J3	0.279	0.327	43.010	37
J4	O.597	0.284	52.503	36
J5	0.567	0.307	61.806	28

Table 8: *Data individual measurements reference device.*

APPENDIX H
ALTERNATIVE DESIGN

In the Bi-Planar Incision Mechanism the linear movements are actuated by the surgeon, while the rotation of the needle is enforced by a spring force. The following alternative design shows the opposite; the surgeon is responsible for the rotation and the spring actuates the linear movement. Fig. 50a shows this system. The blue part is the Base of the system and rests on the surface of the eye. The Base has an Axle, two Bumpers, and two Rings. The index finger and the middle finger can be position in the two blue Rings. The yellow part is the Housing of the system. The housing is able to rotate around the Axle of the Base, the thumb of the surgeon can be placed in the yellow Ring. Inside the Housing, a spring and the Needle Carrier is found. The Needle Carrier is able to translate inside the Housing. Incorporated in the Needle Carrier are two Buttons, if a large enough force is applied to the Button, the arm below the Button will elastically deform. Fig. 50b to Fig. 50d show the steps creating the bi-planar architecture. At first the Needle Carrier is not able to move through the Housing since Button 1 stays stuck behind a hole in the Housing. For the Needle Carrier to move the Button must be pushed inwards. The Bumpers facilitate an inward push when the surgeon rotates the Housing against them, thereby allowing the spring to push the Needle Carrier through the Housing. The Bumpers are located such that when the Bumpers activate the system, the Needle Carrier is at the desired angle which is equal to one of the planes of the bi-planar architecture. Fig. 50b shows the first step, the surgeon rotates the yellow Housing towards Bumper 1. Bumper 1 will push Button 1 inwards causing the Needle Carrier and the attached needle to shoot downwards, thereby creating the oblique incision plane. The Needle Carrier can only moved a certain distance in the oblique direction due to Button 2. The Needle Carrier will stop when Button 2 reaches the hole in the Housing. The Housing must now be rotated to a vertical position, as seen in Fig. 50c. Bumper 2 will push Button 2 inwards which allows the spring to push the Needle Carrier all the way down creating the perpendicular incision plane, as shown in Fig. 50d.

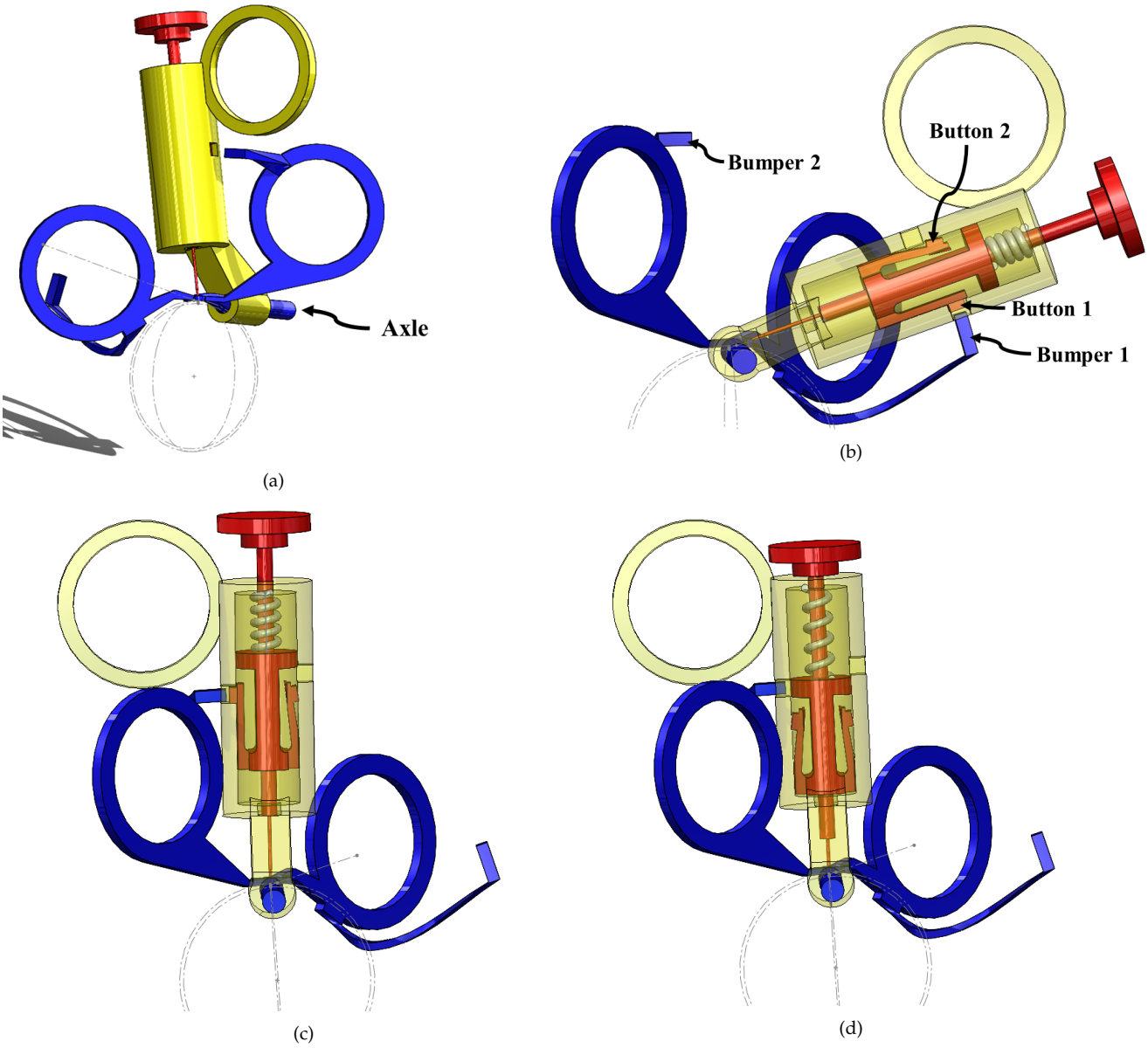

Figure 50: *(a) The alternative design, including the Base in blue, the Housing in yellow and the Needle Carrier in red. (b) Step 1, the yellow Housing is rotated towards Bumper 1, Bumper 1 pushes Button 1 inwards, allowing the Needle Carrie to translate through the Housing, thereby making the oblique incision. (c) Step 2, the Housing is rotated to a vertical position. Bumper 2 pushes Button 2 inwards, allowing the Needle Carrier to translate and create the perpendicular incision. (c) The final position of the Needle Carrier.*

APPENDIX I
TECHNICAL DRAWINGS

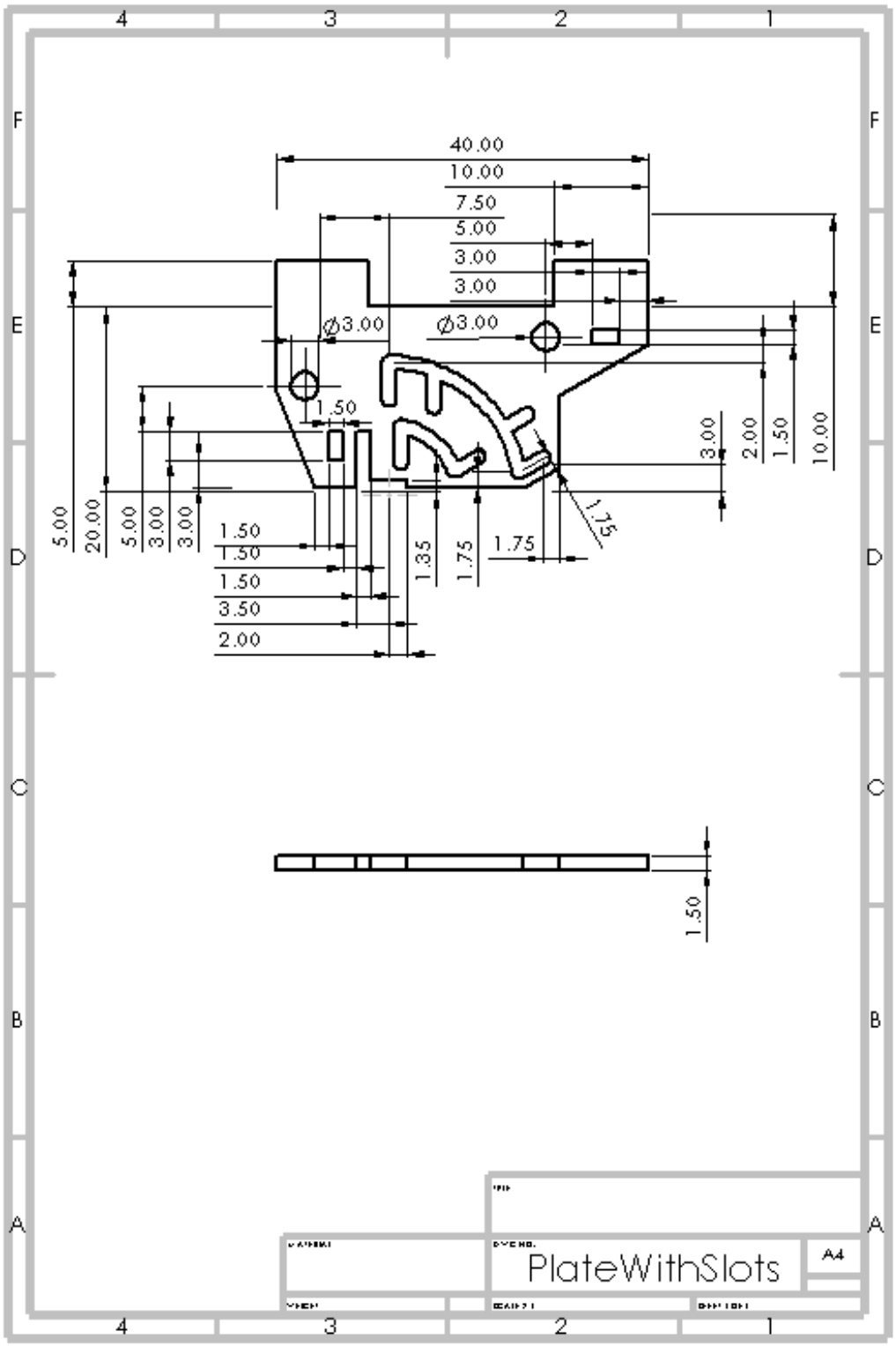

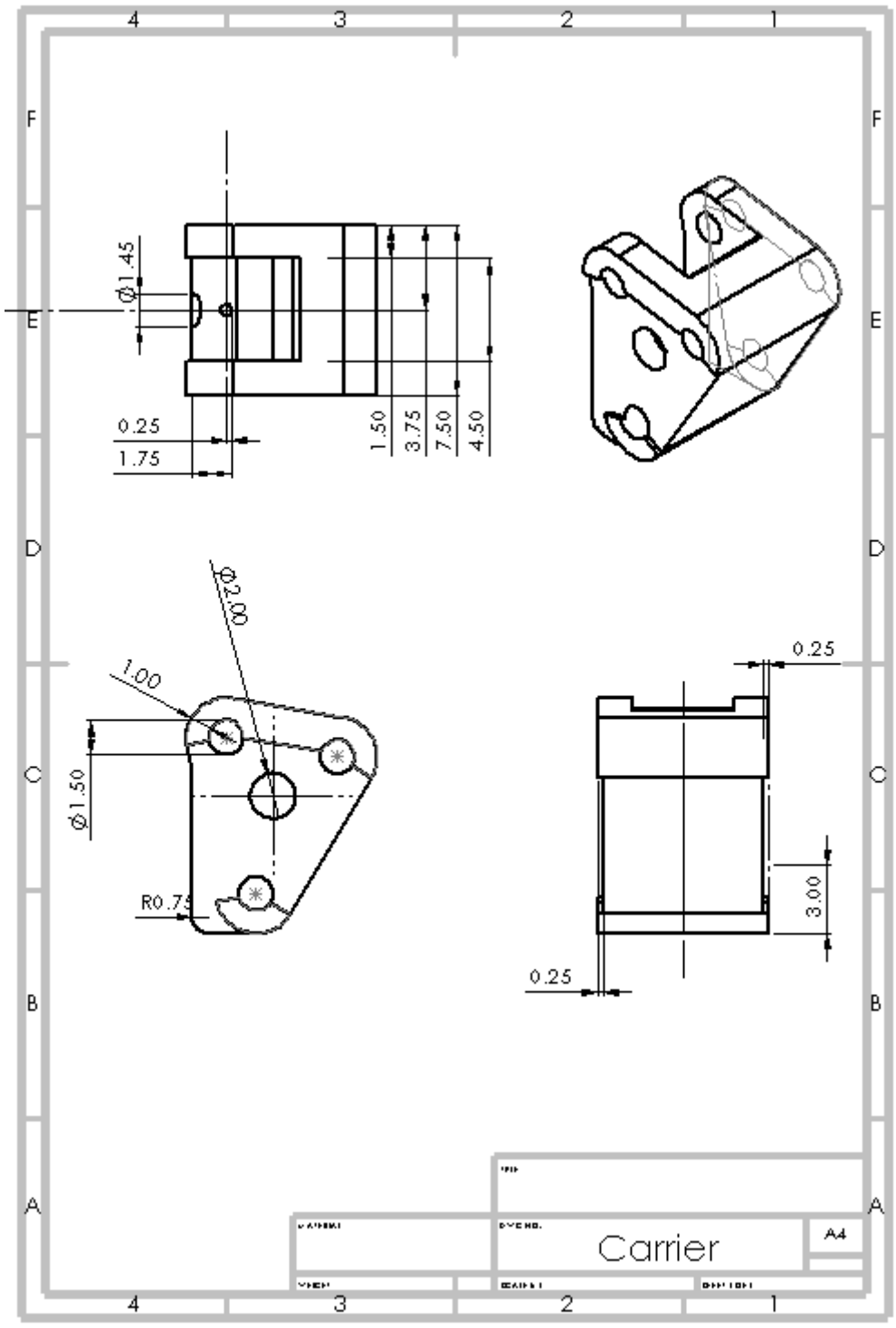
4
3
2
1
F
E
D
C
B
A
Ø1.45
0.25
1.75
1.50
3.75
7.50
4.50
Ø2.00
1.00
Ø1.50
R0.75
0.25
3.00
0.25
Carrier
A4

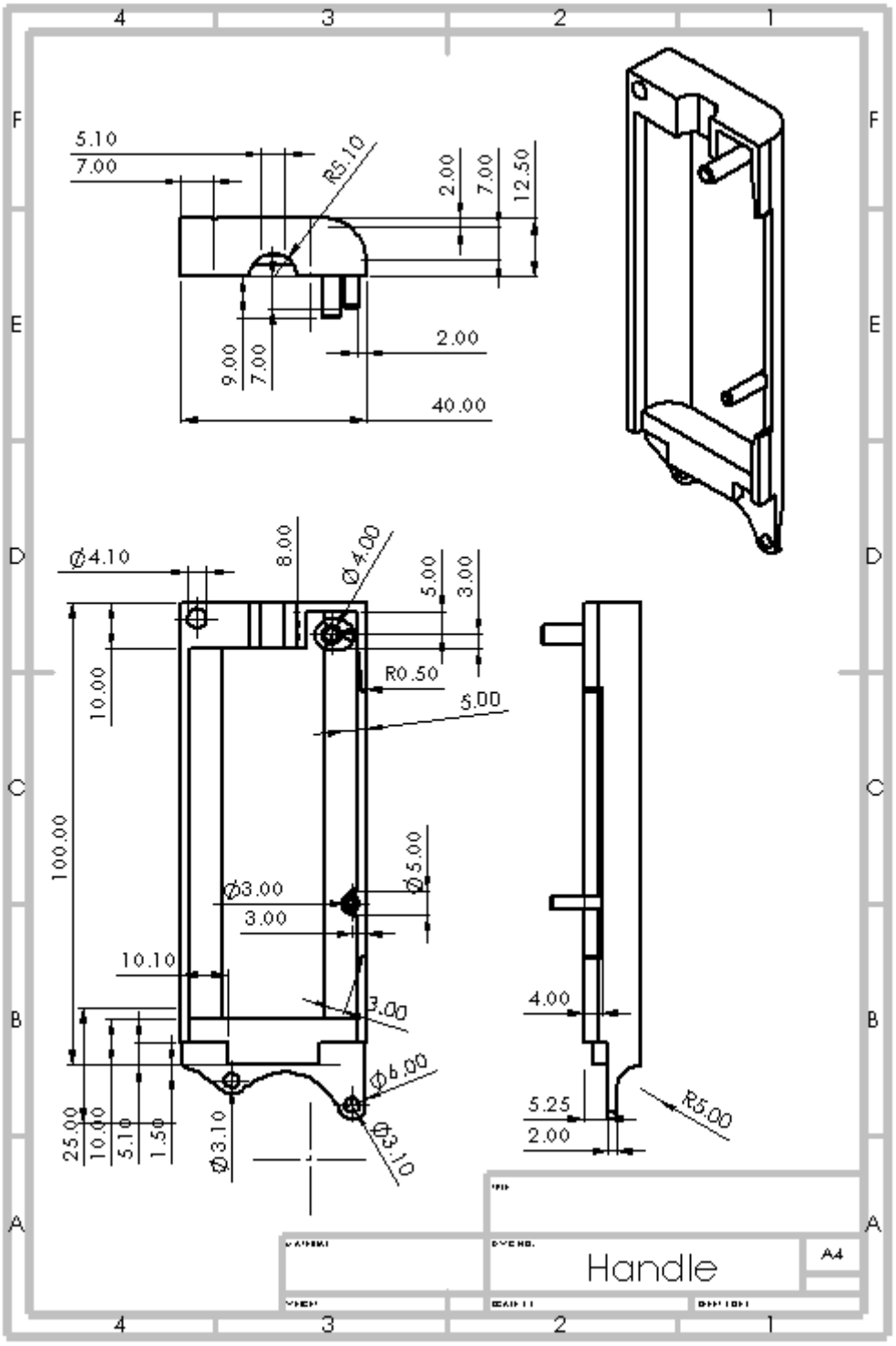
5.10
7.00
R5.10
2.00
7.00
12.50
2.00
9.00
7.00
40.00
Ø4.10
8.00
Ø4.00
5.00
3.00
R0.50
5.00
10.00
100.00
Ø5.00
Ø3.00
3.00
10.10
3.00
Ø6.00
Ø3.10
25.00
10.00
5.10
1.50
Ø3.10
4.00
5.25
2.00
R5.00
Handle
A4

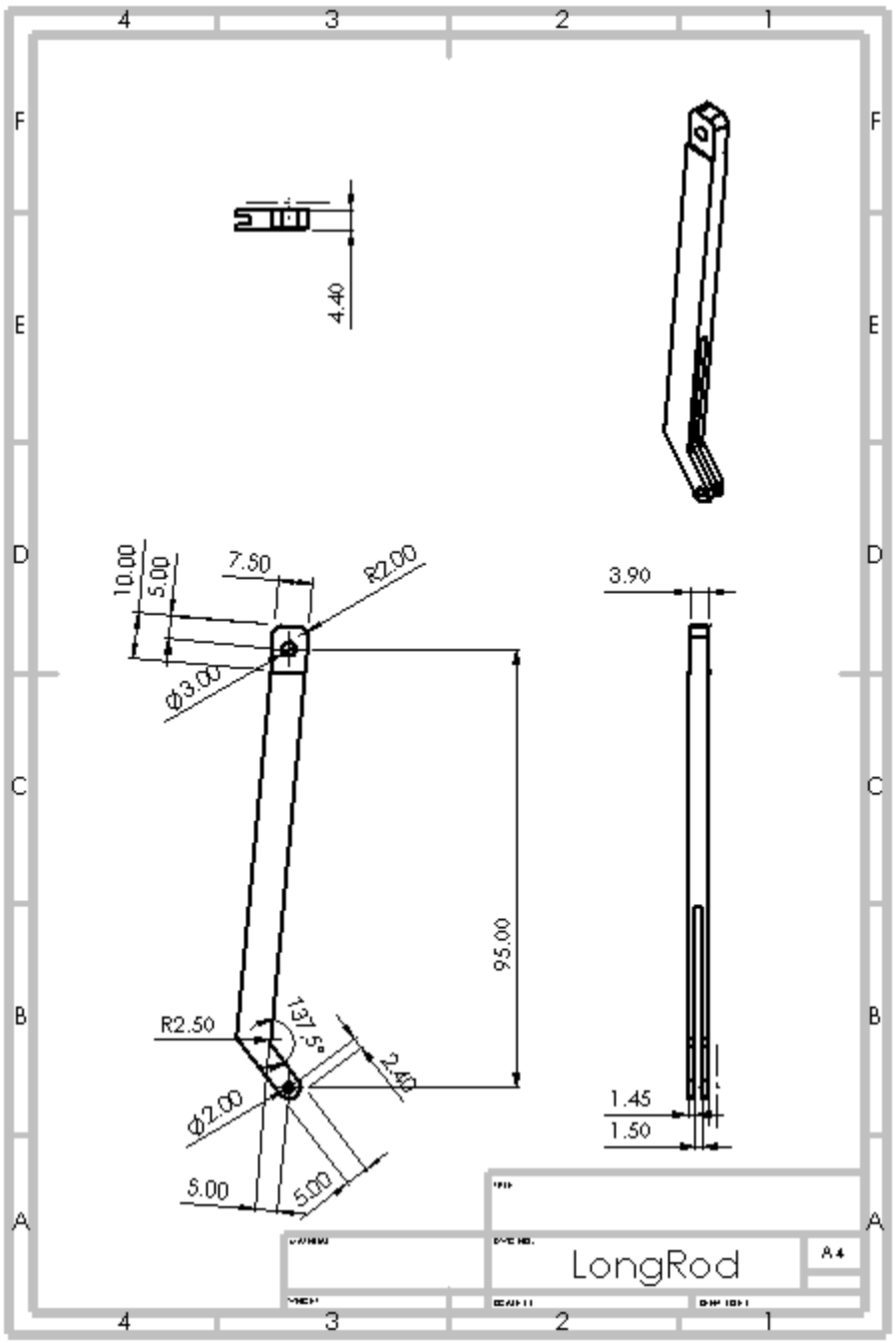
4.40
10.00
5.00
7.50
R2.00
Ø3.00
95.00
R2.50
137.5°
2.40
Ø2.00
5.00
5.00
3.90
1.45
1.50
LongRod
A4

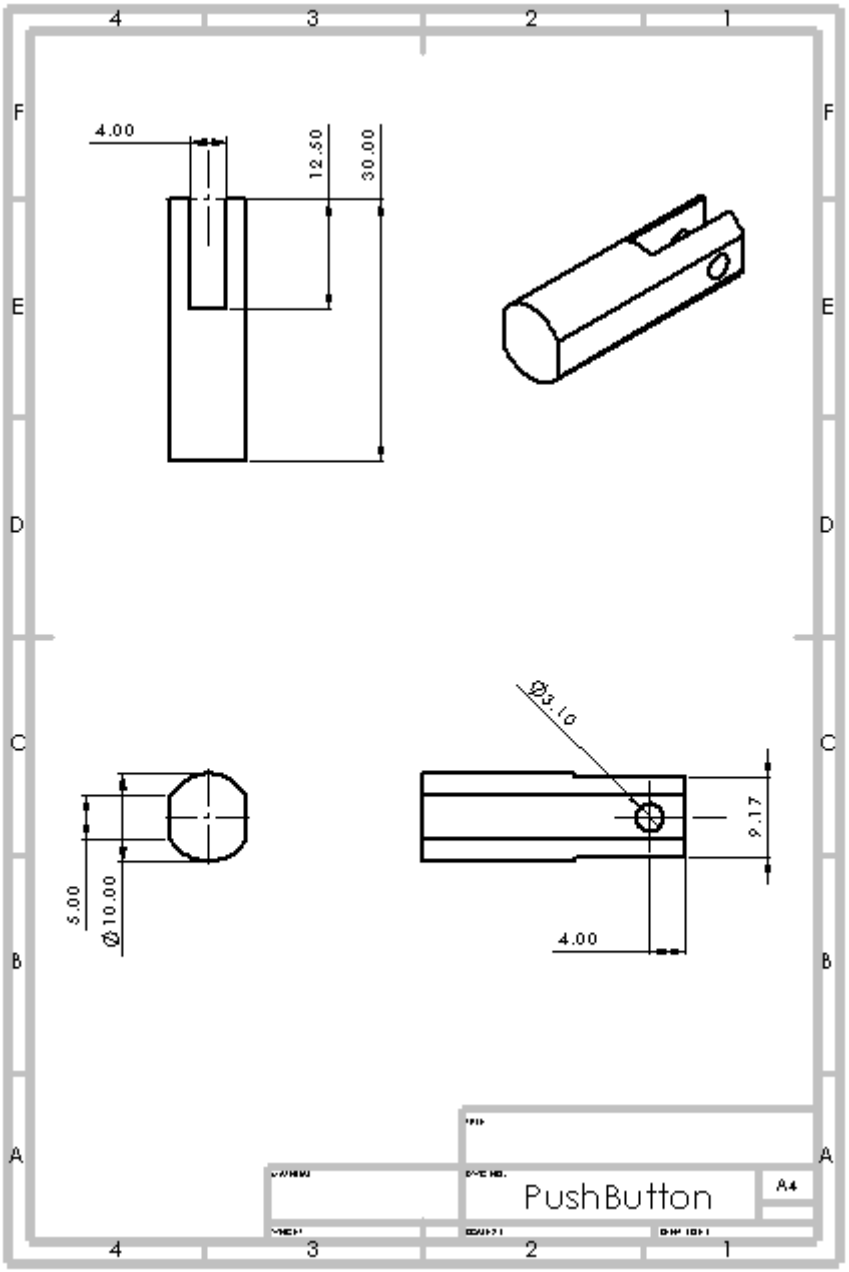
4.00
12.50
30.00
Ø3.10
9.17
4.00
5.00
Ø10.00
PushButton
A4

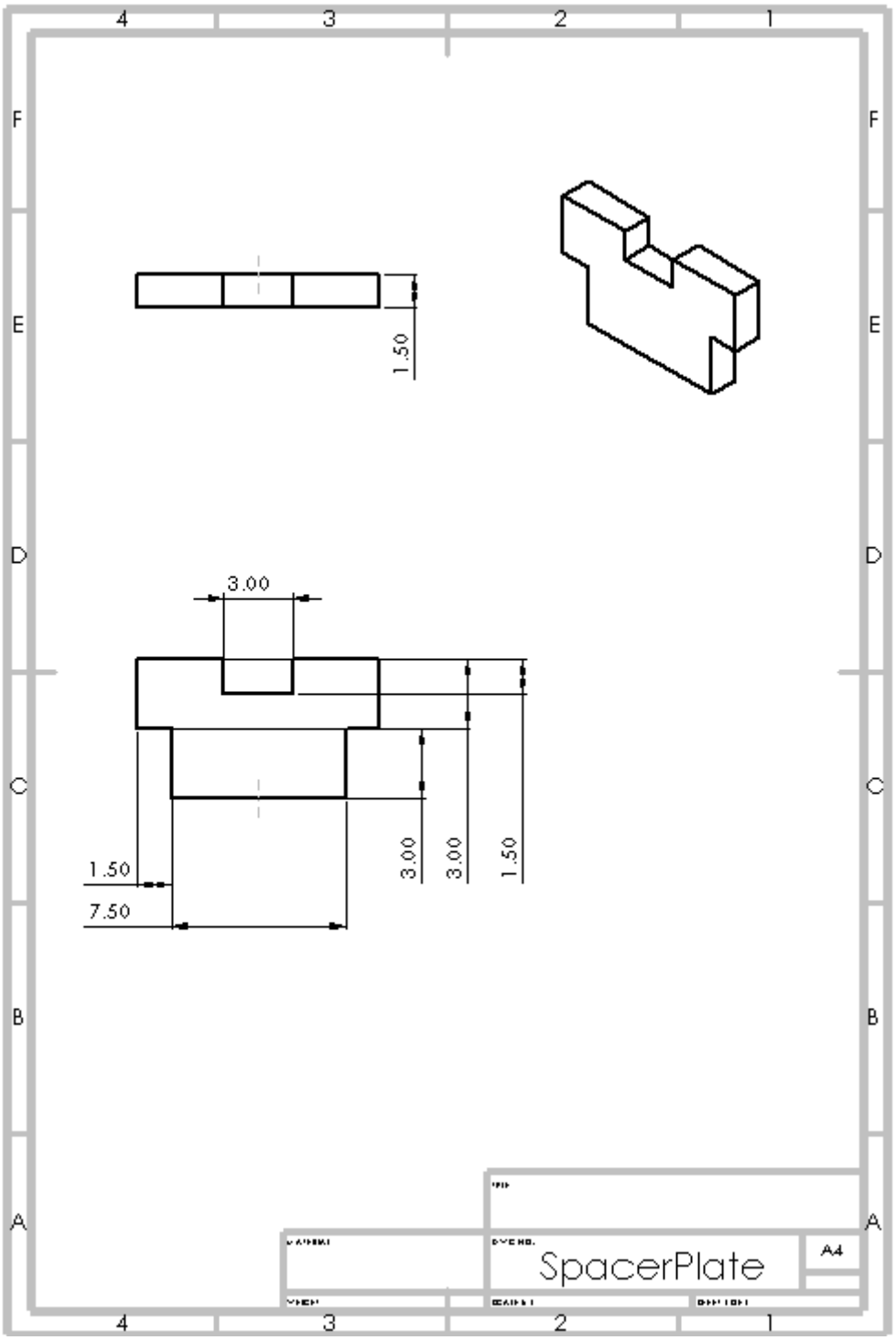
4
3
2
1
F
E
D
C
B
A
1.50
3.00
3.00
3.00
1.50
7.50
SpacerPlate
A4

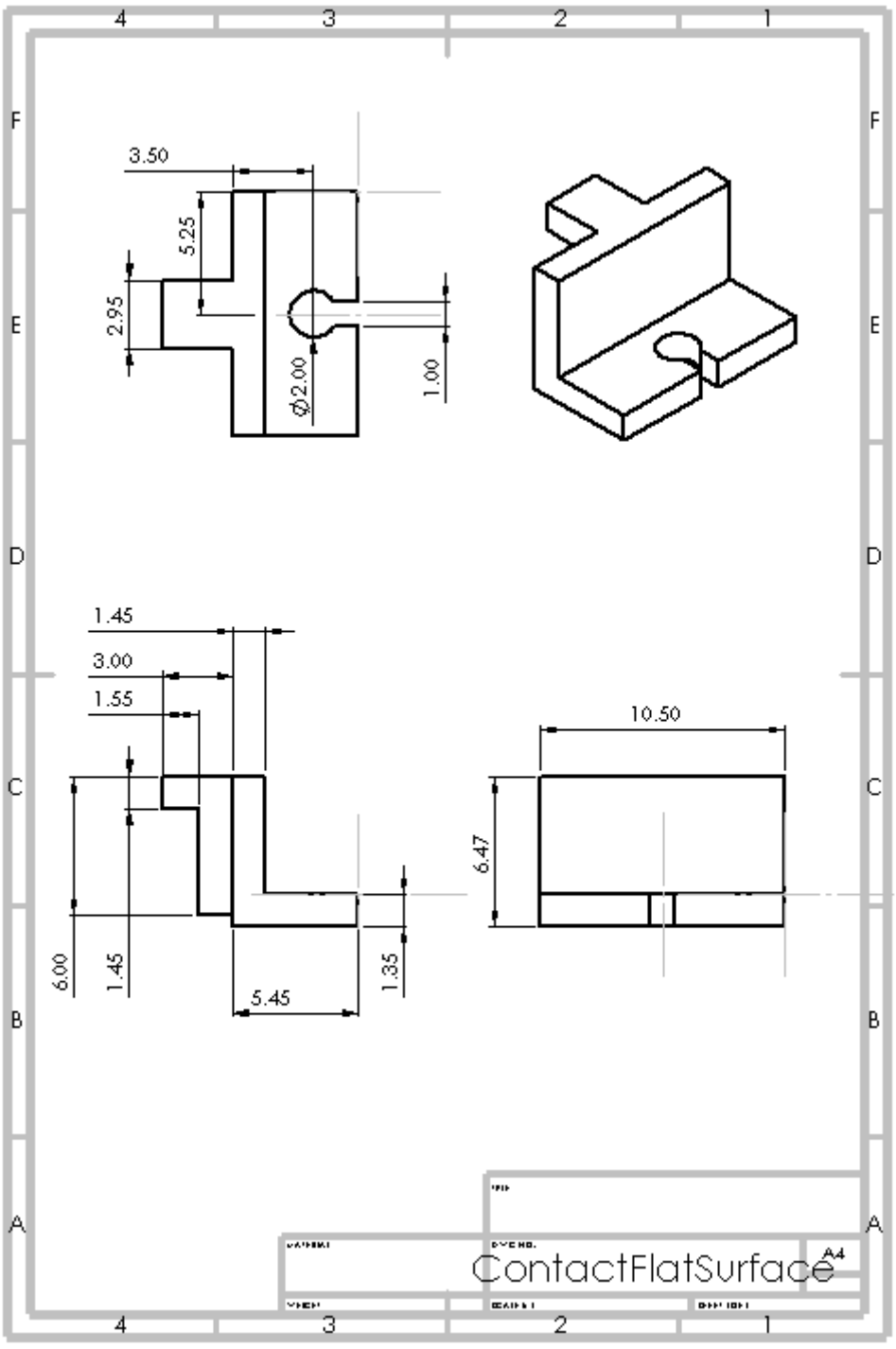
4
3
2
1
F
E
D
C
B
A
3.50
5.25
2.95
Ø2.00
1.00
1.45
3.00
1.55
6.00
1.45
5.45
1.35
10.50
6.47
ContactFlatSurface
A4

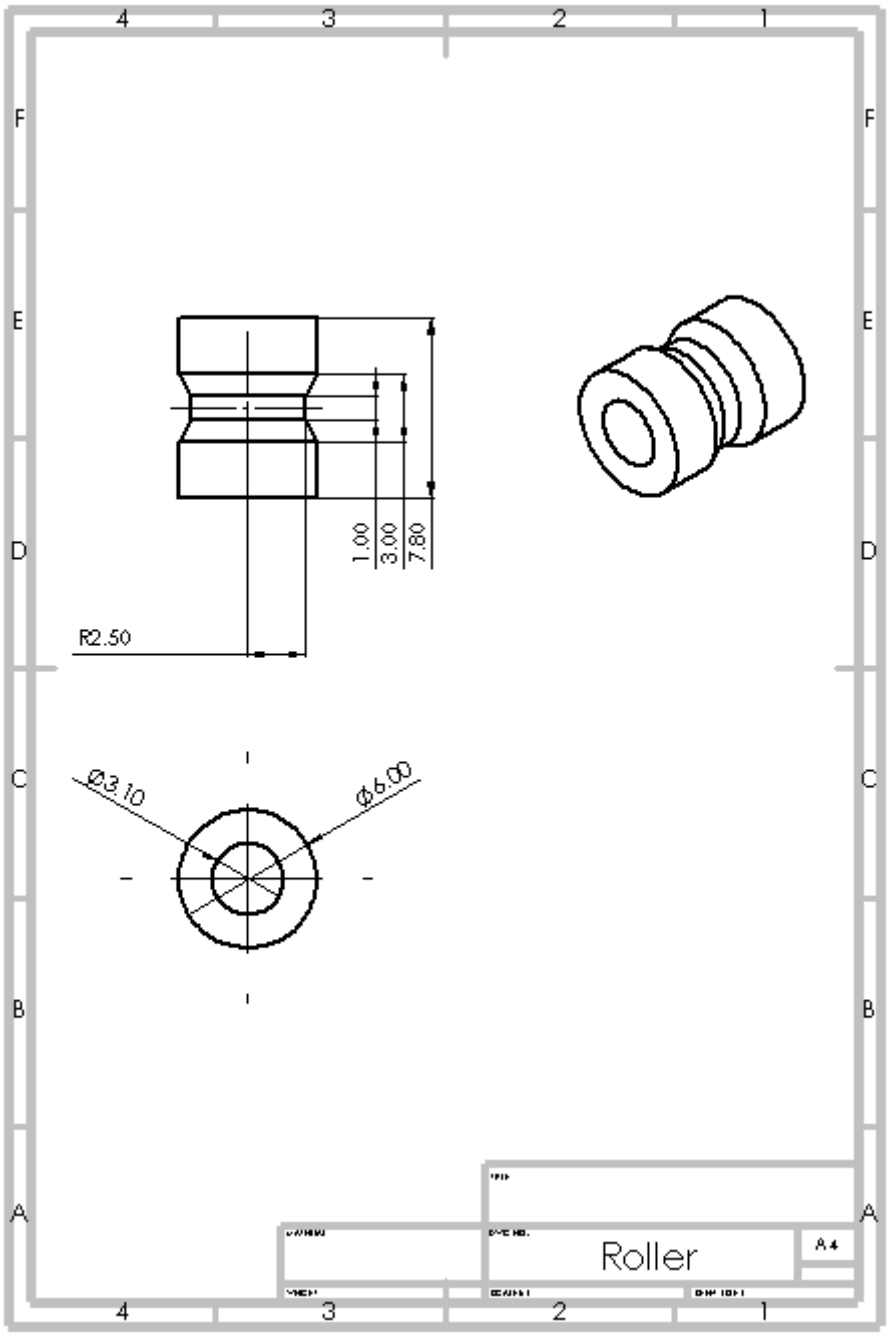
4
3
2
1
F
E
D
C
B
A
1.00
3.00
7.80
R2.50
Ø3.10
Ø6.00
Roller
A4

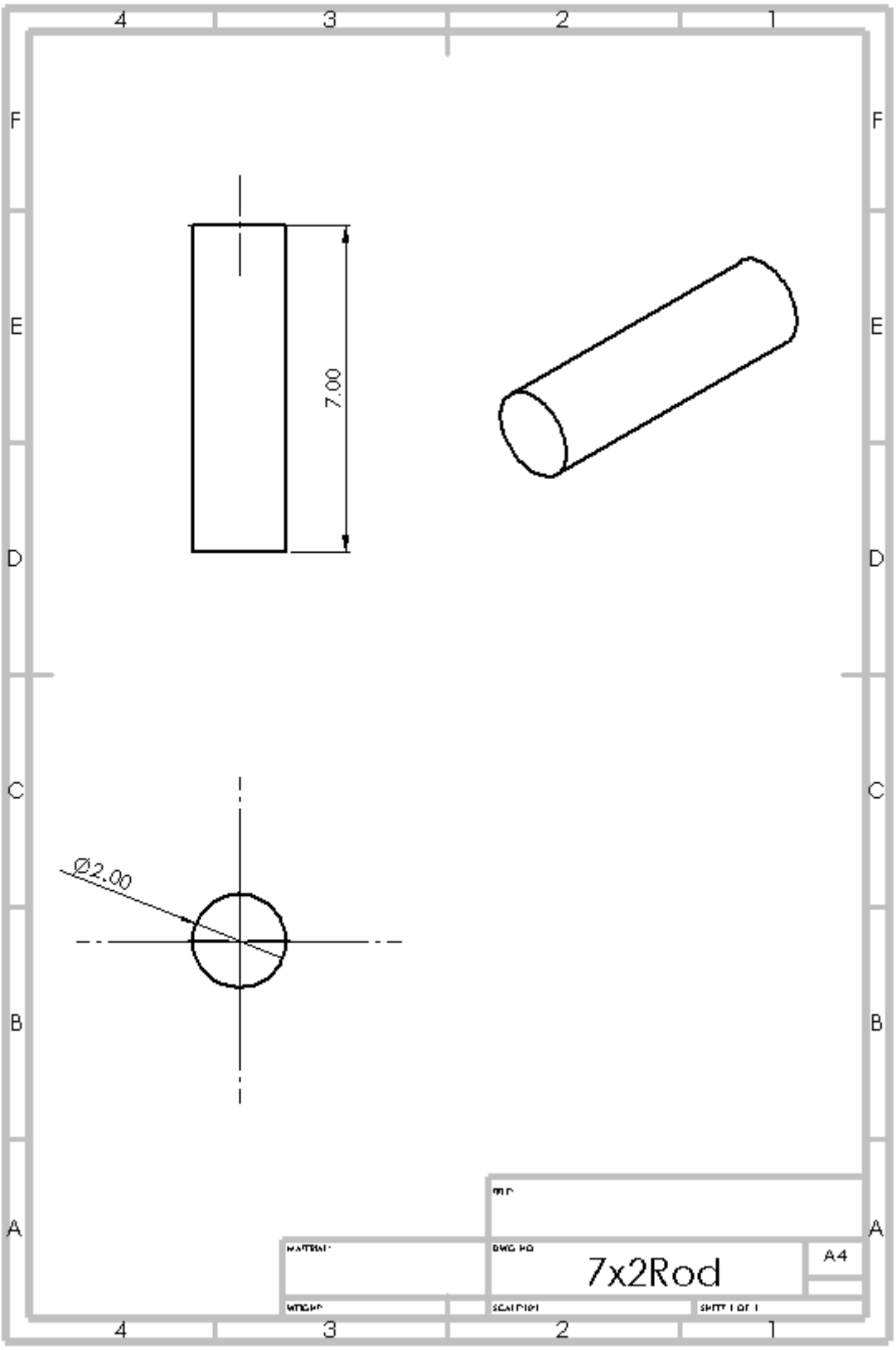
4
3
2
1
F
E
D
C
B
A
7.00
Ø2.00
7x2Rod
A4

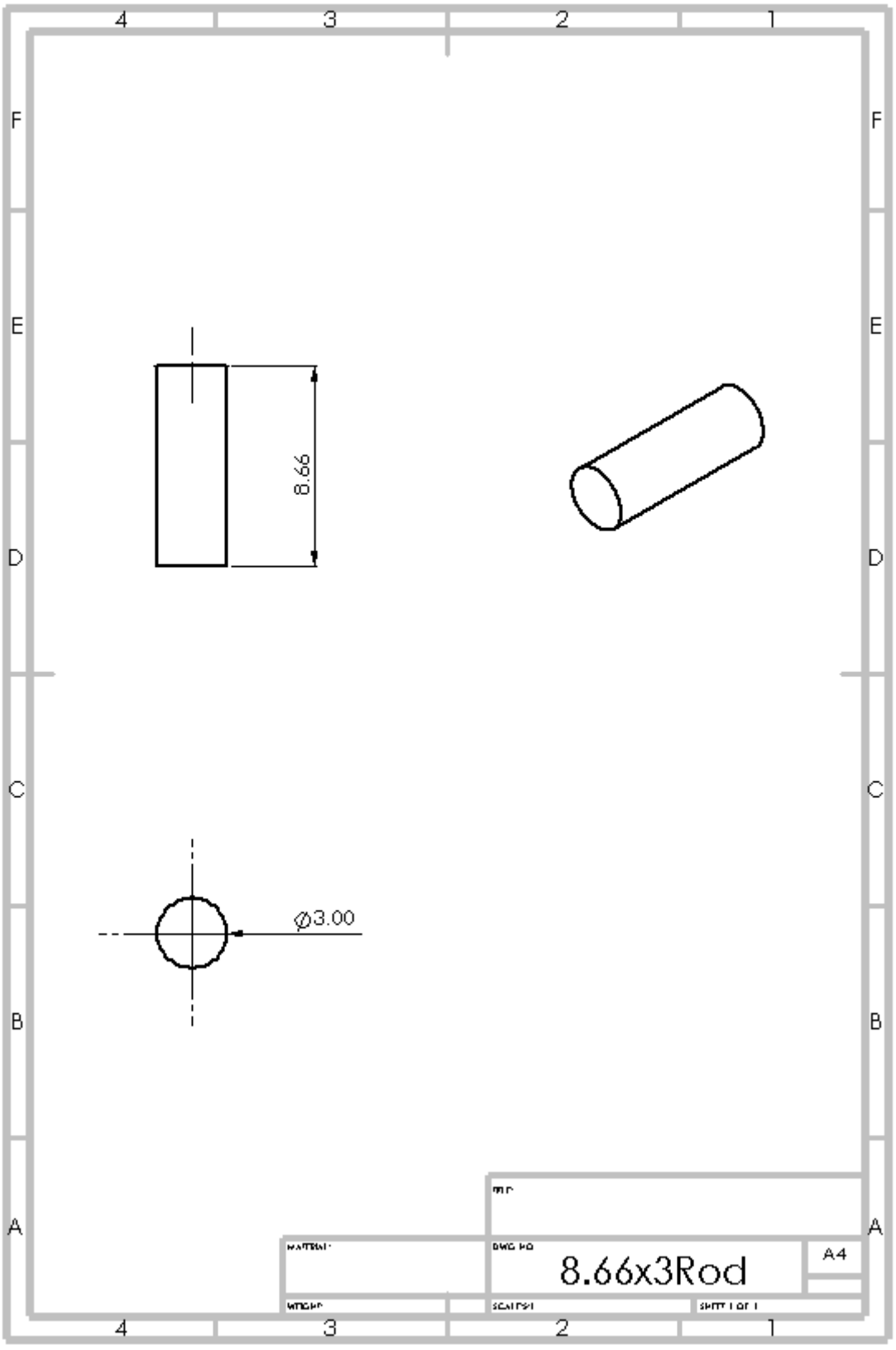
4
3
2
1
F
E
D
C
B
A
8.66
Ø3.00
8.66x3Rod
A4

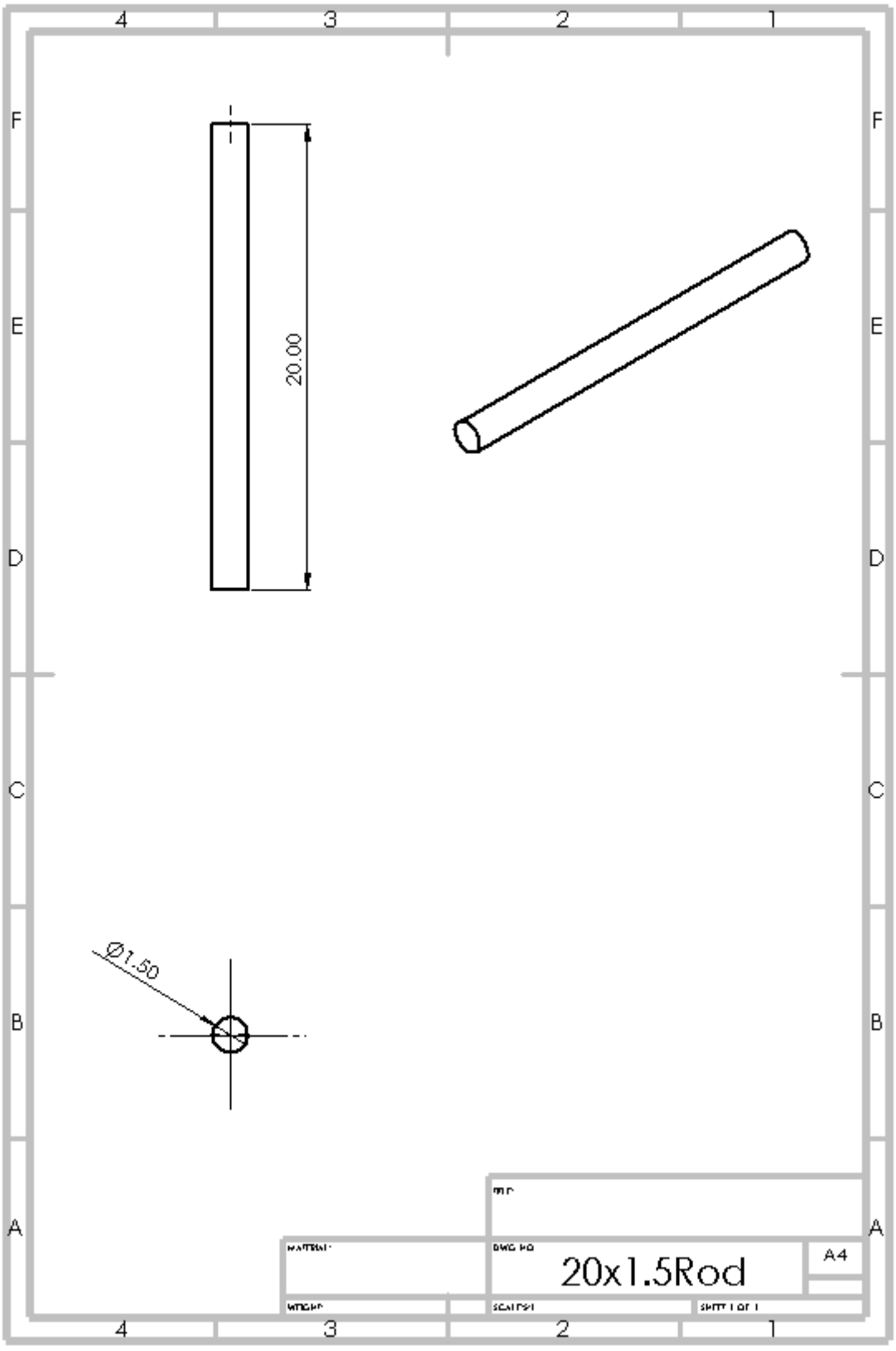
4
3
2
1
F
E
D
C
B
A
20.00
Ø1.50
20x1.5Rod
A4

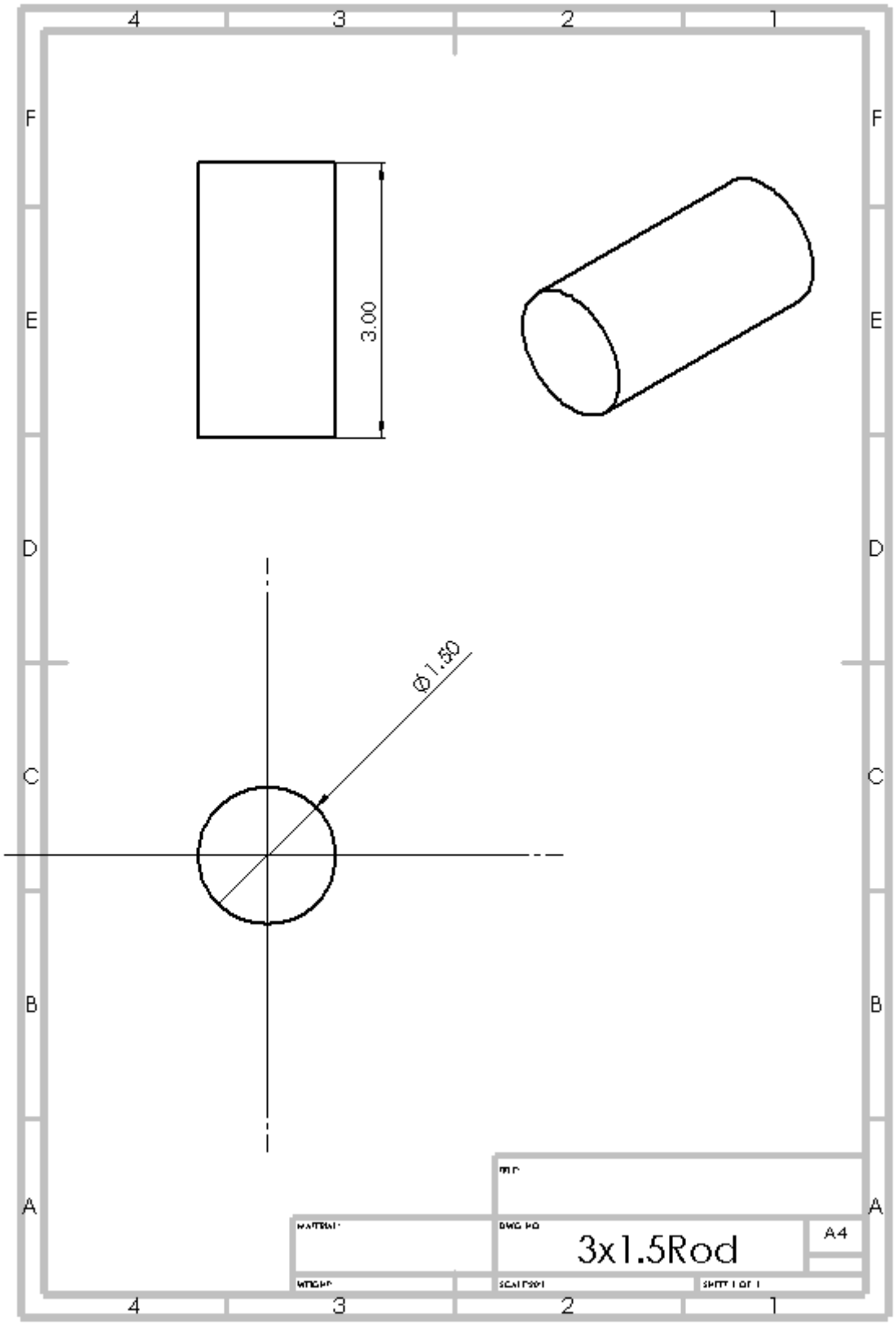
4
3
2
1
F
E
D
C
B
A
3.00
Ø1.50
3x1.5Rod
A4